Technical and Economic Impact of the Deployment of a VSC-MTDC Supergrid with Large-scale Penetration of Offshore Wind

Quanyu Zhao

Supervisor: Dr. Javier García González

ICAI School of Engineering
Institute for Research in Technology
Comillas Pontificial University

This dissertation is submitted for the degree of
Doctor of Philosophy

September 2018

I dedicate this thesis to
all who stay in my heart ...
I love you dearly.

Declaration

I hereby declare that except where specific reference is made to the work of others, the contents of this dissertation are original and have not been submitted in whole or in part for consideration for any other degree or qualification in this, or any other university. This dissertation is my own work and contains nothing which is the outcome of work done in collaboration with others, except as specified in the text and acknowledgements.

Quanyu Zhao
September 2018

Acknowledgements

This thesis summarizes my research activities at the Institute for Research in Technology (IIT) at Comillas Pontificial University, where I started working on September 2014.

And I would like to acknowledge ...

Table of contents

List of figures

List of tables

Nomenclature

Acronyms / Abbreviations

AC	Alternating Current
AWM	Air Warning Marker
B2B	Back-to-Back
CAPEX	Capital Expenditure
CBA	Cost Benefit Analysis
CE	Continental Europe
CSC	Current Source Converter
DC	Direct Current
DCF	Discounted Cash Flow
DL	Distribution Level
DLR	Dynamic Line Rating
EC	European Commission
EMF	Electromagnetic Field
ENTSO-e	European Network of Transmission System Operators for Electricity
EU	European Union
FB	Full-bridge
FOSG	Friend of the Supergrid

GAMS	General Algebraic Modeling System
HB	Half-bridge
HTLS	High Temperature Low Sag
HVDC	High Voltage Direct Current
HV	High Voltage
IEA	International Energy Agency
IEC	International Electrotechnical Commission
IEGT	Injection-Enhanced Gate Transistor
IEM	Internal Energy Market
IGBT	Insulated Gate Bipolar Transistor
IOP	Interoperability
IP	Intellectual Property
IPOPT	Interior Point Optimizer
LCC	Line Commutated Converter
LV	Low Voltage
MAE	Mean Absolute Error
MC	Master Control
MI	Mass Impregnated
MMC	Modular Multilevel Converter
MRTS	Modified RTS
MS	Member State
MTDC	Multi-Terminal High Voltage Direct Current
MT	Multi-Terminal

NLP	Nonlinear Programming
NPC	Neutral-Point Clamped
NSOG	North Sea Offshore Grid
OF	Oil fluid Filled
O.F.	Objective Function
OGEM	Offshore Grid Expansion Model
OHL	Overhead Line
OPEX	OPerational EXpenditure
OPF	Optimal Power Flow
OWF	Offshore Wind Farms
PCC	Point of Common Coupling
PDIP	Primal-Dual Interior Point
PF	Power Flow
PTP	Point-To-Point
PWM	Pulse Width Modulation
RAB	Regulatory Asset Base
RES	Renewable Energy Source
RSE	Ricerca sul Sistema Energetico
RTV	Room Temperature Vulcanizing
SCR	Short Circuit Ratio
SM	SubModule
SOCP	Second-Order Cone Programming
SVC	Static Var Compensator

TEP	Transmission Expansion Planing
TL	Transmission Level
TSO	Transmission System Operator
TYNDP	Ten-Year Network Development Plan
US	United States
VSC-MTDC	VSC based Multi-Terminal High Voltage Direct Current
VSC	Voltage Source Converter
WTG	Wind Turbine Generator

Indexes, sets and subsets

$\mathcal{B}^{ac} \in \mathcal{B}$	Subset of AC buses
$\mathcal{B}^{dc} \in \mathcal{B}$	Subset of DC buses
$g \in \mathcal{G}$	Generating units, running from 1 to G
$i, j \in \mathcal{B}$	Buses, running from 1 to B
$(i,j) \in \mathcal{N}_l$	Pair of buses connected by line l
$l \in \mathcal{L}$	Transmission branches, including lines and transformers, running from 1 to L
$\mathcal{L}^{ac} \in \mathcal{L}$	Subset of AC transmission lines
$\mathcal{L}^{dc} \in \mathcal{L}$	Subset of DC transmission lines
$\mathcal{N}_v^{ac}$	AC bus of converter v
$\mathcal{N}_v^{dc}$	DC bus of converter v
$v \in \mathcal{V}$	VSC converter, running from 1 to V

Parameters

A_g, B_g, C_g	Cost coefficients of generator g

A_v, B_v	Independent and linear terms of the losses function of converter v
$\boldsymbol{B_{ij}}$	AC network susceptance matrix
B_l	Susceptance of line l
B_l^{sht}	Half total line charging susceptance of line l
C_v^{rec}, C_v^{inv}	Quadratic terms of the losses function of converter v acting as rectifier or inverter
$\boldsymbol{G_{ij}^{ac}}$	AC network conductance matrix
$\boldsymbol{G_{ij}^{dc}}$	DC network conductance matrix
G_l	Conductance of line l
$\overline{I}_v$	Maximum current allowed through the converter v
NC_p, NC_q	Costs of non-served real and reactive power
$\overline{P_g}, \underline{P_g}$	Real power limits of generator g
P_{Di}, Q_{Di}	Real and reactive power demand at bus i
$\overline{Q}_g, \underline{Q}_g$	Reactive power limits of generator g
R_l	Resistance of line l
$\overline{S}_l, \overline{P}_l$	Flow limits on transmission line l
$\overline{V}_i, \underline{V}_i$	Voltage limits at bus i

Decision variables

i_v^{inv}	Module of phase current of converter v when functions as an inverter
i_v^{rec}	Module of phase current of converter v when functions as a rectifier
np_i	Non-served active power at bus i
nq_i	Non-served reactive power at bus i
p_g	Active power generation of generator g

p_i	Active power injected at bus i
q_i	Reactive power injected at bus i
q_g	Reactive power generation of generator g
ρ_l	Active power losses of line l
ρ_v	Active power losses of converter v
θ_i	Phase angle at bus i
v_i	Voltage magnitude at bus i

Chapter 1

Introduction

This chapter introduces the context of this thesis, defines its main objectives, and presents the structure of the document.

1.1 Background and Motivation

1.1.1 The concept of the Supergrid

This thesis is inspired and also financed by the European Project named *BestPaths*. The core idea of the project is to repower AC corridors and Multi-Terminal (MT) High Voltage Direct Current (HVDC) systems with various innovative technologies tested in five demonstrations. The final goals is to help decarbonize the European electric system by allowing large-scale penetration of renewable electricity production, and by increasing flexibility of the transmission network.

Providing low-carbon power across Europe will require a more integrated and strong liquid energy market, supported by upgraded and new trans-national transmission networks. This will enable European citizens to benefit from a fully competitive European Internal Energy Market (IEM), and it will be possible to share natural resources among all Member States (MSs) and citizens, based on solidarity and market rules.

Meeting the rising energy requirements in a sustainable, secure and competitive manner is one of the main challenges of current power system. In this context, the

development of the *supergrid*[1] is considered the best solution to allow enormous renewable energy sources in the system, as well as to contribute to the mitigation of global climate change. Some projects that have studied the *supergrid* are Desertec, Twenties or Medgrid (Cole et al., 2011))

Transmitting bulk power through long distances with alternating current (AC) has some limitations (Meah and Ula, 2007). In particular, for underwater transmission systems, direct current (DC) is economically advantageous with respect to AC at much shorter distances. The *supergrid* will allow for bulk power transportation over long distances, from generation centers, where resources are more abundant and economical, to consumption centers. Thanks to the technical developments in the area of power electronics, current converters are able to operate efficiently at high voltage levels, and several initiatives have been launched to move from point-to-point links towards MT configurations in order to increase the reliability of the system and to facilitate the connection between AC and DC grids.

The distinct advantages of Voltage Source Converter (VSC) on controllability and flexibility makes MT HVDC (MTDC) systems a feasible solution from the technical point-of-view. Meanwhile, meshed VSC based HVDC systems with MT configuration (VSC-MTDC) is believed to be the best fit for such a DC grid (Gonzalez-Longatt et al., 2012; Van Hertem and Ghandhari, 2010). Therefore, VSC-MTDC is seen as a viable option that can outperform traditional AC transmission due to its technical, economic and environmental advantages (Okba et al., 2012; Van Hertem and Ghandhari, 2010).

Despite the potential economic, energy security and environmental advantages that could be brought by a *supergrid*, there still remains very substantial obstacles to the actual development. The main challenges can be categorized as technical, regulatory and economic.

- **Technical Barriers**: Compared to conventional AC system, new control and protection devices need to be developed to operate the *supergrid* in a reliable manner. In addition, there is a need to update the power flow, and the optimal power flow models used to plan the optimal operation of the grid.

- **Economic Barriers**: Although the economic opportunities associated with a *supergrid* may be promising, there are also tremendous uncertainties about the balance of expected costs and benefits. It is crucial to demonstrate that such a

[1]The "Supergrid" is defined as "a pan-European transmission network facilitating the integration of large-scale renewable energy and the balancing and transportation of electricity with the aim of improving the European market" (Flourentzou et al., 2009).

large network would bring proclaimed benefits over costs before industrialization and deployment of all innovative technologies into the pan-European transmission system. Towards this end, the project *BestPaths* has devoted one entire work package (WP13), assessing scalability and replicability, on the basis of Cost Benefit Analysis (CBA) of the demonstrated solutions.

- **Regulatory Barriers**: The *supergrid* not only enables large amount of renewable energy integration, but also allows and facilitates international trade and balancing (Van Hertem and Ghandhari, 2010). Consequently, a harmonized European energy policy is necessary in all time horizons, to improve competitiveness, to achieve the security of supply at European level and at the same time, to diminish external dependency. Moreover, financing such a *supergrid* needs a stable and attractive framework and a truly harmonized and collaborative European regulatory environment, which are both significantly challenging.

1.1.2 The European Project BestPaths

In response to the call ENERGY.2013.7.2.3 in order to help overcome the challenges of integrating RES into Europe's energy mix, the EU Project *BestPaths* (http://www.bestpaths-project.eu/) was initiated in year 2014 (BestPaths, 2014 - 2018). It is the last and largest project under the 7^{th} Framework Programme which aims at "demonstrating by early 2018 and through real life, the capability of several critical network technologies in order to increase the pan-European transmission network capacity and electric system flexibility, thus making Europe able of responding to the increasing share of renewable in its energy mix by 2020 and beyond, while maintaining its present level of reliability performance."

The project unites nearly 40 leading organizations from research, industry, utilities, and Transmission System Operators (TSO) around five large-scale demonstrations, in order to develop novel network technologies, as well as to validate the technical feasibility, to assess the costs, impacts and benefits of the tested grid technologies. The focus of the demonstrations is to deliver solutions to allow for transition from HVDC lines to HVDC grids, to upgrade and repower existing AC parts of the network, and to integrate superconducting high power DC links within AC meshed network.

1.1.3 Technology Development Towards the Supergrid

As previously discussed, the *supergrid* is seen as a promising solution for RES integration. The overarching challenge faced by the existing European transmission network is the deficient grid capacity that holds back higher RES integration which might be an obstacle to meet the EU targets in the long term (ECF, 2010). Due to the intermittency of renewable energies, fast balancing is essential to assure system reliability. Transnational interconnections not only are instruments for better security of supply, but also facilitate the cross-border trading and the integration of wholesale electricity markets (Van Hertem and Ghandhari, 2010). In the future, it would serve as a backbone on the basis of existing transmission networks. Presently, high voltage transmission infrastructures have already been constraining the development of renewables which therefore, requires strong upgrades and expansions of the European grid (ECF, 2010; Nature, 2008).

A variety of technical solutions is nowadays available and considered promising for transmission network reinforcement which can be categorized in two classes: AC and HVDC.

From HVDC perspective, converter stations are indispensable components to develop a HVDC grid. However, the development of these converters is subject to a number of challenges such as standard and interoperability issues, DC breakers and hybrid system operation and control. Conductors and cables are other important components to be considered for power transmission and interconnecting systems as connections can either be realized by an Overhead Line (OHL) or by an underground/submarine cable. These technologies are also subject to a number of difficulties: Since there is no reactive power involved in DC transmission, no real physical limit is imposed on the distance. For OHLs, special care needs to be taken for external insulation design accordingly to the particularities of the locations. Special conductor prototypes, i.e., High Temperature Low Sag (HTLS), are designed to increase the transmission capacity. Nevertheless, they are not commercially available yet. As for cables, there are mainly two types (depending on the insulation systems): extruded and paper-lapped (or oil-impregnated) cables. The latter type can be further categorized into oil fluid filled (OF) and mass impregnated (MI). In order to meet future needs on transmission capacity increase and growing deployment of HVDC links worldwidely, both terrestrial and submarine HVDC cables are expected to have better performance in terms of rating and reliability. Consequently, for the past years, different insulation materials and technologies have been used to develop HVDC cable systems (Ghorbani et al.,

2015). Cable size becomes significant when high voltage is targeted. Consequently, transportation and handling of such cables can be very challenging. In particular, for underground land cables, civil works could be a problem in a population-densed area. In addition to technical challenges, regulatory barriers such as (trans)national policies, financial instrument, legal and intellectual property could also exert obstacles.

On the AC side, technologies such as HTLS conductors, insulated cross-arms, Dynamic Line-Rating (DLR) system are proposed under the scope of *BestPaths* project for repowering existing transmission corridors (BestPaths, 2014 - 2018). New materials, tools and technologies are investigated. Nevertheless, similarly as before in the case of HVDC, many challenges remain.

Despite the increasing need, at both national and transnational level, investment levels indicated in the national development plans are lagging behind (Van Nuffel et al., 2017). Adequate technological solutions are prerequisites for building the supergrid, while reasons for insufficient expansion and modernization of the grid are manifold. Towards this end, this thesis has dedicated one chapter (Chapter 6) to identify (not only HVDC, but also AC) the most promising technologies for grid expansion/repowering, and to address the most relevant barriers for the deployment of such technologies.

1.1.4 Optimal Power Flow Modeling for Medium Planning

The impact on power flows derived from Point-To-Point (PTP) interconnections between HVAC and HVDC systems is even more notable in case of having a meshed MTDC system overlaying an AC grid, and the control strategies of the converters become crucial. VSC allows flexible and independent active and reactive power control (Flourentzou et al., 2009), and its forced-commuted feature makes it ideal to connect wind farms at distance as it can mitigate the propagation of voltage and frequency deviations caused by wind variations. However, the operating principles of VSC are completely different from those of Current Source Converter (CSC). Therefore, new algorithms need to be developed for VSC HVDC control and power flow studies.

The problem of finding the Power Flow (PF) solution for the case of hybrid network with VSC-MTDC systems is relatively new (Baradar et al., 2013; Okba et al., 2012). Among the few papers that study the PF problem of a hybrid network in the literature, it is possible to distinguish basically between: 1) the sequential approach as in (Beerten et al., 2012) where AC and DC systems are solved separately under a general formulation that can deal with converter limits and different topologies; and 2) the unified approach as in (Baradar and Ghandhari, 2013) where AC and DC systems are solved together

with an explicit consideration of converter losses that are balanced with a DC slack bus per MTDC grid in the system. Some other authors have been focusing on the transient analysis and stability issues, which is out of the scope of this thesis.

In addition to the PF problem, the Optimal Power Flow (OPF) was firstly introduced by Carpentier in 1962 (Wood and Wollenberg, 2012). The goal is to find the optimal scheduling of the generators while taking into account network constraints (capacity limits and security constraints). In order to assess and fully exploit the potential impact of VSC-MTDC, traditional models that were developed for AC systems need to be extended to cope with hybrid AC/DC networks. Several research works have been proposed to include VSC-MTDC systems into power flow calculation of a hybrid AC/DC system as previously mentioned. However, fewer studies take into account VSC-MTDC systems under an optimization context: (Baradar et al., 2013) applies Second-Order Cone Programming (SOCP) technique, (Cao et al., 2013) solves the hybrid network using the Primal-Dual Interior Point (PDIP) algorithm, with predefined control strategies for DC networks, as well as modified Jacobian and Hessian matrices, and (Feng et al., 2014) utilizes Interior Point Optimizer (IPOPT) to seek solutions for the non-linear model built in General Algebraic Modeling System (GAMS).

OPF models are not only used for short-term system operations. They can also serve as sub modules to assist long-term expansion planning problems (Zhu, 2015). The economic assessment of considering VSC-MTDC systems as an alternative for network reinforcement instead of conventional AC links becomes one of the most important tasks during the overall planning stage. So far, (Feng et al., 2014) is the only found research paper that copes with such a problem. Thus, one of the goals of this thesis is to propose extended OPF tools for AC networks integrated with embedded VSC-MTDC systems of diverse topologies, which could be applied for both operation and planning purposes.

In addition to the problem of lacking appropriate models, there are no previous works that are able to deal with large-scale hybrid networks considering all system losses as well as a detailed technical representation of the generation and the transmission system (both AC and DC). This demands a model that is capable of dealing with large-size systems oriented to medium-term planning analysis.

Finally, technical impacts of modeling system components in different ways within a hybrid network have not been been studied in the existing literature. Among them, converter losses are different depending on whether it functions as a rectifier or as an inverter (Zhao et al., 2017). It requires a deep analysis, as the number of converters

will presumably be very high in case the *supergrid* is built. However, there are no previous research works where a systematic analysis of how much such losses may impact on the optimal solution, and about what level of accuracy is necessary to avoid an unnecessary extra computational burden.

1.1.5 Economic assessment

VSC-MTDC systems have not been paid enough attention in the scientific literature. Most studies, as well as commonly used processes and methodologies for transmission expansion planning focus on conventional AC system, as seen in (L'Abbate et al., 2012) and (de Dios et al., 2007). HVDC systems on the other hand, especially VSC-MTDC, have been considered only in a few papers. Although, advantages of using innovative technologies to repower and expand EU transmission grid are potentially large. The uncertainties associated with the balance between costs and benefits are tremendous. Thus, there is a need to develop new models and extend on the current ones. Meanwhile, the model developed should be complex enough to capture relevant features (derived from a hybrid AC and DC system based on the development of a *supergrid*) but simple enough to allow affordable computation for large-scale systems.

Moreover, CBA intrinsically is a conceptually broad research question, which could be studied in depth. It allows identifying and characterizing the impacts of the studied project. In order to help performing CBA on European projects, the European Network of Transmission System Operators for Electricity (ENTSO-e) has newly approved a guideline, in which, there are a number of benefit indicators (ENTSO-e, 2015b). Nevertheless, implementing all kinds of benefits monetization for different purposes is not as easy and straight forward as categorizing them. Therefore, it requires more research on assessing methodologies and on developing appropriate models to support the analyses. In this thesis, the aforementioned ENSTO-e guideline will be used as a reference in the techno-economic impact assessment that will be carried out.

Besides, what is more challenging and difficult, is to gather enough information and data to perform the CBA or a replicability[2] study from the perspective of the pan-European network, including transmission line parameters, generation and demand information, technical limits, etc. While developing this thesis, massive amount of data were collected and processed in order to prepare a consistent data set that represents adequately the studied system.

[2]Replicability refers to duplication of a system component at another location or time with different boundary conditions (Sigrist et al., 2016).

1.2 Problem Statement and Objectives

As introduced above in Section 1.1, MTDC systems are considered to be one of the most promising and cost-effective ways to integrate a large amount of renewable energies to inland AC system. The new HVDC technology based on VSC has led to the feasibility of meshed MTDC network. This is the main motivation of the present work. Plentiful research need to be carried out in order to disclose the steady state and dynamic behavior of a hybrid system, in addition, to fully explore the advantages of such AC/DC systems in real-size. This thesis will concentrate on the steady-state analysis from a medium-term scope, under different perspectives.

Framed in this context, this thesis endeavors to address the main research question emanating from modeling and analytical perspectives of the MTDC system:

> ***What are the main techno-economic impacts of the of VSC-MTDC systems, under the scope of the pan-European transmission network, considering large integration of offshore wind generation?***

This overall question can be divided in the following objectives, and within each objective, some unresolved issues are identified accordingly:

Objective 1: To contribute to the development of new models that are able to consider simultaneously large AC and DC systems with a high level of wind generation and oriented to medium-term analysis. A special emphasis will be done on the effect that the converters can have on the optimal operation of the system. The time scope of these models will be the medium-term (i.e. one year) in order to assist a posterior cost-benefit analysis where multiple scenarios need to be evaluated.

- Problem Size: There is handful of papers and studies that consider hybrid AC and DC networks. Most of them are oriented to steady-state power flow models. However, as pointed out previously, there is a lack of models that consider MT HVDC under an optimization context (i.e. OPF models). These OPF models are not only necessary tools for operational purposes, but also necessary models to assist medium- and long-term planning problems. On that regard, the size of the studied system can represent a serious obstacle.

- System Components Modeling: Among all the OPF models for hybrid networks proposed in the literature, not enough attention has been paid to the modeling of the converter. In particular, the modeling of converter losses represents an

interesting line of research. Technical impact of appropriate modeling of the losses is not negligible. It could contribute to different generation scheduling, as well as power flow patterns. Moreover, from the long term perspective, ignoring losses would result in underinvestment or even a different expansion solution as shown in (Fitiwi et al., 2015).

Objective 2: To assess the techno-economic impact of the *supergrid* under the scope of a pan-European network. This assessment addresses technical (i.e. changes on the generation pattern, power flows, energy efficiency and congestions all over Europe thanks to the possibility hosting larger amounts of offshore wind generation and to the extra transmission capacity provided by the *supergrid*), economic (i.e. the reduction in operational costs, renewable energy curtailment) and environmental (CO_2 emission reduction) perspectives.

- System Size and Data Acquisition: Without a capable tool that can deal with large-scale systems and a complete data set of the pan-European, it is impossible to perform any economic assessment and demonstrate the potential benefits that the *supergrid* could bring to the system in a quantitative and systematic manner. Apart from the model development, gathering data and construct a consistent, representative data set is also a challenging task that will require the collaboration of institutions such as ENTSO-e.

- Economic Assessment Methodology: The question *how to assess the benefits of the supergrid* is not trivial. ENTSO-e has established some guidelines to perform a general cost-benefit assessment of grid development projects, providing a number of indicators that should be evaluated (ENTSO-e, 2015b). However, the application of such guidelines to the project of the *supergrid* is not straightforward and therefore one of the secondary objectives of this thesis is to help in the elaboration of such CBA through a case study of a practical system.

- Barrier Identification: As *supergrid* would facilitate power transmission and assist IEM Europe-widely, it is necessary to have a stable and attractive framework and a truly harmonized and collaborative European regulatory environment during the development of such network in addition to the removal of all technical barriers. The identification of the main barriers that might prevent from an efficient deployment of the *supergrid* will constitute another objective of this thesis.

1.3 Contributions and Publications

This thesis addresses hybrid AC/DC systems from different perspectives. The main contributions can be grouped into three different aspects of the *supergrid*. The first two contributions are more quantitative. They are: 1) AC/DC hybrid system modeling and 2) AC/DC hybrid system steady-state analysis. The third contribution is more qualitative: 3) barrier identification towards development of the *supergrid*.

1. Contribution to the AC/DC hybrid system modeling.
   An extended OPF model (with full nonlinear PF equations) has been proposed taking into account loss modeling of different converter operation modes (inverter or rectifier). In addition, the impact of some alternative ways of modeling the converter losses in a more simplified manner has been studied.

   A methodology is proposed to assess the effect of the different approaches to model converter losses on the solution of the OPF. This methodology includes the definition of a metric used for the required comparisons.

   Journal Paper:
   Q. Zhao, J. Garcia-Gonzalez, O. Gomis-Bellmunt, E. Prieto-Araujo, and F. M. Echavarren, "Impact of converter losses on the optimal power flow solution of hybrid networks based on VSC-MTDC," ***Electric Power Systems Research*****, vol. 151, pp. 395–403, Oct. 2017.**

2. Contribution to the AC/DC hybrid system analysis.
   A linearized model approximated based on the above mentioned was proposed which can be applied for both operation and planning purposes. It considers detailed hybrid AC/DC transmission representation, i.e., transmission losses are included, meanwhile addresses converter modeling by taking into account that it can function either as an inverter or a rectifier. The model is able to deal with large-scale hybrid AC/DC system at an affordable computational cost.

   Massive amounts of data has been collected and processed to construct a realistic European transmission network. A techno-economic assessment of one year time scope through applying the model has been carried out as a case study in order

to evaluate and compare VSC-MTDC alternatives.

Working Paper:
Q. Zhao, J. Garcia-Gonzalez, "Benefit Evaluation of Large-Scale Hybrid Networks Based on VSC-MTDC," ***Under Drafting.***

3. Contribution to the barrier identification towards development of the *supergrid*. A comprehensive overview of the state-of-the-art and beyond technological developments that are considered promising by industrial professionals, including Transmission System Operators (TSO), manufactures and Renewable Energy Sources (RES) companies, in Europe has been presented. Main features associated with each reviewed technology are also included.

   Barriers that prevents the development and deployment of those technological solutions concerning TSOs, manufactures, RES companies and research centers have been identified and presented systematically.

   Journal Paper (under review):
   Q. Zhao, J. Garcia-Gonzalez, R. Gaspari, "Review of technological solutions and barriers identification for transmission system development to help renewable energy sources integration," ***Submitted to Renewable & Sustainable Energy Reviews.***

Reports:

In addition to the papers either published or submitted above, there are three project deliverables published under the European Project *BestPaths*:

1. Zhao, Q., García-González, J., Rivas, D., & Galan Hernandez, N. (2018). Deliverable D13.2 Definition and Building of BestPaths Scenario. the BestPaths EU Project.

2. Zhao, Q., & García-González, J. (2018). Deliverable D13.3 Identified Barriers for Replicability. the BestPaths EU Project.

3. Azpiri, I. and Veguillas, R. and Despouys, O. and Rebolini, M. and Marzinotto, M. and Palone, F. and Sallati, A. and Kiewitt, W. and Gombert, V. and Lallouet,

N. and Bruzek, C. and Borroy Vicente, S. and González, V. and Lorenzo, M. and D'Arco, S. and García, J. and Zhao, Q. and Siborgs, J. and Finney, S. and Lund, P. and Sorensen, S. and Ugalde, C. and Cirio, D. and Ciapessoni, E. and Eriksson, R. and Berljn, S. (2015). Deliverable: D2.1 Data set, KPIs, tools & methodologies for impact assessment. the BestPaths EU Project.

Other Working Papers:

J. Renedo, A. García-Cerrada, L. Rouco, A.A. Ibrahim, B. Kazemtabrizi, Q. Zhao, J. García-González, 2018. A simplified algorithm to solve optimal power flows in hybrid VSC-based AC/DC systems. Working paper IIT-17-165A. ***Submitted to International Journal of Electrical Power and Energy Systems and under revision.***

J. Sau-Bassols, Q. Zhao, E. Prieto-Araujo, J. García-González, O. Gomis-Bellmunt, 2018. Optimal Power Flow operation of an Interline Current Flow Controller in a hybrid AC/DC meshed grid. ***Submitted to IEEE Transaction on Power System.***

1.4 Outline of the Thesis

The remaining part of the thesis has been divided into several chapters and outlined as follows:

Chapter 2 High Voltage Direct Current Technology presents background information of DC transmission and HVDC technologies are described in detail. How a HVDC *supergrid* can be realized through MTDC configurations based on VSCs, as well as how they can be included in the consideration of transmission planning is briefly explained.

Chapter 3 Optimal Power Flow for AC/DC Hybrid Network first gives an introduction to OPF. Then it provides steady-state modeling of the VSC station, followed by complete non-linear and linear mathematical formulations of the OPF problem of a hybrid AC/DC grid respectively. Both models focus on the steady-state analysis. The nonlinear model means to study converter stations more in detail while the linear model means to target a large-scale hybrid AC/DC system and to serve both for operation and planning purposes. The proposed model has been deployed on the

pan-European system to carry out a techno-economic assessment.

Chapter 4 Impact Assessment of Converter Losses and Case Studies of Non-linear and Linear OPF Models. In this chapter, special attention has been paid to converter losses. How the different ways of modeling losses can impact on the OPF solution is illustrated and explained with a case study. Moreover, to demonstrate the goodness of the linear model, case studies have been conducted on several small IEEE standard system before its application on a practical system.

Chapter 5 Techno-Economic Assessment of pan-European System presents a case study on a pan-European system. The purpose is to show the applicability of the model on a large-scale system and to demonstrate how a techno-economic impact assessment can be carried out for such a system.

Chapter 6 Barriers Towards the European Supergrid addresses the challenges to build a European *supergrid*. The state-of-the-art and beyond technological solutions that are considered promising to expand and reinforced the existing transmission grid are identified, reviewed and highlighted with their features. The main barriers needs to be overcome for the deployment of such technologies are carefully discussed.

Chapter 7 Conclusion and Future Work draws conclusions and suggestions for future work.

Chapter 2

High Voltage Direct Current Technology

In this chapter, a general overview of HVDC systems with the aim of explaining their history and evolution is provided, together with its advantages with respect to the conventional AC grids. First of all, the two main components of an HVDC system, i.e., converters and cables/conductors are reviewed. Secondly, the main HVDC converter technologies (CSC and VSC) are described and the major advantages and drawbacks of each of them are briefly discussed and compared. Then, this chapter presents the concept of MTDC system and reviews technical details of VSC-HVDC (including VSC-MTDC), e.g., system configuration, VSC topologies and modulation methods. These technical details are the foundation of the VSC-MTDC steady-state model, which will be presented in Chapter 3. Finally, an introduction of the basic principles of TEP (in relation with OPF) is given. The need of models able to deal with large-scale MTDC/AC hybrid network operation and simulation is highlighted.

2.1 The War of Currents

Although DC transmission is starting to make its comeback due to its advantages when considering long distances and Offshore Wind Farms (OWFs), the truth is that both AC and DC technology have been around since late 19th century. At then, two

brilliant people, Thomas Edison[1] and Nikola Tesla[2], were embroiled in a nasty war, later known by people as the "War of Currents".

In 1879, Edison developed the world's first incandescent light bulb, and he launched the idea to build a DC system for generating and distributing electricity so businesses and homes could use his new invention. He established his company named Edison Illuminating Company in 1880 and soon after, he opened his first hydroelectric power plant, in New York City, in 1882. In the same year but in Europe, the first long distance DC power line was built, transmitting power from Miesbach (the foothills of the Alps) to Glaspalast (Munich) in Germany by Oskar von Miller[3]. It was operated at a voltage level of 2 kV and the line was 57 km long (EdisonTechCenter, 2015).

Early on, Edison recognized the limitation of his Low Voltage (LV) DC power system. The primary drawback was that it generated and distributed power at the same voltage resulting in high line losses. Consequently,the distance that the DC power could be economically transmitted was seriously limited (EdisonTechCenter, 2014b; Engineering and History, 2010).

Towards this end, Nicola Tesla, a young Serbian-American engineer, was hired to resolve this issue. He set out to redesign Edison's DC generators. Meanwhile, he tried to interest his boss with the idea of an AC induction motor he had been developing. However, Edison dismissed the idea and the *War of Currents* started.

Tesla left Edison in 1885 and received a number of patents for his AC technology in few years. Later, George Westinghouse, who was the owner of Westinghouse Electric Company and also had strong faith in AC transmission, bought his patents. Quickly, Westinghouse become an Edison competitor. With only one year in the business, Westinghouse had already more than half as many generating stations as Edison.

On the other hand, feeling threatened by the rise of AC and not wanting to lose the royalties he had earned from his DC patents, Edison started to discredit AC systems

[1]Thomas Alva Edison (February 11, 1847 - October 18, 1931) was an American inventor and businessman, who has been described as America's greatest inventor. He developed many devices that greatly influenced life around the world, including the phonograph, the motion picture camera, and the long-lasting, practical electric light bulb.

[2]Nikola Tesla (10 July 1856 - 7 January 1943) was a Serbian American inventor, electrical engineer, mechanical engineer, physicist, and futurist who is best known for his contributions to the design of the modern alternating current electricity supply system.

[3]Oskar von Miller was born in Munich in the Kingdom of Bavaria (Germany) in 1855. He is an engineer and business leader of electrical innovation. In 1883, he became the co-director of the German Edison Company. His company built Munich's first power station in 1884. In 1887, the company was renamed Allgemeine Elektricitats Gesellschaft (AEG).

and claimed that they are more dangerous than DC by demonstrating electrocutions of cats, dogs with AC power.

When New York State sought a more humane alternative to execute its death-penalty prisoners, Edison proposed AC power as the most effective option. Eventually, the public campaign resulted in the emergence of electric chair to electrocute people. The penalty to convict criminals became known as “westinghousing” (King, 2011).

In 1893, the Chicago World’s Fair, also known as the World’s Columbian Exposition took place. General Electric bid $554 000 to electrify the fair with Edison’s DC power while Westinghouse offered a price of $399,000 which is more than $150 000 less using Tesla’s AC power. This ultimately led to the final victory of the "War of Currents" to Westinghouse. In the same year, Niagara Falls Power Company awarded the contract to Westinghouse to generate power from Niagara Falls in order to light up street lights of Buffalo. The achievement was regarded as the unofficial end of the "War of Currents" and AC became an industry standard (Lantero, 2014).

In addition, transformer pioneered by Lucien Gaulard[4] and John Dixon Gibbs[5] (which was based on the initial designs of Sebastian Ziani de Ferranti[6]) was firstly demonstrated in London and then Turin (Italy) in 1884 (EdisonTechCenter, 2014a). It had also landed a hand to Tesla.

The *War of Currents* favored AC technology since voltage levels can be easily stepped-up or -down through transformers. It allows different voltage levels at all the stages (generation, transmission and distribution) such that HV power transmission at a long distance with lower power losses is feasible.

Although AC has been dominating the power system for more than a century, DC transmission had never stagnated and kept developing. One of the early predecessors of modern HVDC systems is the *Thury system*. It is named after the Swiss engineer René Thury (August 7, 1860 – April 23, 1938), also known as *the King of DC*.

After spending half a year visiting Edison’s lab in the winter of 1880-1881, he gained a lot of insights and concluded that the designs could be significantly improved. In 1882, he developed a six pole dynamo which yielded a more compact design than those of Edison (la Ville de Genève, 2006). Subsequently, the first DC transmission was built in 1885 from Taubenlochschlucht gorge to supply Bözingen at a capacity of 30kW and a voltage level of 500 Volts (Electrosuisse, 2011).

[4]Lucien Gaulard (1850 – November 26, 1888) was born in Paris, France.

[5]John Dixon Gibbs (1834 – 1912) was a British engineer and financier.

[6]Sebastian Pietro Innocenzo Adhemar Ziani de Ferranti (9 April 1864 – 13 January 1930) was a British electrical engineer and inventor.

Later, he explored the idea to place in series generators and loads so to attain a high transmission voltage. All machines (generator or load) are provided with short-circuiting switches. When a machine is not in use, it is short-circuited. When load varies, generator is switched in and out accordingly to adjust the total voltage (Still, 1913). The first commercial *Thury system* (14kV, 630 kW, 120 km) was put into service in Italy by the Acquedotto de Ferrari-Galliera company in 1889, followed by other *Thury systems*: La Chaux-de-Fonds (1897, 14 kV), between St-Maurice and Lausanne (1899, 22 kV, 3.7 MW), Lyon-Moutiers project (1906, 125 kV, 20 MW, 230 km) (Electrosuisse, 2011; ModernPowerSystems, 2007).

2.2 Comeback of DC systems

With new developments in the area of mercury-arc valves, DC systems started to reemerge and be reconsidered as an alternative for the transmission.

The mercury-arc valve was invented by an American electrical engineer, Peter cooper Hewitt in 1901. With continuous development, mercury-arc valves could be broadly classified into two categories by the mid 1930s: 1) sealed glass envelope for smaller ratings and 2) steel tanks with metal cooling jackets and vacuum pumps for larger ratings. However, technologies back then were proven difficult to withstand HV and achieve low losses at the same time, which made it hard to compete with AC transmission (Tiku, 2014).

In 1939, Dr. August Uno Lamm[7], who in the future was known as *the father of HVDC transmission*, was granted a patent for introducing grading electrodes to mercury-arc valves which increased considerably the voltage withstanding capabilities of the valves (Korytowski, 2017).

In 1941, the first commercial HVDC ($\pm$ 200 kV, 115 km) was contracted to transmit 60 MW of power from Vockerode generating station on the river Elbe to Berlin. The project completed in 1945 but never commissioned due to World War II (Tiku, 2014). As mercury-arc valve technology matured, the first commercial HVDC link (20MW, 100 kV) was finally realized from mainland Sweden to the island of Gotland using submarine cable and started operation in 1954. It marked the modern era of HVDC transmission (Lamm, 1966). Mercury-arc valve based systems were common until

[7]August Uno Lamm (May 22, 1904 – June 1, 1989) was a Swedish electrical engineer and inventor. During his career, Lamm obtained 150 patents.

1975. Since then, HVDC systems use semiconductors (thyristors, then later Insulated Gate Bipolar Transistors (IGBTs)) (Korytowski, 2017; Lescale, 1998).

The first project using thyristor based converters was the Eel River (320 MW) back-to-back (B2B)[8] scheme commissioned in 1972. The main advantages compared to mercury-arc valves were the simpler design, less frequent maintenance and less space needed. Since then, semiconductor based HVDC systems have been steadily developing. Currently, the Shanghaimiao-Shandong ± 800 kV HVDC project under construction will go beyond the world's record up to 6250 A (Zha et al., 2017).

The latest development for HVDC converter technology is the use of IGBT instead of thyristors. The first experimental system (3 MW, ± 10 kV) was tested in Sweden (between Hellsjön and Grängesberg) in 1997. Then in 1999, ABB commissioned the first commercial project rated at 50 MW, ± 80 kV again in Gotland, Sweden (Axelsson et al., 1999).

2.3 Advantages of HVDC systems

Compared to conventional AC transmission, HVDC transmission is a proven technology that outperforms under certain conditions. Mainly they are characterized by the following factors.

- **Investment costs:** A typical PTP link consists of two converter stations and two (or one in case of monopole configuration with ground return) conductors/cables, while a three-phase AC system needs three conductors. This provides DC technology an economically competitive advantage with increasing transmission capacity, when the converter costs can be offset by the lower costs of lines. (Sousa et al., 2012) has provided an economic evaluation on HVDC versus HVAC.

- **Transmission losses:** In AC lines, current density is not equally distributed within a conductor due to "skin effect". The current tends to flow near the conductor surface. The higher the frequency, the shallower the skin depth[9]. DC lines do not have frequency dependency, thus current flows uniformly through

[8] With a back-to-back HVDC configuration, two independent neighboring systems with different and incompatible electrical parameters (Frequency / Voltage Level / Short-Circuit Power Level) are connected via a DC link. Both rectifier (conversion from AC to DC) and inverter (conversion from DC to AC) are located in the same station.

[9] The electric current flows mainly at the "skin" of a conductor. Skin depth is a measure of how closely electric current flows along the surface of the conductor.

the whole conductors. This results in a higher resistance for AC lines compared to DC lines, i.e., higher losses.

- **Long transmission distance:** AC transmission faces a number of challenges when the transmission distance is long. For one example, reactive power compensation is needed in AC transmission system in order to properly energize and operate the link. Otherwise, subsynchronous resonances[10] may occur (Kundur, 1994). On the other hand, DC technology does not encounter limitations on distance.

- **Underground and submarine cables:** Cables have a significantly higher capacitance than OHLs, and hence a much higher charging current. Limitations on transmission distance imposed by charing current of AC cables become significant with the growing need for transmitting bulk power and the trend towards high voltages (Schifreen and Marble, 1956). DC cables exhibit no constraints for cable length and losses can be half of those AC ones. In particular, HVDC system can be a good application allowing efficient integration of offshore wind (Bahrman and Johnson, 2007).

- **Right of way:** As mentioned previously, DC transmission requires less conductors. Therefore tower design of DC lines is more compact than for AC lines and less right-of-way is needed. This is particularly advantageous for population-densed areas. A schematic illustration can be found in (SiemensAG, 2014).

- **Controllability and Flexibility:** One of the fundamental advantages of HVDC technology is the ease of controlling active power in the link independently (by setting the proper operating point), as long as power balance is guaranteed. This allows a more flexibility control and operation of the system and can also improve the performance (e.g., stability) of AC power systems (Wang and Redfern, 2010).

- **Asynchronous interconnections:** DC technology allows to interconnect AC systems that are asynchronous through B2B configuration (e.g., Eel River project commissioned in 1972) or through DC links.

From above, advantages of using HVDC technology to expand transmission grid are potentially large, especially when long distance power transmission is needed. However,

[10]Subsynchronous resonance is a condition where the electric network has natural frequencies below the nominal frequency of the system (Lei et al., 2000).

the uncertainties associated with the balance between costs and benefits are very significant and careful CBA has to be carried out for each project.

From the cost side, in addition to expenses on physical infrastructure, environmental impacts have drawn more attention nowadays. Environmental costs can vary notably depending on the country or region due to specific environmental impact regulation (ENTSO-e, 2015b). Yet benefits on the other hand, are even more complex to assess. To start with, there are different ways or criteria for categorizing benefits. Each one requires an appropriate tool for assessment (L'Abbate et al., 2012). Nevertheless, some of them are difficult to model and consequently have not been taken into account explicitly (ENTSO-e, 2015b), while others are quantitatively difficult to measure with indicators or to be monetized (Wang, 2013b). Moreover, depending on the viewpoints taken by different players, i.e., TSO, generation companies, consumers, each considered benefit can be evaluated based on different methodology.

Therefore, economic viability needs to be carefully examined before any huge investment in transmission network reinforcement take place and as stated in Chapter 1, this thesis aims to assess the performance of a hybrid system from both technical and economic point-of-view. More discussion has been carried out in Chapter 5 and 6.

2.4 Configurations of HVDC Systems

There are several configurations available for HVDC systems which can be classified as 1) monopolar 2) homopolar 3) bipolar and 4) B2B with alternative grounding strategies. This section is dedicated to describe all these configurations and their relative advantages and drawbacks.

2.4.1 Monopolar configuration

The monopolar configuration is the most basic one for HVDC transmission system (CIGRE, 2013a). In this configuration, two converters are connected by a single pole line, and a positive or a negative DC voltage (usually negative due to less corona effects (Sood, 2004)) is used. The grounding or earthing is an important part with significant roles in the operation of the HVDC systems to provide a current return path (CIGRE, 2017; Hamzehbahmani et al., 2015). In some applications, the ground or sea is implemented as a conductive path for the return current. This configuration

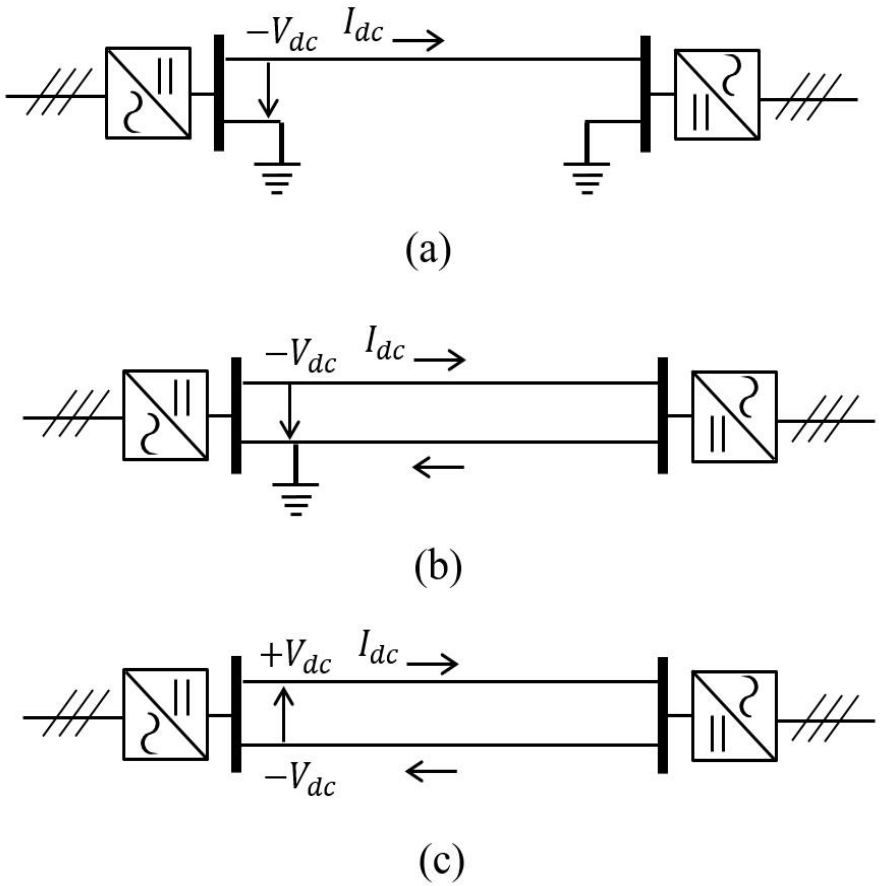

Fig. 2.1 Monopolar HVDC System Configurations: (a) Asymmetric monopole ground return (b) Asymmetric monopole metallic return (c) Symmetric monopole

(Fig. 2.1 (a)) can be referred to as "asymmetric monopole with ground/sea return" which is the simplest and least expensive HVDC system.

Due to large DC current injection into the ground, concerns are raised with respect to metallic corrosion of objects in the vicinity of the grounding electrodes. In the case where a sea electrode is used, DC current can also cause chemical pollution in the water surrounding the electrode (Girdinio et al., 2012). In addition, when the use of ground/sea return is constrained (e.g., heavily congested areas, fresh water cable crossings, or areas with high earth resistivity), a metallic neutral or a low voltage conductor can be used as the current return path. In this case, the conductor needs to be insulated to withstand the voltage drop (along the conductor) and rise (during fault conditions) (CIGRE, 2013a), resulting in higher costs and system losses. This configuration (Fig. 2.1 (b)) is known as “asymmetric monopole with metallic return” (Hamzehbahmani et al., 2015).

Another comparable scheme (Fig. 2.1 (c)) is the "symmetric monopole". In this case, two DC cables with full insulation are needed. The grounding can be provided through various methods. For instance, by connecting to the DC capacitors’ mid-point (CIGRE, 2013a).

For all monopolar configurations, there is one main drawback: the failure of a converter or a cable leads to the complete lost of the entire system.

2.4.2 Homopolar configuration

In the homopolar configuration (Fig. 2.2), two conductors are operated in the same polarity with either ground or a metallic return. Usually a negative polarity is used due to smaller corona losses and reduced radio interferences (Arrillaga et al., 2007). The insulation costs are reduced due to parallel operation of the two poles. However, this configuration is usually not feasible due to environmental concerns raised by large earthing current (Sood, 2004).

2.4.3 Bipolar configuration

A bipolar configuration consists of four converters and two conductors. Unlike homopolar links, it operates with two polarities, carrying currents in opposite directions. A schematic diagram is shown in Fig. 2.3. Bipolar schemes are usually considered for higher transmission capacity than monopolar links due to its heavy investment costs. However, system reliability can be improved due to the double usage of converters at

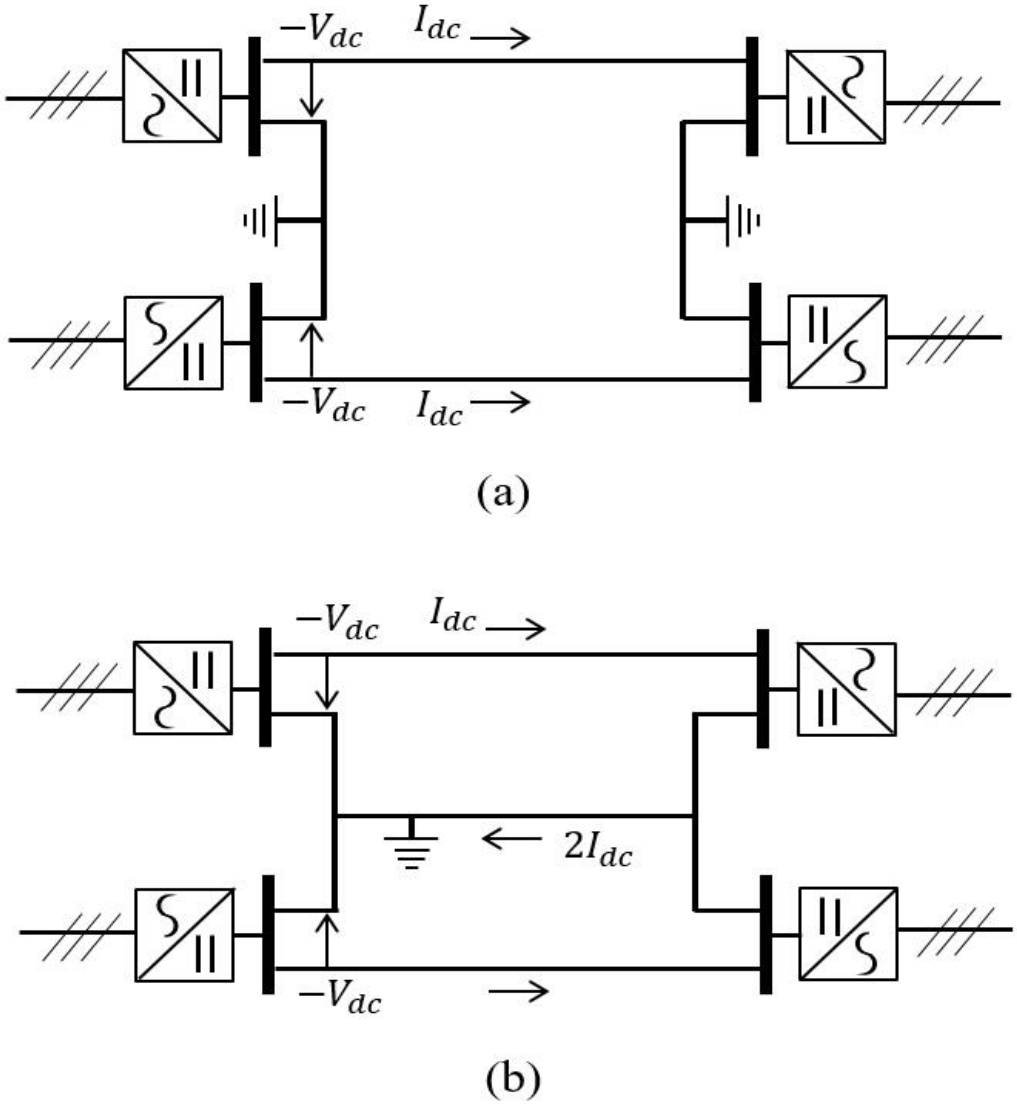

Fig. 2.2 Homopolar HVDC System Configurations: (a) Ground return (b) Metallic return

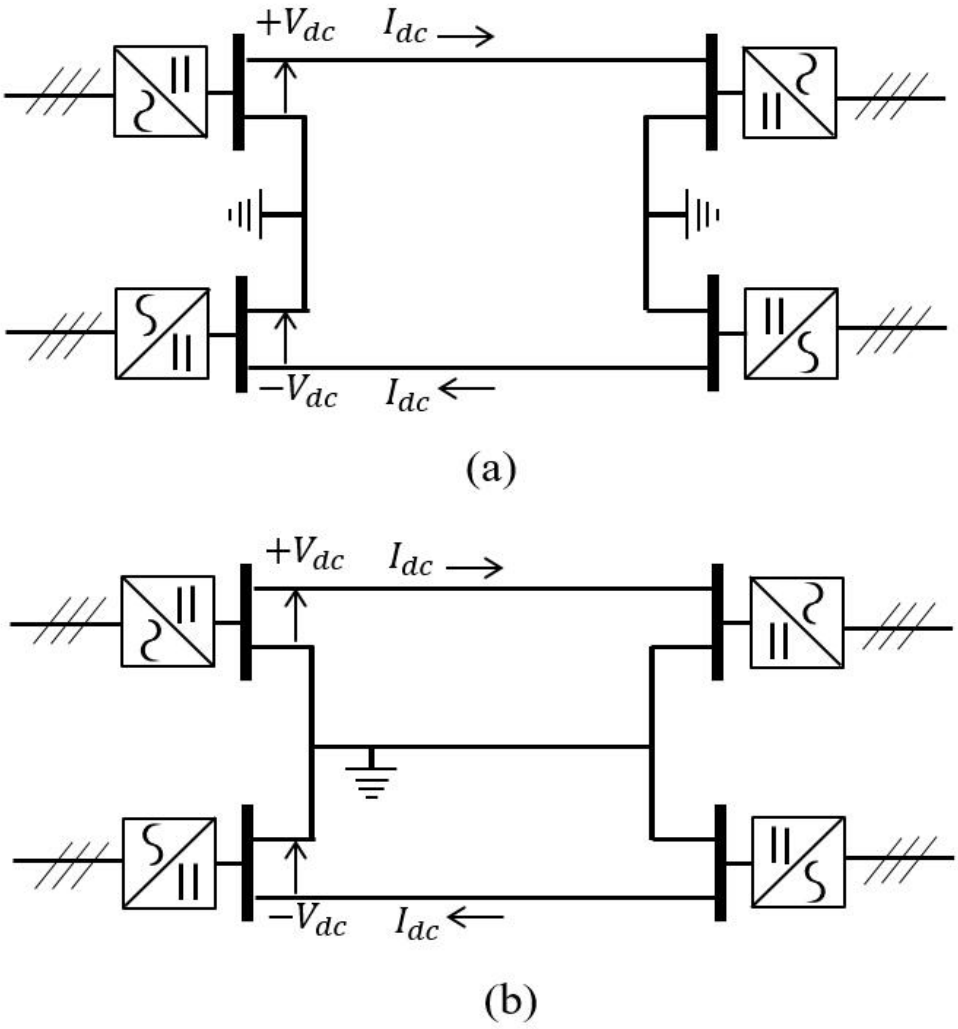

Fig. 2.3 Bipolar HVDC System Configurations: (a) Ground return (b) Metallic return

each HVDC terminal (CIGRE, 2013a; Dorf, 2000). Under normal operation and a balanced load, the current rating in both poles are identical and there is no ground current. The earthing current can either flow through ground if there are no environmental restrictions (Fig. 2.3 (a)) or through a metallic return cable (Fig. 2.3 (b)) (Hamzehbahmani et al., 2015).

In the case of unbalanced load, the grounding may carry a significant current. Unlike monopolar configuration, with bipolar configuration if any converter or conductor fails, power transmission can continue in the other pole.

2.4.4 Back-to-Back (B2B) configuration

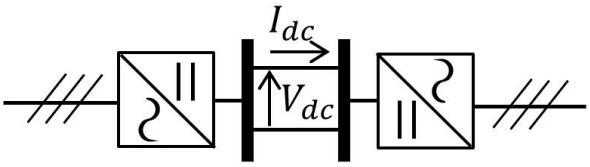

Fig. 2.4 Back-to-Back HVDC System Configuration

With a back-to-back configuration, two asynchronous AC systems, which may have the same or different frequencies, can be interconnected. Two converter stations are located at the same site and long transmission line or cable is not needed (Flourentzou et al., 2009). A schematic illustration is shown in Fig. 2.4.

2.5 Converter Technologies

Converters are one of the main components constituting HVDC transmission systems, being responsible for the conversion between AC and DC voltage. Power conversion has been historically an overwhelming challenge as seen in Section 2.2. The original technologies based on mercury -arc valves are subject to arc-back problems which can damage the valves. Thanks to the semiconductor technologies development, this problem has been overcome and it has enabled the progress of DC transmission (Korytowski, 2017). There are currently two dominant technologies used in HVDC transmission system: conventional line-commutated CSCs, and self-commutated VSCs.

2.5.1 Line-Commutated Current Source Converter (CSC)

HVDC system based on line-commutated CSCs can be either referred to as Line-Commutated Converter (LCC) HVDC or alternatively CSC HVDC. The power reversal of an CSC based HVDC system requires to change the DC voltage polarity and this limits the flexibility of the DC system.

CSCs are based on thyristor valves. Voltage rating can be raised by connecting thyristor in series as a "stack" while current rating can be raised by connecting those stacks in parallel (Cole, 2010). Latest development (the third generation) of thyristor shows a blocking capability ranging from 7.2 to 8.5 kV and rating currents from 5.5 to 6.25 kA as required for the state-of-the-art ultra HVDC (Vobecky et al., 2017). Nowadays, the largest CSC HVDC in operation has a rating of ± 800 kV and 6.4 GW (Åström et al., 2010), and even a higher rating, i.e., ± 1100 kV and 10 GW, is planned (Liu et al., 2012).

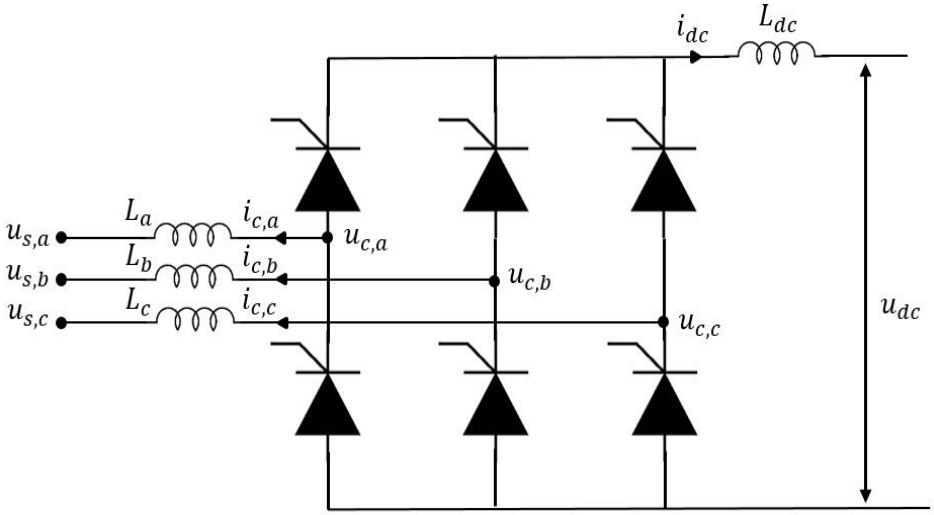

Fig. 2.5 CSC HVDC Graetz Bridge

The basic building block of a CSC is the three-phase full-wave bridge circuit referred to as a Graetz bridge (Fig. 2.5). In normal state, the thyristors block the current (i.e., off state), and can be switched on when a current is flowing into the gate terminal. The thyristor will not turn off autonomously even after the gate current is removed. To stop conducting, current needs to flow in the opposite direction through it (Rimez, 2014).

Although CSC HVDC have been deployed largely for the past decades (Oni et al., 2016), CSC has several drawbacks (Beerten, 2013; Rimez, 2014; Zhang, 2010):

CSCs rely on a strong AC network which can be expressed in terms of the Short Circuit Ratio (SCR)[11] at the Point of Common Coupling (PCC). Typically, an AC network with short-circuit power at least 2.5 times of the HVDC rating is required for satisfactory operation (Andersen, 2006). This type of converter also introduces a significant amount of harmonics on both AC and DC sides which causes distortion of voltage waveforms. Therefore filters are needed to minimize the effects. Moreover, the converters consume reactive power, which could amount to 50% - 60% of the converter rating. Thus, compensation is necessary, e.g., capacitor banks, Static Var Compensator (SVC), a nearby generator or a synchronous condenser. Subsequently, the converter station can occupy large space. In addition, commutation failures may occur to the inverter station that are typically caused by disturbance in the AC system. It is common and occur for any AC fault that causes a sudden phase shift or a voltage drop of more than about 0.15 p.u. at an inverter terminal (Adapa, 2012). HVDC line tripping can be resulted from a number of repeated commutation failures.

2.5.2 Forced-Commutated Voltage Source Converter (VSC)

The development of IGBT in the 1990s opened up new possibilities for HVDC technology. VSC is another type of converter technology utilizing IGBTs as core components. Unlike thyristor, IGBTs are fully-controllable switches that can be switched on and off. Currently, IGBTs have a maximum voltage rating of 6.5 kV and current rating up to 3.6 kA (Trzynadlowski, 2015).

Since IGBTs are self-commutated, no external grid is needed for commutation. Besides, it offers a number of other advantages as opposed to CSCs, such as: independent control of both active and reactive power rapidly, so there is no need for reactive power compensation; no commutation failure induced by disturbance from AC network; possible connection to a "weak" AC network or even a passive one where no generation source is available, i.e., low SCR; power reversal is done through current reversal instead of polarity reversal as for CSCs; absence of lower order harmonics and hence small filter size (Flourentzou et al., 2009).

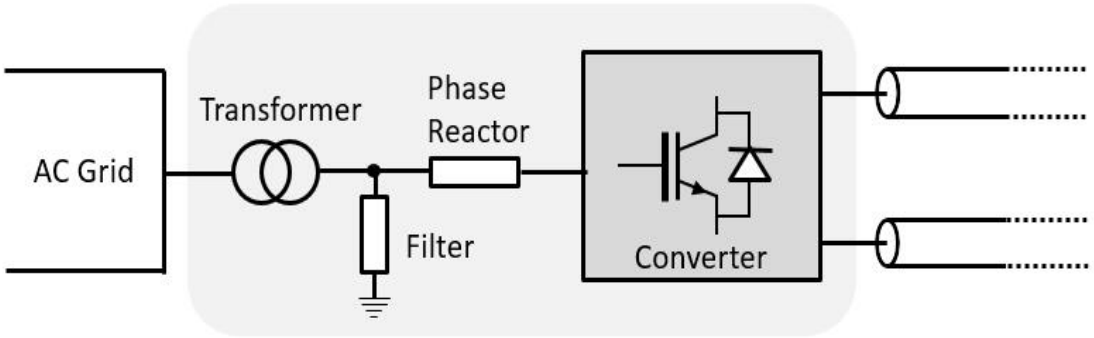

Fig. 2.6 VSC HVDC scheme

Voltage Source Converter Technology

A typical VSC HVDC converter station configuration is shown in Fig. 2.6. It consists of the following parts:

- **Converter transformer:** is an essential component to match the AC grid voltage with the operating voltage of the converter. Compared to CSC, absence of low order voltage harmonics allows a simpler design, similar to standard transformers.
- **Filter/Phase reactor:** Since only high order harmonics exists in VSCs due to high switching frequency, it can be easily substituted by a low-pass filter which is formed by the filter together with the phase reactor.
- **Converter:** is the most important element of the HVDC system that convert DC voltage to an AC voltage of an arbitrary size and shape by switching the IGBTs.The switching of IGBTs are controlled by the control scheme as to control the complex current, thereby the active and reactive power are controlled independently.

The topology of VSC based on IGBTs can be roughly categorized into three types, following a chronological order of development: two-level converter, three-level converter and Modular Multilevel Converter (MMC).

The first generation of VSCs was based on a two-level converter topology, which were firstly developed by ABB and commercially known as "HVDC Light". Fig. 2.7

[11]SCR is defined as the ratio of system short circuit level MVA to the DC power MW, which has been used to indicate system strength (Gavrilovic, 1991).

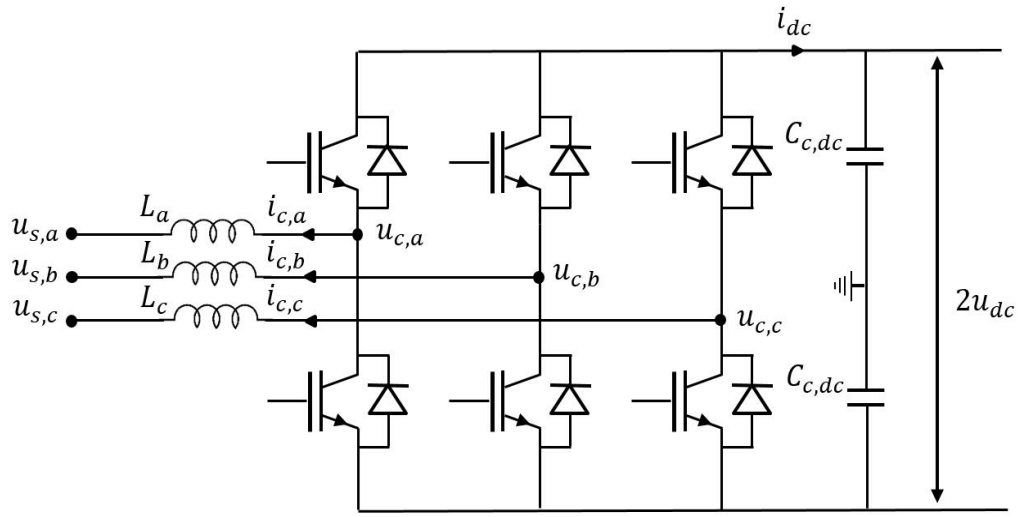

Fig. 2.7 Two-level Voltage Source Converter

provides a simplified schematic illustration. Each valve is represented by only one switching element. The well known Pulse Width Modulation (PWM) technique is used to synthesize voltage waveform. Although conduction losses are low for IGBTs, losses resulted from switching elements are high. A two-level converter can yield losses up to 3% of the total power going through the converter. The comparable losses for a CSC is 0.8% (CIGRE, 2005).

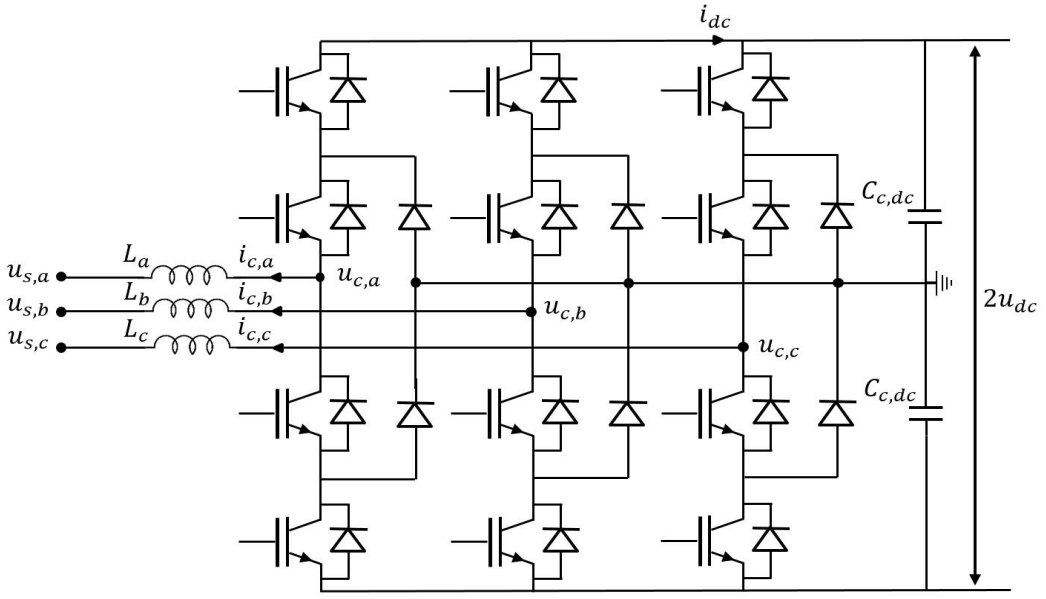

Fig. 2.8 Three-level Neutral-Point Clamped Voltage Source Converter

The second generation of VSCs used a three-level topology with Neutral-Point Clamped (NPC), as depicted in Fig. 2.8. In each phase, two diodes are added clamping the switch voltage to half of the DC voltage. Thereby, it provides a third voltage level to switch between leading to lower switch losses. Consequently, converter losses can be reduced to approximately 1.8% (CIGRE, 2005).

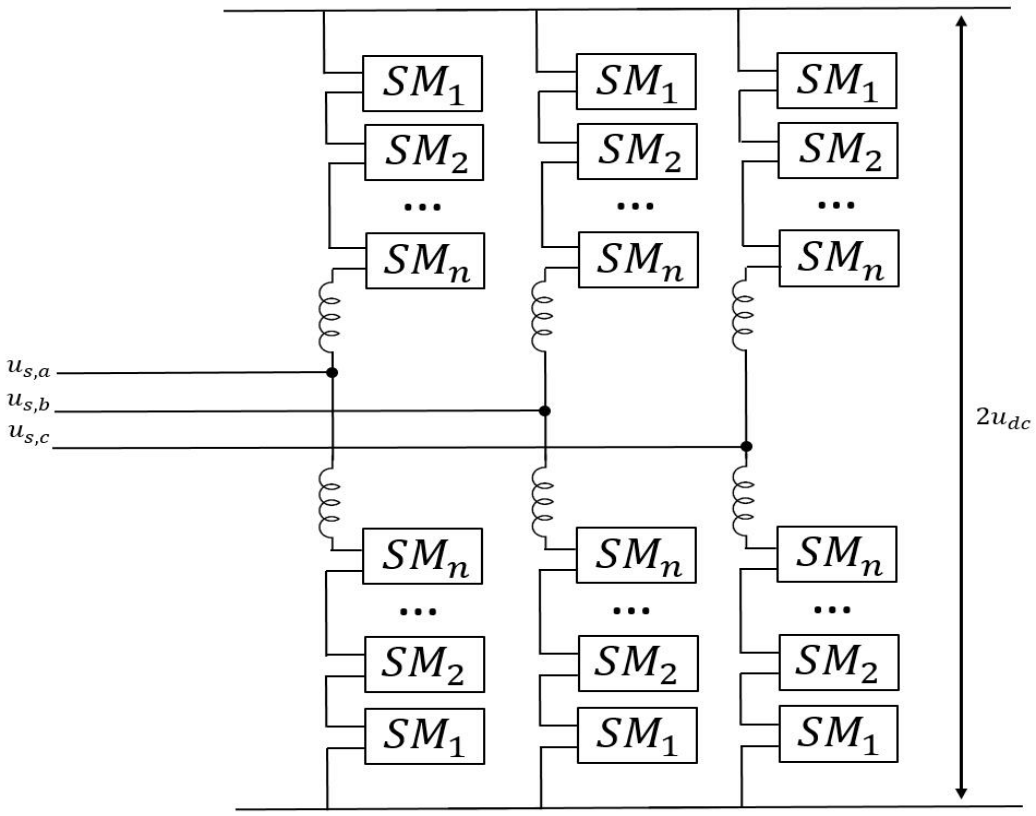

Fig. 2.9 Modular Multilevel Voltage Source Converter

The latest development of converter topology introduces the so-called MMC, as depicted in Fig. 2.9. Instead of switching elements, each valve consists of a large number of controlled SubModules (SM). In MMC, each SM is responsible for a distinct voltage step, typically in the order of magnitude of a single IGBT voltage. There are a few hundred SMs per arm resulting a low switching frequency. Consequently, the converter losses drop to roughly 1% (Jovcic and Ahmed, 2015).

Within each SM, there are two schemes available: 1) half-bridge (HB) module (Fig. 2.10 (a)) consisting of two IGBTs and one capacitor and 2) full-bridge (FB) module (Fig. 2.10 (b)) that doubles the number of switching devices compared to HB module. Yet, FB MMC offer the capability to block DC faults. Compared to the other two

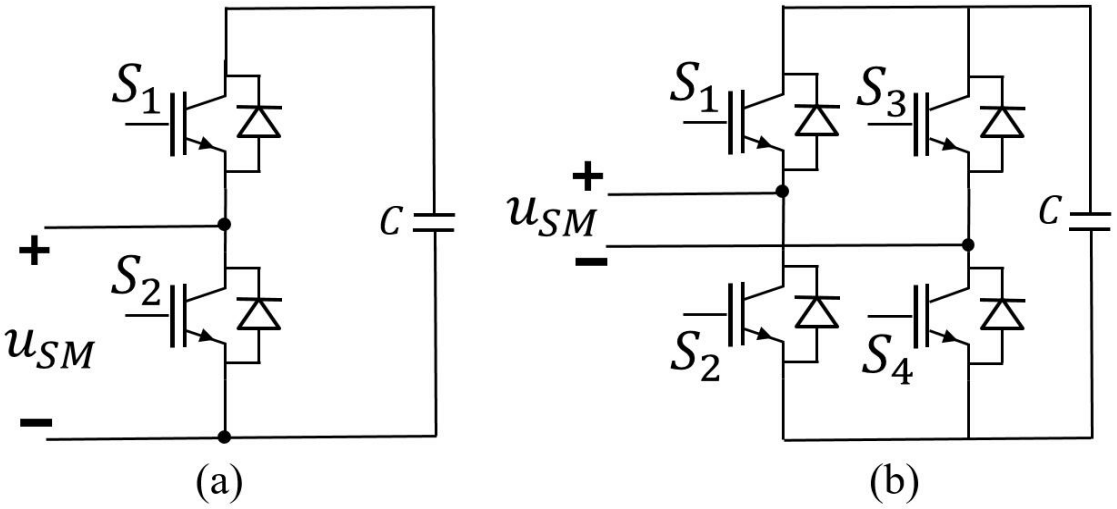

Fig. 2.10 MMC Building Blocks: (a) half-bridge and (b) full-bridge

topologies, the downside of MMC is that it requires twice the number of switches (or fourfold in the case of FB MMC). In addition, the design and control strategy are more complex (Abildgaard and Molinas, 2012).

2.5.3 CSCs versus VSCs

Having discussed in Section 2.5.1 and 2.5.2, the main difference between CSC and VSC is that, CSC keeps a constant current in the DC line with a small ripple, while VSC functions exactly the opposite way: it keeps a constant voltage source on the DC side. Table 2.1 summarizes some key characteristics of CSC and VSC technology (Oni et al., 2016). Mode technical details and comparison can be seen in Chapter 2 of (Sood, 2004).

Although CSC is an interesting option for bulk power transmission, it is not considered a preferred option for offshore application for several reasons. Firstly, cost of offshore platform highly depends on the size. As CSC takes up more space than VSC which would result in more costs. In addition, CSC relies on a strong AC grid for commutation and is not capable of black start. In case of a blackout, unlike CSC, VSC can restore the grid without external power supply given its capacitors are charged and can function as a voltage source (Flourentzou et al., 2009). Finally, VSC is suitable for MTDC system as it is more immune to AC disturbances, has independent multidirectional flow and operates with a common voltage polarity.

Feature	CSC	VSC
Semiconductor type	Thyristor	IGBT
Switching control	Turn on	Turn on and off
AC grid	Strong grid	Weak grid, Black start capability
Converter station losses	Low (~0.8%)	High (~1% - 3%)
Cost	Lower	Higher
Harmonics	Large filter	Small filter
Occupation area	Large site	Compact site
Power reversal by	Voltage polarity	Current direction
AC disturbances impact	Commutation failures	No influence
Maturity	High	Low
Suitability for MTDC	Problematic	Good
Energy store	Inductive	Capacitive
Independent P & Q Control	No	Yes

Table 2.1 Comparison of CSC and VSC

2.6 VSC based MTDC System

Although HVDC systems have been in operation for more than 50 years, majority of the projects are either PTP or B2B schemes. Despite great interest raised in industry, technical challenges imposed by CSC technology, such as polarity reversal and commutation failure, do not make it a suitable option to extend the HVDC grid to a MT configuration (Van Hertem and Ghandhari, 2010).

There are currently only two MTDC based on CSC nowadays in operation (Adapa, 2012). The first one was originally built with only two terminal between the Italian mainland and the island of Sardinia in 1965 at ± 200 kV and 200MW. The capacity was increased to 300 MW in 1992. A third terminal was added in 1988 in Corsica providing up to 50 MW, making it a MTDC scheme (Chaudhuri et al., 2014). The other one is the Quebec - New England link between Canada and the United States (US). It was a five-terminal design. However, the original two-terminal link between Des Cantons in Quebec and Comerford in New Hampshire was never integrated into the other three-terminal (Radisson, Nicolet, Sandy Pond) link due to anticipated performance problems (Arrillaga et al., 2007). So the link is now operating as a three-terminal system. Fig. 2.11 gives a schematic illustration of how a PTP HVDC system and a MTDC system could look like.

Compared to CSCs, VSC allows a relatively simple extension plan to a meshed grid since VSCs are not subject to voltage polarity reversal, thus avoiding complex

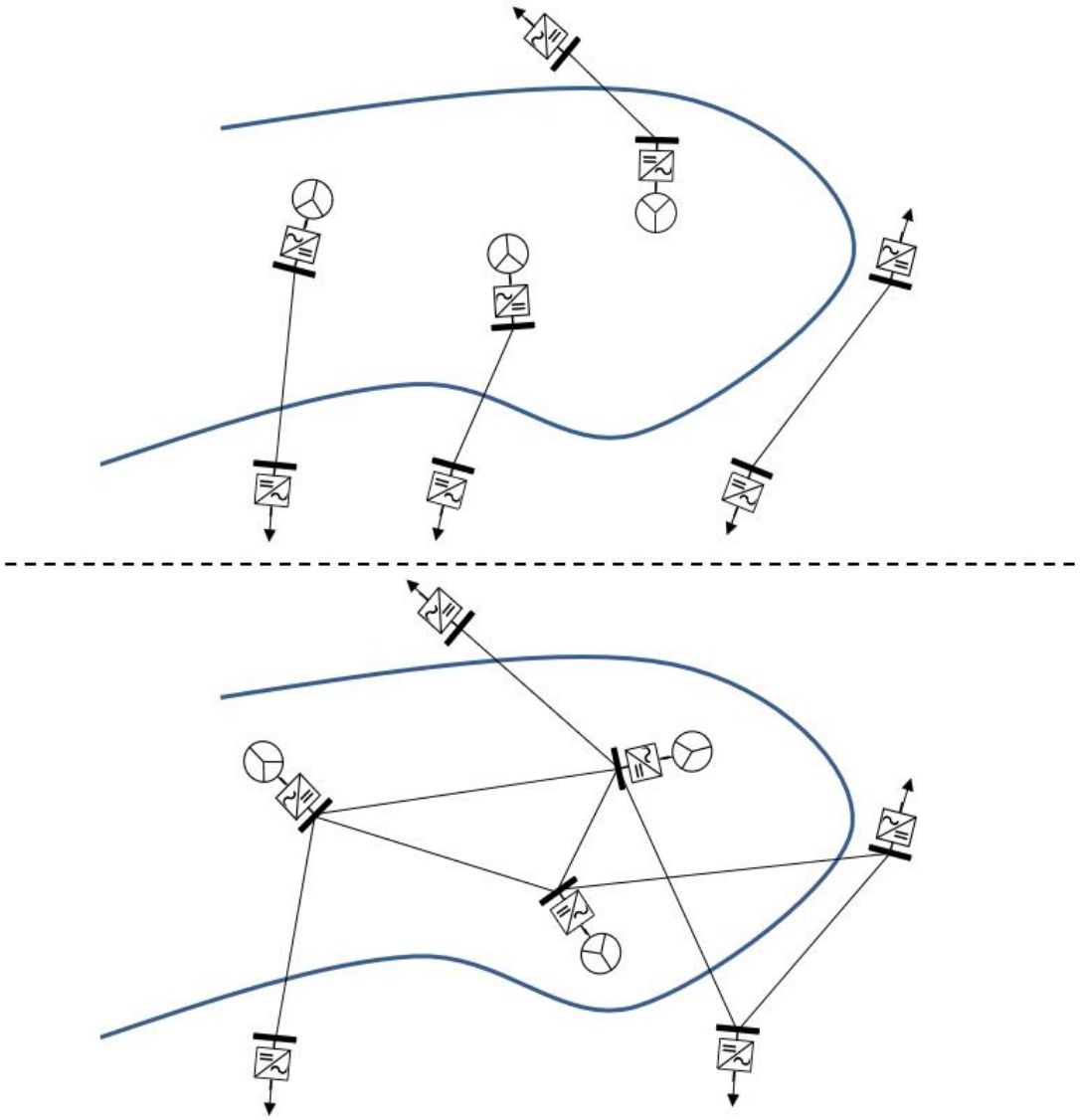

Fig. 2.11 Schematic illustration of PTP HVDC (up) and MTDC (down) systems

mechanical switchgear. In addition, it functions as an ideal current source on the DC side allowing the parallel connection of several DC terminals without technical difficulties. Moreover, VSC offers significant advantages regarding offshore transmission (Barnes and Beddard, 2012).

The great potential offered by VSC MTDC has led to the proposition of the concept *supergrid* (Gordon, 2006). The world's first VSC MTDC is the Nan'ao project located in China which was commissioned at the end of year 2013. It consists of three terminals (± 160 kV) aiming at absorbing wind generation from Island of Nan'ao to the bulk power system of mainland. More information can be found in (Fu et al., 2014; Li et al., 2014; Rao, 2015).

2.7 Transmission Expansion Planning considering VSC-MTDC

Transmission planning is a complex process and also one of the most critical issues that needs to be constantly addressed for meeting the demand while maintaining system stability and reliability among power system studies. It has become even more challenging due to the broad spectrum of technological solutions (such as HVDC transmission) and the growing integration of RES (Migliavacca et al., 2011).

Before liberalization of the market, in a vertically integrated and managed power system, the transmission investment decisions were made by a single agent in coordination with generation expansion decisions, based on cost- (both generation and transmission costs) minimizing principle (Cagigas and Madrigal, 2003). Nowadays, in a competitive environment, generation, transmission and distribution activities are unbundled. TSOs are only responsible for transmission assets. In this framework, to provide nondiscriminatory access to all the market players and to facilitate fair competition, it is crucial that previous Transmission Expansion Planning (TEP) criteria need to be revised and extended. More robust planning methodologies are necessary to address the above uncertainties and challenges. In addition, environmental impacts must also be adequately considered in the planning process (L'Abbate et al., 2012).

TEP issues are reviewed in (Hesamzadeh et al., 2008) and (Hemmati et al., 2013), methodological approaches and models are revealed in (L'Abbate et al., 2012) and (Latorre et al., 2003). Among all these studies, only few of them have considered HVDC systems. (Wang et al., 2008) has categorized the societal economic benefits into three

parts: consumer, producer and transmission surplus, and quantified them based on a market simulation program, GridView. On the other hand, (Sousa et al., 2012) assesses the economic limit based on cost minimization criteria through comparisons of costs on physical components and losses. However, only PTP interconnections are considered in these papers. (Kong and Jia, 2011) takes offshore wind farms of different structure and wind turbines of different topology into account, combining with either VSC HVDC or HVAC systems, a techno-economic analysis was implemented through a Discounted Cash Flow (DCF) approach incorporating investment costs, discounted annual costs and revenues, to obtain cost-effectiveness. (Feng et al., 2014) proposes a model to obtain the optimal operation of a hybrid network. The model is developed in GAMS and uses the IPOPT solver for obtaining the solution. However, this model includes all nonlinearities in the formulation which makes it impossible to tackle a system of large-scale and cannot guarantee a global optimum. Hybrid transmission expansion models are proposed recently in (Escobar et al., 2016) and (Dominguez et al., 2016) to minimize costs taking into consideration of two-terminal HVDC links. However, (Escobar et al., 2016) uses a DC equivalent model for network representation neglecting completely system losses which could lead to underinvestment (Alguacil et al., 2003). (Dominguez et al., 2016) includes transmission losses , yet converter losses are overlooked. Without proper converter losses modeling, the solution of the OPF can vary significantly.

Taking into account all these issues, in order to be able to assess the profitability of HVDC systems, it is necessary to develop a new model that is able to deal with large-scale hybrid networks considering all system losses as well as a detailed technical representation of the generation and the transmission system (both AC and DC). In this PhD thesis, such a model is proposed. The mathematical formulation is shown in Chapter 3.

Chapter 3

Optimal Power Flow for AC/DC Hybrid Networks

This chapter first introduces the basic principles of OPF. Then a nonlinear OPF formulation incorporating MTDC systems for steady-state analysis is described. This nonlinear version of is then reformulated as a linear model to be able to deal with large-scale systems in order to serve both operation and planning purposes. Both formulations include transmission and converter losses, taking into account that converter losses can be different when the converter acts as an inverter or as a rectifier. The models are implemented in GAMS and verified with the Leuven 5-bus system (Beerten et al., 2010). Finally, this chapter dedicates to further compare the two models (NLP-OPF vs. LP-OPF) described and presents more results. A smaller 14-bus system and a larger 50-bus system are used to perform case studies.

3.1 Introduction to Optimal Power Flow (OPF)

The OPF problem has a long history of development since Carpentier firstly discussed it in 1962 (Wood and Wollenberg, 2012). It is is a nonlinear and non-convex optimization problem which may contain both continuous and discrete control variables. The difficulty of solving such problems increases significantly with system size and complexity[1]. Extensive research has been conducted for the past decades. (Huneault

[1]The fast development of power electronics based on new and powerful semiconductor devices has led to innovative developments of such as HVDC and flexible AC transmission system (FACTS). In addition to introducing new power electronics in the grid, overall network may become heavily meshed with more and more transmission infrastructures.

and Galiana, 1991) reviews the first developments. Recent literature surveys are given in (Frank et al., 2012a,b).

Nowadays, OPF is a commonly used tool for both power system operation and planning purpose. The objective is to determine the optimal setting of a given power system network that optimize the objective functions (e.g., operating costs, system losses, load shedding, total emissions, etc.) while respecting a set of constraints (e.g., power flow equations, generator operating limits, etc.).

A general OPF formulation can be expressed in the following form:

$$min \quad f(u,x) \tag{3.1}$$

subject to

$$g(u,x) = 0 \tag{3.2}$$

$$h(u,x) \leq 0 \tag{3.3}$$

where x and u represent state and decision (or control) variables respectively. $f(u,x)$ represents the objective function. Vector functions $g(u,x)$ and $h(u,x)$ characterize system equality and inequality constraints correspondingly. Depending on the f, g and h functions, the OPF problem may be formulated as a linear, non-linear, mixed integer linear or mixed integer non-linear problem.

3.2 Modeling of VSC

The VSC station comprises all the elements that connect the AC and the DC networks. Each VSC will be referred to with the index v. As discussed previously, voltage waveform at the converter is synthesized either by PWM techniques or by a MMC approach. In the steady states analysis, VSC modeling does not distinguish between the different types of modulation and the different number of switching levels (two-level, three-level or multilevel) (CIGRE, 2014; Haileselassie, 2012). Therefore, a typical approach for VSC modeling can be depicted as in Fig. 3.1.

The filter bus is connected to the AC network through a transformer and the power can flow in both directions. When the active power is taken from the AC side and injected at the DC side, the converter is said to be operated as a rectifier. Otherwise, the converter is operated as an inverter. The converter can also inject or absorb reactive

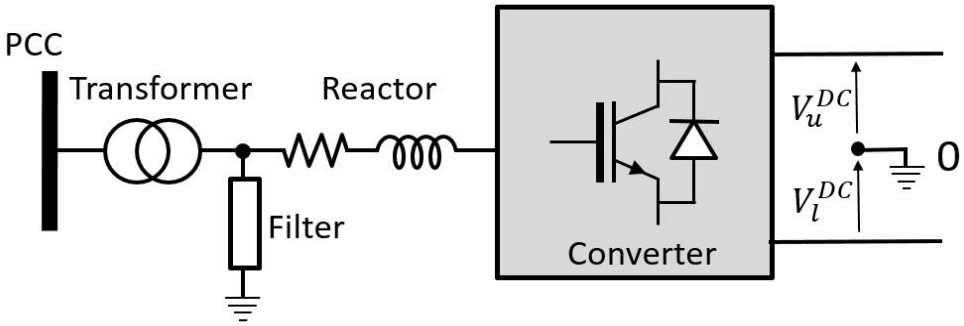

Fig. 3.1 Three phase scheme and single-phase diagram of the VSC

power from the AC side. The variables that represent the active and reactive power injected to the AC side of the converter v are defined as p_v^{ac} and q_v^{ac}. These variables can be either positive or negative depending on the operation mode of the converter. The same applies to the power injected to the DC side of the converter, i.e. p_v^{dc} .

3.2.1 Equivalent circuit of VSC

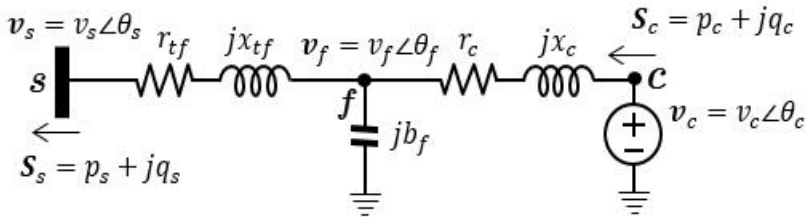

Fig. 3.2 Equivalent circuit of the VSC

It shall be clarified that all variables presented in this section are in [p.u.], and units of corresponding parameters are adapted accordingly.

Fig. 3.2 shows the equivalent circuit of the VSC. As described in (Beerten et al., 2012; Feng et al., 2014), VSC converter is generally modeled as a controllable voltage source $\underline{v}_c = v_c\angle\theta_c$ connected by a phase reactor $\underline{z}_c = r_c + jx_c$ to an intermediate node where a lossless shunt filter is connected ($\underline{z}_f = -j/b_f$). The voltage at this intermediate node is $v_f\angle\theta_f$. The transformer can be represented by its impedance: $\underline{z}_{tf} = r_{tf} + jx_{tf}$.

It is important to notice that for each VSC converter station, two more AC buses are added to the system: the filter bus (voltage $v_f\angle\theta_f$), and the converter bus (voltage $v_c\angle\theta_c$). In case of not being necessary to install the filter (or when its effect can be

neglected), both the phase reactor and the transformer impedance can be lumped together, eliminating from the equations the corresponding voltage magnitude and phase angle of the filter bus. As a consequence, the power flow within the VSC converter station between the nodes c, f, and s have to comply with the standard AC power flow equations. In that case, the shunt susceptance only affects the diagonal terms of the matrix $\mathbf{B}$ at the position of the filter buses. Depending on the level of accuracy (transformer- or filter-less), converter power injection to the AC network $p_v^{ac} + jq_v^{ac}$ can be treated equivalent as $\boldsymbol{s_c} = p_c + jq_c$ or $\boldsymbol{s_s} = p_s + jq_s$.

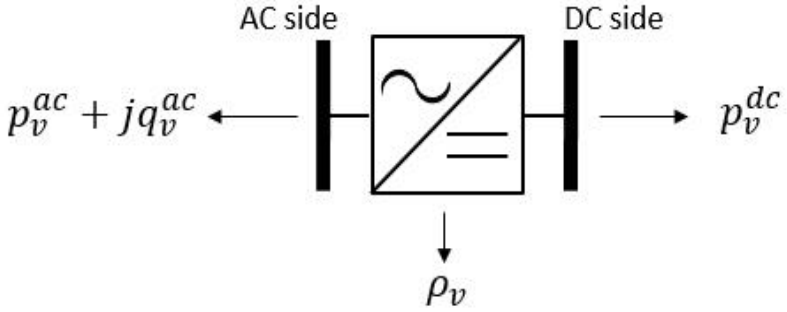

Fig. 3.3 Power balance at the VSC station

Regarding the power balance at the converter, Fig. 3.3 shows the criterion adopted in this thesis where the arrows indicate when the injected power is considered positive. The corresponding active power balance equation is established in (3.4), where power losses at the converter can take only positive values, i.e., $\rho_v \geq 0$.

$$0 = p_v^{dc} + p_v^{ac} + \rho_v, \forall\, v \in \mathcal{V} \tag{3.4}$$

3.2.2 Converter losses

During the conversion process, the available real power at one side of the converter will be lower than the active power injected at the other side due to the converter losses, ρ_v.

There are several sources of losses within an MMC, such as semiconductor losses in each of the SMs, arm reactor losses, phase reactor losses or transformer losses. Focusing on the semiconductor losses, two different types can also be distinguished, the switching and the conduction losses (Rohner et al., 2010). Several publications show different methods addressing the losses calculations of and MMC (Gnanarathna et al., 2011; Oates and Davidson, 2011; Rohner et al., 2010; Zhang et al., 2014). Similarly,

several components contribute to the losses of PWM based converters which can be potentially complex as well (CIGRE, 2005). However, such detailed procedures cannot be included directly in an optimization model. For this reason, a polynomial expression is adopted, as it is conventionally used in the PF state-of-the-art models.

The state-of-the-art modeling of converter losses for steady-state PF analysis is the one presented in (Beerten et al., 2012), and later on included in the CIGRE report (CIGRE, 2014). In that work, the authors differentiate between the operation of the converter as a rectifier or as an inverter, and therefore, the coefficients of the polynomials used to model the losses can be different depending on the direction of the active power transferred. In a PF model, the converter operation mode (inverter or rectifier) must be known in advance. By contrast, under the optimization context, the operation mode is a decision variable, and the optimization problem determines the optimal operation of every converter taking into account the very same representation of the losses as the one presented in (Beerten et al., 2012). Thus, in the proposed OPF model fully presented in Section 3.3, converter losses are expressed as a quadratic function that depends on both the value and the direction of the phase current of the converter. This has not been taken into account in the previous OPF studies of hybrid networks such as (Cao et al., 2013; Feng et al., 2014).

Following the same criteria as above for the active power, the phase current i_v will take positive values when the converter injects it at the AC bus (inverter), or as negative in the opposite case (rectifier). Therefore, the mathematical expression of the losses is shown in (3.5):

$$\rho_v = A_v + B_v \cdot |i_v| + C_v^{inv} \cdot \left(i_v^{inv}\right)^2 + C_v^{rec} \cdot (i_v^{rec})^2 \tag{3.5}$$

where $i_v = i_v^{inv} - i_v^{rec}$ and i_v^{inv}, $i_v^{rec} \geq 0$; A_v, B_v and C_v^{rec}, C_v^{inv} are corresponding converter loss coefficients. Adding as an extra condition that either i_v^{inv} or i_v^{rec} can be different to zero, only one of the quadratic terms $C_v^{inv} \cdot (i_v^{inv})^2$ or $C_v^{rec} \cdot (i_v^{rec})^2$ will be activated. In addition, the absolute value used in the linear term could be computed as $|i_v| = i_v^{inv} + i_v^{rec}$.

3.2.3 VSC operation limits

Under the optimization context, there are mainly three factors limiting the operation of VSC based HVDC systems (Cao et al., 2013; Cole, 2010), which are described next.

Maximum current through the IGBTs

This limit is meant to safeguard the switching elements of the VSC as the arms of the converter support the whole phase current i_v during some parts of the cycle. As the maximum current that the IGBTs can support is limited, one way to ensure that they are not overloaded is by imposing the following limits:

$$-\overline{I}_v \leq i_v \leq \overline{I}_v, \forall\, v \in \mathcal{V} \tag{3.6}$$

DC and AC voltage level coupling

Apart from the voltage limits imposed at both sides of the converter, it is necessary to take into account that the voltage level on the DC side exerts a limit on the maximum voltage that can be obtained at the AC side of the converter (Cole, 2010). This can be simplified as a ratio between the AC and DC side voltages that can be defined as (3.7).

$$v_c \leq k_v \cdot v_i \qquad \forall\, v \in \mathcal{V}, c \in \mathcal{N}_v^{ac}, i \in \mathcal{N}_v^{dc} \tag{3.7}$$

In this thesis, the factor k_v is set to be 1.1 for all case studies (Feng et al., 2014). Converters are assumed to be operated in nominal conditions. However, if other modulation mode or methods are used to obtain higher voltages for VSC AC buses, this factor could be modified accordingly (Feng et al., 2014).

Maximum current through the DC cables

The maximum current through a DC cable is limited due to its technical characteristics. Given that DC voltage does not have much variation with respect to the nominal value, the limit imposed on current thereby can be treated as equivalent to setting the maximum DC power transfer allowed as in (3.23) (Zhao et al., 2017).

PQ capability curves

Capability curves that relate the active and reactive power limits are conventionally used for PF applications. Following the proposed OPF approach, there is no requirement to include the explicit capability curve limitations, as they are implicitly present in the equations included to represent the electrical network.

In addition to the above three constraints to ensure the safe operation of the converters

in steady-state, previous imposed limits have further derived boundaries on active and reactive power injected to the AC network (Beerten et al., 2012; Feng et al., 2014). The reactive power q_v injected to the AC side will be considered positive in case of being capacitive:

$$p_v^2 + q_v^2 = (v_c \cdot i_v)^2 \qquad \forall\, c \in \mathcal{N}_v^{ac}, v \in \mathcal{V} \tag{3.8}$$

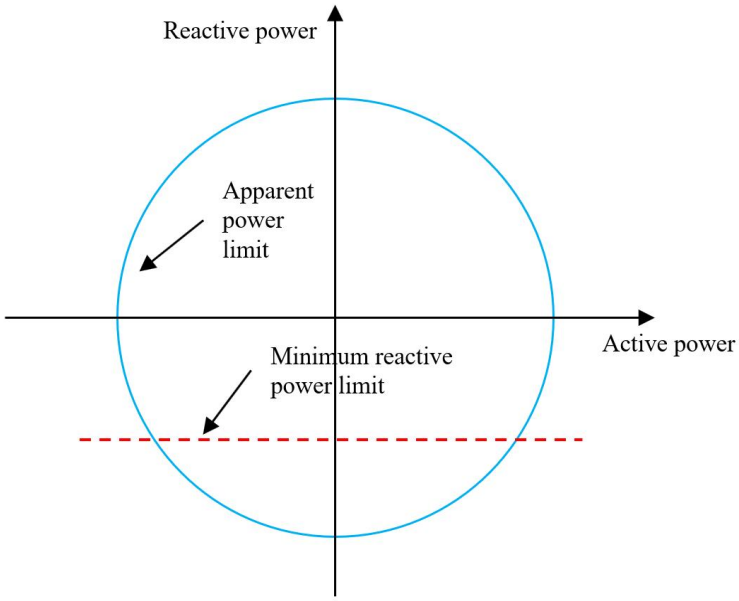

Fig. 3.4 P-Q diagram of VSC station

Moreover, as explained in (Vormedal, 2010), presumably a steady-state minimum DC voltage can exist and prohibit continuous operation while absorbing reactive power (Fig. 3.4), thus a minimum of -0.5 p.u. is imposed to the converters as in (Feng et al., 2014), where $\overline{Q}_v$ is the maximum allowed reactive power. This is also illustrated with a P-Q diagram provided for HVDC Light of ABB (Vormedal, 2010):

$$q_v \geq \underline{q_v} = -\frac{\overline{Q}_v}{2} \qquad \forall\, v \in \mathcal{V} \tag{3.9}$$

3.3 Mathematical Formulation of the Nonlinear OPF

In this section, the detailed mathematical formulation is presented for the proposed nonlinear programming (NLP) OPF model. It shall be clarified that all variables presented in this section are in [p.u.], and units of corresponding parameters are adapted accordingly.

3.3.1 AC Network Constraints

AC Power Flow Equations

Every bus i of the AC grid is characterized by its voltage magnitude v_i and phase angle θ_i. By denoting $\theta_{ij} = \theta_i - \theta_j$, power injections at node i and power flows (from i to j) on branch l, i.e., $(i,j) \in \mathcal{N}_l$, are (Wood and Wollenberg, 2012):

$$p_i = v_i \sum_{j \in \mathcal{B}^{ac}} v_j \left[G_{ij}^{ac} \cos(\theta_{ij}) + B_{ij} \sin(\theta_{ij}) \right], \forall\, i \in \mathcal{B}^{ac} \tag{3.10}$$

$$q_i = v_i \sum_{j \in \mathcal{B}^{ac}} v_j \left[G_{ij}^{ac} \sin(\theta_{ij}) - B_{ij} \cos(\theta_{ij}) \right], \forall\, i \in \mathcal{B}^{ac} \tag{3.11}$$

$$p_l = v_i^2 G_l - v_i v_j \left[G_l \cos(\theta_{ij}) + B_l \sin(\theta_{ij}) \right] \tag{3.12}$$

$$q_l = -v_i^2 \left(B_l + B_l^{sht} \right) - v_i v_j \left[G_l \sin(\theta_{ij}) - B_l \cos(\theta_{ij}) \right] \tag{3.13}$$

Notice that transformers are modeled as regular lines with pre-defined tap ratios. Conservation of power are established through (3.10) and (3.11) taking into account active power injections from VSCs:

$$p_i = \sum_{g \in \mathcal{G}_i} (p_g) - P_{Di} + \sum_{v \in \mathcal{V}_i} p_v^{ac} + np_i, \forall\, i \in \mathcal{B}^{ac} \tag{3.14}$$

$$q_i = \sum_{g \in \mathcal{G}_i} (q_g) - Q_{Di} + \sum_{v \in \mathcal{V}_i} q_v^{ac} + nq_i, \forall\, i \in \mathcal{B}^{ac} \tag{3.15}$$

AC Bus Voltage Limits

$$\underline{V}_i \leq v_i \leq \overline{V}_i, \forall i \in \mathcal{B}^{ac} \tag{3.16}$$

AC Transmission Line Capacity Limits

$$\sqrt{p_l^2 + q_l^2} \leq \overline{S}_l, \forall\, l \in \mathcal{L}^{ac} \tag{3.17}$$

This constraint can also be formulated according to the equivalent expression below:

$$p_l^2 + q_l^2 \leq \overline{S}_l^2, \forall l \in \mathcal{L}^{ac} \tag{3.18}$$

3.3.2 DC Network Constraints

DC Power Flow Equations

Every bus i of the DC grid is characterized by its voltage magnitude v_i. Every line l connecting a pair of DC buses can be represented by its resistance R_l. Assuming that the extreme nodes of such line are i and j, the real power injected at node i and power flows (from i to j) on line l of the DC grid satisfy the following expression:

$$p_i = n \cdot v_i \sum_{j \in \mathcal{B}_{\mathrm{dc}}} G_{ij}^{dc} \left(v_i - v_j\right), \forall\, i \in \mathcal{B}^{dc} \tag{3.19}$$

$$p_l = n \cdot \left[v_i \left(v_i - v_j\right) / R_l\right], \ (i,j) \in \mathcal{N}_l \tag{3.20}$$

where n represents the number of poles. In this thesis, for all case studies, a symmetric monopole configuration is assumed, i.e., $n = 2$.
VSC losses ρ_v are incorporated for power conservation seen from DC side:

$$p_i = \sum_{v \in \mathcal{V}_i} \left(p_v^{dc} + \rho_v\right), \forall\, i \in \mathcal{B}^{dc} \tag{3.21}$$

DC Bus Voltage Limits

The voltage at the DC bus must comply with the voltage limits for system stability concerns (Cui and Sun, 2018).

$$\underline{V}_i \leq v_i \leq \overline{V}_i, \forall i \in \mathcal{B}^{dc} \tag{3.22}$$

DC Transmission Line Capacity Limits

The power can be transmitted through a DC cable is bounded by its technical characteristics.

$$-\overline{P}_l \leq p_l \leq \overline{P}_l, \forall l \in \mathcal{L}^{dc} \tag{3.23}$$

3.3.3 Additional VSC constraints

In addition to the operating limits imposed on VSC as described in Section 3.2.3, converter losses depend on whether it operates as a rectifier or as an inverter (seen in Section 3.2.2). In case it acts as an inverter, i.e., the converter injects power in the AC bus, i_v will take positive values; in case the converter acts as a rectifier, i.e., the converter absorbs power in the AC bus, i_v will take negative values. Consequently, (3.24) is included to force the phase current to be the same direction with the power injected to the corresponding AC bus:

$$0 \leq i_v \cdot p_v^{ac}, \forall v \in \mathcal{V} \tag{3.24}$$

3.3.4 Generator Capacity

When the generation unit is on, the maximum active and reactive power that can be produced is limited due to the technical characteristics of the unit. The same applies to the minimum generation. In case of active power, the minimum stable load is due to minimum requirement of the output power to satisfy pressure and temperature conditions in thermal units, or minimum outflow requirements in hydro units. Regarding the minimum reactive power, the limits are related to the P-Q curve of the generators.

$$\underline{P}_g \leq p_g \leq \overline{P}_g, \forall\, g \in \mathcal{G} \tag{3.25}$$

$$\underline{Q}_g \leq q_g \leq \overline{Q}_g, \forall\, g \in \mathcal{G} \tag{3.26}$$

3.3.5 Objective Function/Optimization Criterion

The considered Objective Function (O.F.) is to minimize the total operating costs plus the penalty from the non-served active and reactive power as shown in (3.27) assuming $np_i \geq 0$, $nq_i \geq 0$ respectively. A_g, B_g and C_g are cost coefficients of generators. NC_p and NC_q represent the unitary costs of non-served real and reactive power respectively. There are some other alternatives, such as minimization of network losses as in (Cao et al., 2013), which could also be easily adapted.

$$\min \sum_{g \in \mathcal{G}} \left(C_g + A_g \cdot p_g + B_g \cdot p_g^2 \right) + \sum_{i \in \mathcal{B}} \left(NC_p \cdot np_i + NC_q \cdot nq_i \right) \tag{3.27}$$

In this thesis, the penalty cost for non-served active and reactive power is set to be 1000 \$/MW and 1000 \$/Mvar respectively (Leveque, 2007).

3.4 Mathematical Formulation of Linear OPF

As discussed in Section **??**, the TEP problem can be viewed as an extension of the OPF problem with binary variables that determines the status of potential transmission lines and makes the TEP formulation "mixed-integer" in nature (Kyriakides et al., 2015). Essentially, it solves a series of OPF problems with different network topologies. Consequently, an OPF model can be seen as a *submodule* of a TEP model (Zhu, 2015).

Although, the OPF model presented above is a complete formulation for steady-state analysis that includes no approximations, it is nonlinear and non-convex which makes it hard to solve and does not guarantee a global optimum. Given the complexity of the problem, large-scale systems are intractable at affordable computational costs. Thus, the well-known DC-OPF[2] model is often adopted in which, reactive power and system losses are neglected (Zhang, 2013). Research on this topic is still under way. A through overview is provided in (Stott et al., 2009).

[2]The model proposed is called LP-OPF instead of DC-OPF to avoid confusion, and both AC and DC grids are considered.

To the author's knowledge, (Wiget and Andersson, 2013) is the only work that studies the OPF problem incorporating MTDC network in a linear manner. However, neither transmission nor converter losses are taken into consideration. Oversimplified OPF formulation is not adequate for TEP problems since they neglect key aspects, such as system losses, that could significantly impact the solution. A thorough comparison among network representations is provided in (Fitwi, 2016). It is essential to strike a balance between the complexity of the network representation and computational effort. Therefore, a linear new model (later referred to as "LP-OPF") is proposed in this thesis to cope with hybrid AC/DC networks based on our previous work (Zhao et al., 2017) targeting large-scale systems, in order to serve both operation and planning purpose.

It considers a detailed hybrid AC/DC transmission representation, i.e., transmission losses are included, meanwhile addresses converter modeling by taking into account that it can function either as an inverter or a rectifier which hasn't been paid enough attention to in literature (Zhao et al., 2017). At the same time, it allows affordable computation time for large-scale systems.

In the rest part of the section, a detailed mathematical formulations is provided with objective functions and constraints respectively. It shall be noted that, all variables presented in this section are in [p.u.], and units of corresponding parameters are adapted accordingly.

This model is built based on the DC-OPF formulation described in (Wood and Wollenberg, 2012), and has been extended to include MTDC networks, converters and transmission losses. No reactive power is considered in the model, thus AC voltage magnitudes are assumed to take nominal values. Notation to indicate certain branch l between pair of extreme buses (i, j) is added in this formulation in case of parallel lines with limiting maximum capacity needs to be represented. Quadratic terms in (3.30), (3.36) and (3.43) will be explained and clarified in detail in Section 3.4.6.

3.4.1 AC Network Constraints

AC Power Flow Equations

Every bus i of the AC grid is characterized by its phase angle θ_i. By denoting $\theta_{ij} = \theta_i - \theta_j$, following DC-OPF convention, power injections at node i and power flows

(from i to j) on branch l, i.e., $(i,j) \in \mathcal{N}_l$, are (Wood and Wollenberg, 2012):

$$p_i = \sum_{j \in B^{ac}} B_{ij}\theta_{ij} + \sum_{l \subset [(i,j) \cup (j,i)]} \frac{\rho_l}{2}, \forall\, i \in \mathcal{B}^{ac},\ (i,j) \in \mathcal{N}_l,\ (j,i) \in \mathcal{N}_l \tag{3.28}$$

$$p_l = B_l \theta_{ij}, \forall\, l \in \mathcal{L}^{ac},\ (i,j) \in \mathcal{N}_l \tag{3.29}$$

where ρ_l represents the branch losses. These losses can be treated as additional loads at the two extreme nodes of the line (Ramos and Sanchez-Martin, 1997) where each fictitious load represents half of the branch losses. Instead of expressing losses as a function of angle difference, it can be expressed as a function of flows on the line. losses can be readily derived as follows assuming in p.u. (Fitiwi et al., 2015):

$$\rho_l = f\left(p_l\right) = R_l p_l^2, \forall\, l \in \mathcal{L}^{ac} \tag{3.30}$$

and with active power injections, p_v^{ac}, from VSCs taken into account, conservation of power at every nodes are established through (3.31):

$$p_i = \sum_{g \in \mathcal{G}_i} \left(p_g\right) - P_{Di} + \sum_{v \in \mathcal{V}_i} p_v^{ac} + np_i, \forall\, i \in \mathcal{B}^{ac} \tag{3.31}$$

AC Transmission Line Capacity Limits

$$-\overline{P}_l \leq p_l \leq \overline{P}_l, \forall\, l \in \mathcal{L}^{ac} \tag{3.32}$$

AC Bus Phase Angel Limits

$$\underline{\theta}_{ij} \leq \theta_{ij} \leq \overline{\theta}_{ij}, \forall\, i,j \in \mathcal{B}^{ac},\ (i,j) \in \mathcal{N}_l \tag{3.33}$$

3.4.2 DC Network Constraints

DC Power Flow Equations

For every DC line l connected between nodes i and j through its resistance R_l, the two extreme nodes are characterized by their voltage magnitudes v_i and v_j. The real power injected at node i and the power flow p_l on line l leaving bus i can be expressed

as follows:

$$p_i = n \cdot \sum_{j \in B^{dc}} G_{ij}^{dc} \left(v_i - v_j\right) + \sum_{l \subset [(i,j) \cup (j,i)]} \frac{\rho_l}{2}, \forall\, i \in \mathcal{B}^{dc},\ (i,j) \in \mathcal{N}_l,\ (j,i) \in \mathcal{N}_l \quad (3.34)$$

$$p_l = n \cdot \left[\left(v_i - v_j\right) / R_l\right], \forall\, l \in \mathcal{L}^{dc},\ (i,j) \in \mathcal{N}_l \quad (3.35)$$

where n represents the number of poles. Similar as in the AC network, ρ_l represents the transmission losses:

$$\rho_l = f\left(p_l\right) = R_l p_l^2, \forall\, l \in \mathcal{L}^{dc} \quad (3.36)$$

While VSC losses ρ_v are incorporated for power conservation seen from DC side:

$$p_i = \sum_{v \in \mathcal{V}_i} \left(p_v^{dc} + \rho_v\right), \forall\, i \in \mathcal{B}^{dc} \quad (3.37)$$

DC Transmission Line Capacity Limits

$$-\overline{P}_l \leq p_l \leq \overline{P}_l, \forall l \in \mathcal{L}^{dc} \quad (3.38)$$

DC Bus Voltage Limits

$$\underline{V}_i \leq v_i \leq \overline{V}_i, \forall\, i \in \mathcal{B}^{dc} \quad (3.39)$$

3.4.3 VSC Constraints

Maximum current through the IGBTs

It is the same as in Section 3.2.3.

$$-\overline{I}_v \leq i_v \leq \overline{I}_v, \forall v \in \mathcal{V} \quad (3.40)$$

DC and AC voltage level coupling

It is the same as in Section 3.2.3.

$$v_c \leq k_v \cdot v_i \qquad \forall v \in \mathcal{V}, c \in \mathcal{N}_v^{ac}, i \in \mathcal{N}_v^{dc} \quad (3.41)$$

Maximum power constraint

Given a maximum allowed phase current, apparent power injected to the AC network needs to be constrained as shown in (3.8). Nevertheless, it can be further simplified to the following expression provided that entire formulation is made in [p.u.]:

$$0 = i_v - p_c, \forall\, v \in \mathcal{V},\ c \in \mathcal{N}_v^{ac} \tag{3.42}$$

Converter losses

The same expression as before in the NLP formulation is adopted which distinguishes different behavior when acting as a rectifier or an inverter. Linearization of the quadratic terms will be further explained in Section 3.4.6:

$$\rho_v = A_v + B_v \cdot |i_v| + C_v^{inv} \cdot \left(i_v^{inv}\right)^2 + C_v^{rec} \cdot (i_v^{rec})^2 \tag{3.43}$$

Conservation of power

Power balance within the converter is established by the same expression as in (3.4). Power can be injected on both sides, depending on the flow direction variables, p_v^{ac} and p_v^{dc} can be either positive or negative. However, converter losses ρ_v cannot be negative, i.e., $\rho_v \geq 0$.

3.4.4 Generator Capacity

In the linearized model, only the generation limit of the active power produced by the generator will be considered.

$$\underline{P}_g \leq p_g \leq \overline{P}_g, \forall\, g \in \mathcal{G} \tag{3.44}$$

3.4.5 Objective Function/Optimization Criteria

The O.F. considered in this model is to minimize the total operating costs plus the penalty on the non-served active power as shown in (3.45) assuming $np_i \geq 0$. A_g and C_g indicate cost coefficients of generators, NC_p represents the unitary costs of non-served active power. Other alternatives such as minimization of network losses as

in (Cao et al., 2013) could also be adapted accordingly.

$$\min \sum_{g \in \mathcal{G}} (C_g + A_g \cdot p_g) + \sum_{i \in \mathcal{B}} (NC_p \cdot np_i) \tag{3.45}$$

3.4.6 Linearization of Quadratic Terms

As previously mentioned, neglecting transmission losses to reduce the computational burden in case of large-scale system can jeopardize the accuracy of TEP solutions leading to underinvestment. Transmission losses modeling in relation with TEP problems is thoroughly reviewed in Chapter 3 of (Fitwi, 2016). There are mainly two issues needs to be paid close attention to: 1) accuracy (including the capability to limit *artificial losses* (Fitiwi et al., 2015) or *fictitious losses* as in (Ramos and Sanchez-Martin, 1997)), and 2) computational complexity resulted from linearization. Thus, the losses representation should be accurate enough to address key problems such as avoidance of artificial losses, but simple enough to allow affordable computation for large-scale systems.

Existing linear loss models are reviewed in (Fitiwi et al., 2015). Among the three methods, *Model 3a* or piecewise linear approximation model is able to achieve certain level of accuracy, while limiting artificial losses at a price that additional variables are needed to represent power flow segments. This model is described in (Alguacil et al., 2003; de la Torre et al., 2008; Ramos and Sanchez-Martin, 1997; **?**) with further details.

In addition, (Fitiwi et al., 2015) has also proposed some other loss models to improve the accuracy. Results show that although binary variables help with the precision, it is very computationally intensive which reduce its applicability for large-scale systems. With an additional constraint (compared to *Model 3a*), *Model 3b* is able to represent losses more accurately given an reasonable extra amount of computation time.

Thus in this thesis, *Model 3b* formulation is adopted for the LP-OPF model and therefore all quadratic terms appeared are approximated by a set of linear constraints. In order to illustrate the linearizion, the loss ρ_l in (3.30) is used as an example hereafter.

The first step is to discretize the maximum allowed line flow $\overline{P}_l$ into a desired number of segments N. Each segment is of a positive step-size $\Delta\overline{P}_l$ and corresponds to a term in the final linear expression. In this thesis, N has taken the value of 4 as suggested in (Fitiwi et al., 2015) and (Ramos and Sanchez-Martin, 1997). Consequently a quadratic losses function can be extrapolated by pieces of linear functions. In this way, every

segment has a flow variable Δp_l^n associated with the n^{th} partition. By adding losses calculated for each segment Δp_l^n, losses for every line can be approximated. Following constraints are included:

$$\rho_l = R_l \sum_{n=1}^{N} (2n-1) \Delta \overline{P}_l \Delta p_l^n, \forall\, l \in \mathcal{L}^{ac} \tag{3.46}$$

$$0 \leq \Delta p_l^n \leq \Delta \overline{P}_l \tag{3.47}$$

$$\sum_{n=1}^{N} \Delta p_l^n = |p_l| = p_l^+ + p_l^- \tag{3.48}$$

$$\Delta p_l^{n+1} \leq \Delta p_l^n \tag{3.49}$$

providing that $p_l = p_l^+ - p_l^-$, where p_l^+ and p_l^- are two non-negative auxiliary variables (i.e., $p_l^+,\ p_l^- \geq 0$), representing the flow in the opposite directions for the line. In addition, only one of them (p_l^+ and p_l^-) could be different from zero.

3.5 Validation

Previous work (Wang, 2013a) on the hybrid AC/DC OPF had followed an approximate verification since there was no commercial software which can be utilized to accurately verify the results of the model back then. In this thesis, a more analytical and precise approach is followed to validate the models.

The OPF models presented in this chapter have been implemented in GAMS (Brooke et al., 1992) on an Intel-i7 2.93GHz personal computer with 4GB of RAM memory. The obtained OPF solutions are compared with the solution of the VSC MTDC power flow model MatACDC presented in (Beerten et al., 2010), which is based on the Matlab toolbox MATPOWER. MatACDC is a PF solver (Beerten, 2013). In a PF problem of an AC network, each bus provides two PF equations and four unknowns (P, Q, V, θ), which entails two of them needs to be specified. The known and unknown variables depend on the type of buses. Each bus can be categorized into three types, i.e., PV (a bus at which the magnitude of the voltage is defined, as well as the real power injection), PQ (a bus at which the real and reactive power are specified)

and slack or swing (its voltage is assumed to be fixed in both magnitude and phase) (Gomez-Exposito et al., 2008). To make an analogy with DC networks, since reactive power does not exist, the number of equations and variables is reduced with respect to AC system. Either the voltage magnitude (for slack bus) or active power is unknown. Therefore, by fixing power generation, bus voltage and phase angle accordingly to the MatACDC solution, the two OPF models can be used as PF solvers.

3.5.1 System Description

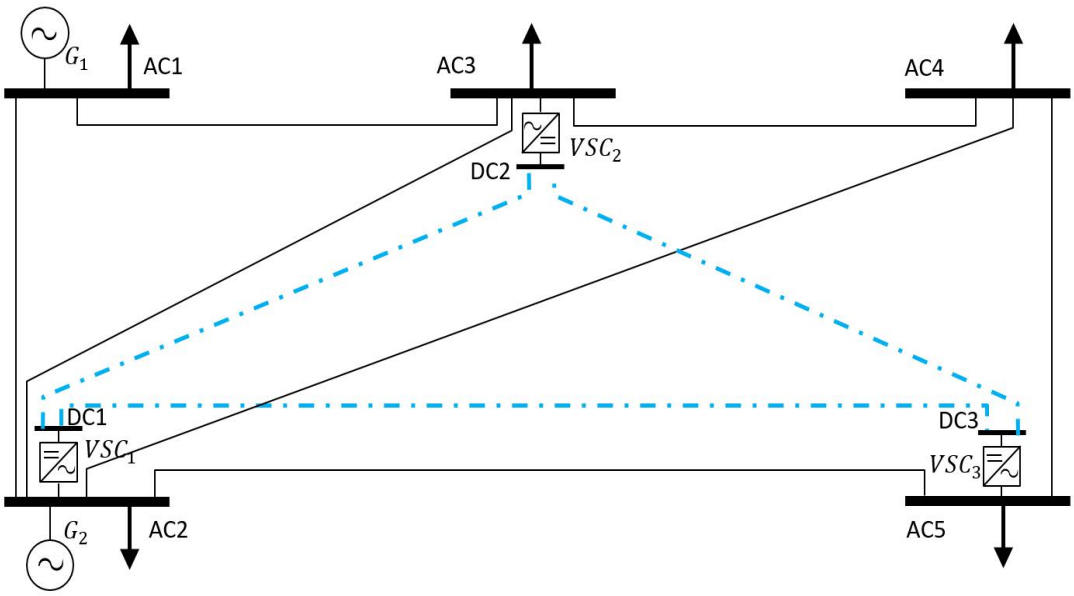

Fig. 3.5 Leuven 5-bus System

The test system presented in (Beerten et al., 2010) has been chosen, as shown in Fig. 3.5. The grid has 5 AC buses ($AC1$ to $AC5$) and three DC buses ($DC1$ to $DC3$). The DC buses are connected to the AC grid via converter stations (VSC_1 to VSC_3). Two generators (G_1 and G_2) are located at bus $AC1$ and $AC2$ respectively. AC transmission lines are presented in black solid line, while DC transmission lines are represented in blue dash dotted lines. The detailed converter and grid data are available in Appendix A (Beerten and Belmans, 2015; Beerten et al., 2010).

3.5.2 Results

The complex model (NLP-OPF) takes into account all nonlinearities and successfully replicates exactly the results produced by MATACDC with IPOPT solver. IPOPT

is commonly applied in solving large-scale nonlinear optimization problems (Wang, 2013a) using "interior point line search filter" method (GAMS, 2015). On the other hand LP-OPF is solved with CPLEX 12.6 (GAMS, 2015). Power flow results of the simplified model are provided below.

Branch	**NLP**	**LP**
$P_{AC1-AC2}$	98.38	97.58
$P_{AC1-AC3}$	35.26	34.54
$P_{AC2-AC3}$	13.25	13.53
$P_{AC2-AC4}$	17.08	17.30
$P_{AC2-AC5}$	25.33	25.41
$P_{AC3-AC4}$	23.09	22.60
$P_{AC4-AC5}$	−0.07	−0.27
$P_{DC3-DC2}$	−30.66	−30.36
$P_{DC3-DC5}$	8.52	8.70
$P_{DC2-DC5}$	27.96	27.83
$P_{AC2-DC2}$	60.00	60.00
$P_{AC3-DC3}$	−20.76	−20.20
$P_{AC5-DC5}$	−35.00	−35.00

Table 3.1 Power Flow [MW] of both AC and DC Branches

It can be observed in Table 3.1 that LP-OPF provide quite precise approximations for almost all lines. Big discrepancy happens on AC line $P_{AC4-AC5}$, which is almost 4 times the exact value accordingly. Average mismatch of these 13 line flows is 0.3 MW, while the average flow is 30.41 MW, making the error around 0.99%.

Branch	**NLP**	**LP**
V_{DC1}	1.00791	1.00789
$V_{DC2^{(slack)}}$	1.00000	1.00000
V_{DC3}	0.99778	0.99774

Table 3.2 DC voltage [p.u.] Level Comparison

Table 3.2 shows a comparison of the DC voltage level within the 3-terminal MTDC network. Bus $DC2$ is assumed to be the DC slack bus to cover all the losses in DC network. As can be seen from the table, the differences between the exact nonlinear model and the linear one are very small.

3.6 Case Studies of Nonlinear and Linear OPF Models

Previously, two models are presented for steady-state analysis of hybrid AC/DC network. One aims at obtaining the exact OPF solution, while the other targets systems of large-scale in order to serve planning purpose. In order to further assess and compare the performance of proposed models, two more case studies are carried out with larger test systems. The purpose is to compare the proposed simplified OPF model so to understand the impact on the accuracy level of the LP-OPF approximation when HVDC systems are embedded in the AC grid. The first case study focus on a small modified IEEE standard system, in which, solutions between LP-OPF and NLP-OPF are compared. The second case study investigates two hybrid AC/DC systems with different DC grid configurations. It is meant to highlight the impact that such differences have on the OPF solution. Comparisons are made not only between different models (LP-OPF vs. NLP-OPF), but also across different systems.

All the OPF problems are solved using the proposed models with default values of solver parameters (relative optimality tolerance, maximum number of iterations, etc.). Please note that NLP model does not guarantee global optimum. In this thesis, the focus is on the formulation of the OPF models rather than on the development of the advanced solution algorithms for the global optimum of the nonlinear optimization problem. Therefore to minimize such effect, when carrying out the case studies for OPF solutions comparisons, both systems are solved with initialization of solving the LP first. The obtained solution then is used as the starting point for solving the NLP.

3.6.1 Comparison Metrics

In order to assess the goodness of the simplified OPF solution, two indicators proposed in (Zhao et al., 2017) are used which are defined as follows:

- **System costs**

Given that the NLP-OPF provides the benchmark value of the O.F., the deviation of the LP-OPF model can be measured in relative terms (3.50):

$$\Delta OF_{\%}^{LP-OPF} = \frac{OF^{LP-OPF} - OF^{NLP-OPF}}{OF^{NLP-OPF}} \times 100\% \tag{3.50}$$

- **Active power flow differences**

After solving the OPF, as many power flows as number of branches will be generated. To measure how close the solution of the LP-OPF model is with respect to the NLP-OPF model, the Mean Absolute Error (MAE) is used.

$$MAE^{LP-OPF} = \frac{1}{n}\sum_{l=1}^{n}\left|f_l^{LP-OPF} - f_l^{NLP-OPF}\right| \tag{3.51}$$

where n is the total number of observations (i.e., number of lines), f_l^{LP-OPF} stands for the active power flow at branch l obtained with the LP-OPF model, and $f_l^{NLP-OPF}$ is the exact value obtained with the NLP-OPF model.

3.6.2 Case Study #1

System Description

The studied system is modified based on the one used in (Wiget, 2015). The AC part originates from the IEEE 14-bus test case available at (Christie, 1993) (later referred to as "IEEE14"). The DC grid remains the same. Fig. 3.6 provides the single line diagram of the system.

The grid has fifteen AC buses (1 to 15) and five DC buses ($DC1$ to $DC5$), which are connected via converter stations. The system contains six generators. AC transmission lines are presented in black solid line, while DC transmission lines are represented in blue dash dotted lines. The AC buses are connected with twenty lines, of which five are transformers. The DC grid has seven transmission lines. The detailed grid data is available in Appendix B.

Results

O.F. and deviation of the two models is presented in Table 3.3. Branch power flows (both AC and DC) and power generation levels are shown in Table 3.4, Table 3.5 and Table 3.6 respectively below.

Systems	**NLP [€]**	**LP [€]**	**Deviation [%]**
$IEEE14$	172.74	172.66	0.05

Table 3.3 O.F. and deviation in percentage [%] (IEEE14)

It can be observed that results from NLP- and LP-OPF models are quite close. O.F. difference is merely 0.05%. MAE for AC branches is only 2.03 MW. Considering the

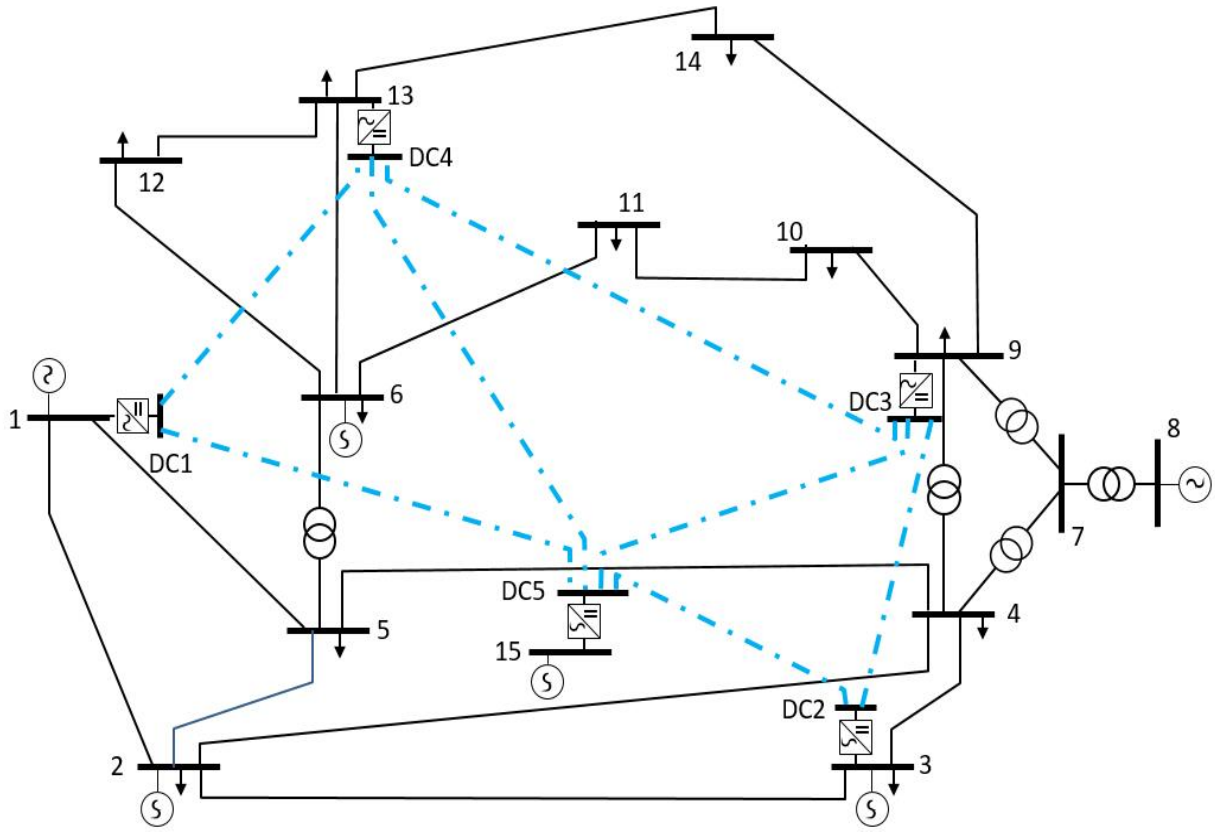

Fig. 3.6 IEEE 14-bus Test System with 5-bus MTDC network

Bus No.	Unit	NLP	LP
1	g_1	2.56	0.0
2	g_2	0.0	0.0
3	g_3	99.42	100
6	g_4	69.83	71.86
8	g_5	48.95	50
15	g_6	45.06	44.23

Table 3.4 Active Power Generation Level [MW] of All Units (IEEE14 System)

average flow of the twenty lines is 11.39MW, the error amounts to approximately 17.8%. For DC branches, MAE is 3.32 MW. There is not very much difference between the OPF solution in the 5-terminal network (Table 3.6). Considering all branches together, average mismatch of these twenty-seven line flows is 2.36 M, while the average flow is 10.86 MW, making the error around 21.7%. Calculated error percentage is notable in this case although MAE is insignificant. This can be considered reasonable since the entire system is lightly loaded. For all lines, the average capacity occupied is only 20.8% which could magnify the error percentages. Therefore, in case study #2, a larger system is used.

Branch	**NLP**	**LP**	**Branch**	**NLP**	**LP**
P_{1-2}	10.94	14.76	P_{6-11}	10.29	12.50
P_{1-5}	-2.33	0.0	P_{6-12}	6.26	6.30
P_{2-3}	-0.99	-0.96	P_{6-13}	12.81	12.50
P_{2-4}	-3.33	-1.03	P_{7-8}	-48.95	-50.00
P_{2-5}	-6.47	-5.02	P_{7-9}	17.24	23.16
P_{3-4}	-1.79	0.0	P_{9-10}	2.37	0.17
P_{4-5}	-12.82	-16.51	P_{9-14}	6.26	4.58
P_{4-7}	-31.70	-26.84	P_{10-11}	-6.65	-8.88
P_{4-9}	-8.41	-5.51	P_{12-13}	0.11	0.15
P_{5-6}	-29.27	-29.19	P_{13-14}	8.85	10.46

Table 3.5 Power Flow [MW] of AC branches (IEEE14 System)

Branch	**NLP**	**LP**
$P_{DC1-DC4}$	5.03	1.88
$P_{DC1-DC5}$	-12.22	-17.87
$P_{DC2-DC5}$	-7.83	-5.26
$P_{DC2-DC3}$	12.70	8.95
$P_{DC3-DC4}$	-4.07	0.63
$P_{DC3-DC5}$	-13.80	-9.53
$P_{DC4-DC5}$	-9.74	-10.15

Table 3.6 Power Flow [MW] of DC branches (IEEE14 System)

3.6.3 Case Study #2

System Description

The used test system is the same as for the converter loss impact assessment, as described in Section 4.1.3 and shown in Fig. 4.1 and Fig. 4.2.

Results

O.F. and deviation of 7T and 9T system is presented in Table 3.7. Branch power flows and power generation levels are shown respectively below.

Systems	**NLP [k€]**	**LP [k€]**	**Deviation [%]**
$7T$	122.70	117.83	3.97
$9T$	122.55	117.88	3.81

Table 3.7 O.F. and deviation in percentage [%] (7T and 9T)

- **7T System**

Generation levels (Table 3.8) of all generators play a important role as part of a complete optimal power flow solution. It can be easily observed from the table that, only generators from buses No. 107, 207, 213 and 302 have different outputs, while all others keep the same generation for the two models.

Bus No.	**Unit**	**NLP**	**LP**	**Bus No.**	**Unit**	**NLP**	**LP**
101	g_1	16	16	201	g_{33}	16	16
	g_2	16	16		g_{34}	16	16
	g_3	76	76		g_{35}	76	76
	g_4	76	76	202	g_{36}	16	16
102	g_5	16	16		g_{37}	16	16
	g_6	16	16		g_{38}	76	76
	g_7	76	76		g_{39}	76	76
	g_8	76	76	207	g_{40}	70.66	100
107	g_9	57.71	92.70		g_{41}	70.66	70.93
	g_{10}	57.71	25		g_{42}	70.66	100
113	g_{11}	69	69	213	g_{43}	85.68	69
	g_{12}	69	69		g_{44}	85.68	69
	g_{13}	69	69		g_{45}	85.68	69
114	g_{14}	0	0	214	g_{46}	0	0
115	g_{15}	2.4	2.4	215	g_{47}	2.4	2.4
	g_{16}	2.4	2.4		g_{48}	2.4	2.4
	g_{17}	2.4	2.4		g_{49}	2.4	2.4
	g_{18}	2.4	2.4		g_{50}	2.4	2.4
	g_{19}	2.4	2.4		g_{51}	2.4	2.4
	g_{20}	155	155		g_{52}	155	155
116	g_{21}	155	155	216	g_{53}	155	155
118	g_{22}	400	400	218	g_{54}	400	400
121	g_{23}	400	400	221	g_{55}	400	400
122	g_{24}	50	50	222	g_{56}	50	50
	g_{25}	50	50		g_{57}	50	50
	g_{26}	50	50		g_{58}	50	50
	g_{27}	50	50		g_{59}	50	50
	g_{28}	50	50		g_{60}	50	50
	g_{29}	50	50		g_{61}	50	50
123	g_{30}	155	155	223	g_{62}	155	155
	g_{31}	155	155		g_{63}	155	155
	g_{32}	350	350		g_{64}	350	350
				302	g_{65}	199.07	220.20

Table 3.8 Active Power Generation Level [MW] of All Units (7T System)

Branch	NLP	LP	Branch	NLP	LP
$P_{101-102}$	10.94	11.73	$P_{201-203}$	-10.61	-12.38
$P_{101-103}$	-0.85	-5.47	$P_{201-205}$	55.12	57.11
$P_{101-105}$	65.91	69.06	$P_{202-204}$	-6.29	-8.53
$P_{102-104}$	44.90	43.09	$P_{202-206}$	48.72	49.44
$P_{102-106}$	53.04	54.49	$P_{203-209}$	15.66	13.82
$P_{103-109}$	25.19	29.50	$P_{203-224}$	-206.34	-206.95
$P_{103-124}$	-206.05	-215.78	$P_{204-209}$	9.75	7.10
$P_{104-109}$	-29.82	-31.50	$P_{205-210}$	-16.80	-14.36
$P_{105-110}$	-6.35	-2.54	$P_{206-210}$	-89.66	-87.77
$P_{106-110}$	-85.69	-82.80	$P_{207-208}$	86.97	144.23
$P_{107-108}$	87.87	88.53	$P_{208-209}$	-52.74	-28.21
$P_{108-109}$	-47.82	-52.00	$P_{208-210}$	-32.62	-0.58
$P_{108-110}$	-36.63	-32.08	$P_{209-211}$	-87.65	-76.46
$P_{109-111}$	-102.21	-101.30	$P_{209-212}$	-116.27	-106.54
$P_{109-112}$	-126.99	-129.04	$P_{210-211}$	-153.66	-134.39
$P_{110-111}$	-150.41	-143.06	$P_{210-212}$	-183.10	-164.47
$P_{110-112}$	-175.97	-170.80	$P_{211-213}$	-124.17	-105.38
$P_{111-113}$	-132.79	-127.98	$P_{211-214}$	-114.89	-107.54
$P_{111-114}$	-120.53	-117.78	$P_{212-213}$	-75.43	-52.62
$P_{112-113}$	-87.36	-80.16	$P_{212-223}$	-224.91	-222.41
$P_{112-123}$	-216.57	-223.92	$P_{213-223}$	-211.81	-218.78
$P_{113-123}$	-196.98	-205.29	$P_{214-216}$	-309.58	-304.30
$P_{114-116}$	-315.28	-314.72	$P_{215-216}$	87.50	65.74
$P_{115-116}$	78.51	69.61	$P_{215-221}$	-205.82	-214.90
$P_{115-121}$	-219.34	-221.50	$P_{215-224}$	210.53	209.14
$P_{115-124}$	210.17	218.14	$P_{216-217}$	-269.64	-285.75
$P_{116-117}$	-314.80	-312.77	$P_{216-219}$	97.77	98.27
$P_{116-119}$	128.17	118.31	$P_{217-218}$	-203.15	-188.15
$P_{117-118}$	-179.28	-176.63	$P_{217-222}$	-141.81	-141.25
$P_{117-122}$	-138.29	-139.44	$P_{218-221}$	-68.46	-60.91
$P_{118-121}$	-56.43	-55.11	$P_{219-220}$	-41.75	-41.63
$P_{119-120}$	-26.64	-31.60	$P_{220-223}$	-105.84	-106.03
$P_{120-123}$	-90.68	-95.93	$P_{221-222}$	-153.55	-156.13
$P_{121-122}$	-157.10	-157.92	$P_{301-302}$	-199.07	-200.20
$P_{201-202}$	-44.50	-45.33			

Table 3.9 Power Flow [MW] of AC branches (7T System)

Branch	**NLP**	**LP**
$P_{DC1-DC3}$	-99.57	-100.00
$P_{DC2-DC3}$	-92.05	-92.98
$P_{DC4-DC5}$	-38.85	-25.00
$P_{DC4-DC6}$	-31.78	-24.14
$P_{DC4-DC7}$	-13.54	-17.25
$P_{DC5-DC7}$	13.07	4.88
$P_{DC6-DC7}$	-51.22	-18.57

Table 3.10 Power Flow [MW] of DC branches (7T System)

Branch power flows of both AC and DC grids are shown in Table 3.9 and Table 3.10 respectively. MAE, i.e., average mismatch, for AC branches is 6.50 MW, while the average flow is 114.36 MW, which amount to an error of 5.68%. For DC branches, MAE is 9.63 MW. There is near negligible difference between the OPF solution in the 3-terminal network ($P_{DC1-DC3}$ and $P_{DC2-DC3}$). Big discrepancies only occur on the 4-terminal network. Considering all branches together, average mismatch of these 84 line flows is 6.76 MW, while the average flow is 108.88 MW, making the error around 6.21%.

- **9T System**

Similarly as before, generation levels for all generators are illustrated in Table 3.11. Major differences are observed at buses No. 107, 207, 213 and 302.

Bus No.	Unit	NLP	LP	Bus No.	Unit	NLP	LP
101	g_1	16	16	201	g_{33}	16	16
	g_2	16	16		g_{34}	16	16
	g_3	76	76		g_{35}	76	76
	g_4	76	76	202	g_{36}	16	16
102	g_5	16	16		g_{37}	16	16
	g_6	16	16		g_{38}	76	76
	g_7	76	76		g_{39}	76	76
	g_8	76	76	207	g_{40}	69.82	56.42
107	g_9	63.28	33.36		g_{41}	69.82	100
	g_{10}	63.28	100		g_{42}	69.82	100
113	g_{11}	70.87	69	213	g_{43}	79.96	69
	g_{12}	70.87	69		g_{44}	79.96	69
	g_{13}	70.87	69		g_{45}	79.96	69
114	g_{14}	0	0	214	g_{46}	0	0
115	g_{15}	2.4	2.4	215	g_{47}	2.4	2.4
	g_{16}	2.4	2.4		g_{48}	2.4	2.4
	g_{17}	2.4	2.4		g_{49}	2.4	2.4
	g_{18}	2.4	2.4		g_{50}	2.4	2.4
	g_{19}	2.4	2.4		g_{51}	2.4	2.4
	g_{20}	155	155		g_{52}	155	155
116	g_{21}	155	155	216	g_{53}	155	155
118	g_{22}	400	400	218	g_{54}	400	400
121	g_{23}	400	400	221	g_{55}	400	400
122	g_{24}	50	50	222	g_{56}	50	50
	g_{25}	50	50		g_{57}	50	50
	g_{26}	50	50		g_{58}	50	50
	g_{27}	50	50		g_{59}	50	50
	g_{28}	50	50		g_{60}	50	50
	g_{29}	50	50		g_{61}	50	50
123	g_{30}	155	155	223	g_{62}	155	155
	g_{31}	155	155		g_{63}	155	155
	g_{32}	350	350		g_{64}	350	350
				302	g_{65}	199.07	220.20

Table 3.11 Active Power Generation Level [MW] of All Units (9T System)

Branch	**NLP**	**LP**	**Branch**	**NLP**	**LP**
$P_{101-102}$	7.54	0.11	$P_{201-203}$	-1.6	-5.65
$P_{101-103}$	7.31	-0.07	$P_{201-205}$	54.08	56.55
$P_{101-105}$	76.24	75.27	$P_{202-204}$	3.00	0.00
$P_{102-104}$	17.73	26.56	$P_{202-206}$	31.44	35.09
$P_{102-106}$	61.72	59.36	$P_{203-209}$	10.94	12.78
$P_{103-109}$	18.39	25.35	$P_{203-224}$	-192.64	-199.05
$P_{103-124}$	-191.11	-206.09	$P_{204-209}$	12.61	9.93
$P_{104-109}$	15.61	-3.58	$P_{205-210}$	-17.61	-14.91
$P_{105-110}$	3.69	3.55	$P_{206-210}$	-35.50	-42.15
$P_{106-110}$	-77.40	-78.07	$P_{207-208}$	84.45	130.02
$P_{107-108}$	97.87	104.00	$P_{208-209}$	-48.99	-31.04
$P_{108-109}$	-45.37	-45.53	$P_{208-210}$	-38.75	-11.83
$P_{108-110}$	-29.36	-23.10	$P_{209-211}$	-85.44	-76.73
$P_{109-111}$	-79.28	-85.19	$P_{209-212}$	-85.44	-76.73
$P_{109-112}$	-108.35	-114.57	$P_{210-211}$	-128.24	-117.00
$P_{110-111}$	-135.14	-132.23	$P_{210-212}$	-160.04	-147.63
$P_{110-112}$	-165.15	-161.61	$P_{211-213}$	-117.59	-100.26
$P_{111-113}$	-107.28	-105.18	$P_{211-214}$	-96.58	-94.54
$P_{111-114}$	-107.65	-113.45	$P_{212-213}$	-62.68	-47.45
$P_{112-113}$	-55.28	-54.53	$P_{212-223}$	-214.42	-211.15
$P_{112-123}$	-219.02	-225.76	$P_{213-223}$	-206.41	-209.09
$P_{113-123}$	-215.81	-221.47	$P_{214-216}$	-291.04	-291.10
$P_{114-116}$	-302.23	-310.31	$P_{215-216}$	65.13	71.14
$P_{115-116}$	65.40	65.82	$P_{215-221}$	-205.63	-213.49
$P_{115-121}$	-205.00	-214.49	$P_{215-224}$	196.11	201.08
$P_{115-124}$	194.60	208.25	$P_{216-217}$	-256.08	-284.06
$P_{116-117}$	-281.80	-297.98	$P_{216-219}$	81.00	115.30
$P_{116-119}$	95.52	104.41	$P_{217-218}$	-203.50	-190.60
$P_{117-118}$	-146.15	-161.75	$P_{217-222}$	-141.79	141.61
$P_{117-122}$	-137.86	-139.31	$P_{218-221}$	-68.64	-62.15
$P_{118-121}$	-71.28	-62.27	$P_{219-220}$	-50.12	-52.30
$P_{119-120}$	-42.87	-38.56	$P_{220-223}$	-114.27	-116.76
$P_{120-123}$	-106.96	-102.93	$P_{221-222}$	-153.58	-155.75
$P_{121-122}$	-157.54	-158.05	$P_{301-302}$	-199.07	-200.20
$P_{201-202}$	-52.48	-51.40			

Table 3.12 Power Flow [MW] of AC branches (9T System)

Branch	NLP	LP
$P_{DC1-DC3}$	-100.00	-100.00
$P_{DC1-DC4}$	1.65	0.00
$P_{DC2-DC3}$	-100.00	-90.50
$P_{DC2-DC6}$	-26.33	-20.11
$P_{DC2-DC9}$	40.87	23.06
$P_{DC3-DC5}$	-8.66	2.51
$P_{DC4-DC5}$	-40.80	-25.00
$P_{DC4-DC7}$	-31.00	-21.09
$P_{DC5-DC7}$	10.01	3.91
$P_{DC6-DC7}$	-62.52	-25.00
$P_{DC6-DC8}$	34.59	3.46
$P_{DC8-DC9}$	32.84	39.71

Table 3.13 Power Flow [MW] of DC branches (9T System)

Branch power flows of both AC and DC grids are shown in Table 3.12 and Table 3.13 respectively. MAEs for AC branches is 7.36MW, while the average AC flow is 107.95 MW, which amount to an error of 6.82%. Considering all these 89 lines, MAE is 8.04 MW, while the average flow is 98.89 MW, making the error around 8.13%.

3.6.4 Computational Perspective of Case #1 and #2

Problem size is compared by indicating number of constraints, number of variables and nonzero elements, reflecting essentially the complexity of the two formulations. While CPU time and number of iterations used, which defines the computational burden, are shown subsequently. Table 3.14 presents the result for IEEE14 system. Table 3.15 and Table 3.16 show the result for both 7T and 9T respectively.

Problem Features	NLP	LP
Constraints	340	437
Variables	351	503
Nonzero Elements	1485	1523
CPU Time [*s*]	0.797	0.016
Iterations	60	411

Table 3.14 Problem Size and Computational Burden Comparison (IEEE14 System)

Problem Features	**NLP**	**LP**
Constraints	880	703
Variables	969	1246
Nonzero Elements	4072	3151
CPU Time $[s]$	2.719	0.031
Iterations	262	553

Table 3.15 Problem Size and Computational Burden Comparison (7T System)

Problem Features	**NLP**	**LP**
Constraints	948	780
Variables	1041	1374
Nonzero Elements	4346	3479
CPU Time $[s]$	5.234	0.047
Iterations	508	723

Table 3.16 Problem Size and Computational Burden Comparison (9T System)

Although for NLP, problem size is slightly bigger, it takes less iterations to reach the solution, but each iteration takes a longer time to solve. The resulted computation time is almost 90 times slower than the LP for 7T (and 111 times slower as for 9T). Another observation is that moving from 7T to 9T, system complexity does not increase much, however, computation time almost double for NLP. LP also experience a raised computation time, yet not as much as NLP. Therefore, computational efficiency could be better achieved through the LP-OPF model as expected, especially when problem size is getting bigger.

Chapter 4

Impact Assessment of Converter Losses and Case Studies of Non-linear and Linear OPF Models

First, this chapter analyzes the impact on the power flow solution as a result of embedding VSC-MTDC systems into an AC grid. A case study on the 7T and 9T MRTS systems using the NLP-OPF proposed in Chapter 3 is carried out. The case study results are presented and carefully analyzed[1].

4.1 Converter Losses Impact Assessment

Despite the existence of many barriers such as the cost of converter stations, less standardized equipment as compared with AC systems, need of new control algorithms, difficulty to build DC breakers, etc., MTDC configuration are seen as a viable option that can outperform traditional AC transmission due to its technical, economic and environmental advantages (Meah and Ula, 2007).

Compared to CSC, VSC offers some great advantages (Flourentzou et al., 2009). Due to completely different operating principles, new algorithms have been developed for VSC HVDC control and PF studies (Beerten et al., 2012). The problem of finding the PF solution for the case of a hybrid network with VSC-MTDC systems is relatively new (Baradar et al., 2013; CIGRE, 2005). The OPF problem for hybrid networks is

[1]This chapter draws on Q. Zhao, J. García-González, O. Gomis-Bellmunt, E. Prieto-Araujo, and F. M. Echavarren, "Impact of converter losses on the optimal power flow solution of hybrid networks based on VSC-MTDC," Electric Power Systems Research, vol. 151, pp. 395–403, Oct. 2017.

even a less developed research line, and the converter's operation introduces additional decision variables that increase the complexity of the resulting optimization problem, (Baradar et al., 2013; Cao et al., 2013; Feng et al., 2014).

In case of a large deployment of HVDC networks, the impact of their converter stations on the control, operation and planning of the whole power system needs to be carefully examined. For instance, the ratio between the voltage levels at the AC and DC sides of the converter is limited due to the constraints imposed by the power electronic equipment. In addition, the amount of active and reactive power injected or withdrawn at the AC node has to respect the P-Q capability curves. Among the converter characteristics, this chapter aims to study the effect of the losses incurred during the converter operation. As in any energy transformation process, the converter operation is not 100 % efficient, and therefore, there will be always a difference between the active power injected at one terminal, and the active power withdrawn at the other. Typical values of such losses ranges from 1 % up to 3 % of the total power going through the converter (CIGRE, 2005). Therefore, for a hypothetical case of a large HVDC Supergrid, the active power losses of the converters could represent a significant portion of all the system losses.

From the optimal operation point of view, it is common to model AC and DC transmission losses so that the OPF solution takes into account them when deciding the optimal generators scheduling. Due to the non-linear nature of the power flow equations, such transmission losses are in many cases approximated by means of simplified formulations (for instance as piecewise linear functions (Fitiwi et al., 2015)) or even neglected.

The proper modeling of converter losses is neither a simple task as there are several source of losses such as semiconductor losses, phase reactor losses and transformer losses (CIGRE, 2005; Rohner et al., 2010). Following the NLP-OPF model proposed in Chapter 3, the theoretical converter losses will be calculated as a polynomial function that depends on the phase current of the converter, and taking into account that losses can be different when the converter acts as an inverter or as a rectifier (i.e. active power injected at the AC bus or at the DC bus respectively). Given that such detailed modeling of converter losses could lead to a heavy computational burden, this Chapter will dedicate to analyze the impact of some alternative ways of modeling the converter losses in a more simplified manner. In this sense, conventional DC and AC transmission losses will be modeled by means of the exact power flow equations, so that the obtained results allow isolating the effect of the approach followed to model converter losses.

4.1.1 Converter Losses

State-of-the-art modeling ("*Complete*")

The state-of-the-art mathematical expression of the losses will be used as benchmark values for the comparison (later referred to as "*Complete*" modeling). It is previously presented as (3.5) in the NLP-OPF formulation:

$$\rho_v = A_v + B_v \cdot |i_v| + C_v^{inv} \cdot \left(i_v^{inv}\right)^2 + C_v^{rec} \cdot (i_v^{rec})^2 \tag{4.1}$$

Average modeling ("*Avg*")

It models the converter losses without differentiating between the inverter/rectifier modes by selecting the quadratic coefficient equal to the average of C_v^{inv} and C_v^{rec}, i.e.,$C_v^{avg} = {}^{(C_v^{inv}+C_v^{rec})}/_2$, as shown below:

$$\rho_v = A_v + B_v \cdot |i_v| + C_v^{avg} \cdot |i_v|^2 \tag{4.2}$$

Proportional modeling ("*Prop*")

In this case, the converter losses are assumed to be proportional to the absolute value of the real power p_c (see Fig. 3.2) injected from the converter to the c node on the AC side with certain ratio α. ρ_v is depicted in Fig. 3.3 and explained with (3.4). The constraint thereby can be written as follows:

$$\rho_v = \alpha \cdot |p_c| \tag{4.3}$$

Lossless modeling ("*Lss*")

This model simply assumes a lossless converter, thus only transmission losses (AC and DC lines) are considered.

4.1.2 Analysis Methodology

In this section, an approach to evaluate the impact of converter losses on the OPF solution of AC/DC hybrid systems is proposed using the NLP-OPF model described in Chapter 3. Firstly, it is necessary to define a comparison metric in order to compare the goodness and accuracy of the solution obtained when a simplified representation of the losses is used. Secondly, as the differences between the benchmark case and

the simplified-losses cases could depend on the particular characteristic of the system under study, it is proposed to replicate the analysis for different deployments of the HVDC grid, and for a full range of possible levels of the demand.

Comparison Metrics

The solution of the OPF of a hybrid AC/DC system consists of a large amount of output variables: active and reactive power injected by all the generators, voltage magnitudes and phase angles at every AC bus, active and reactive power flows at every AC line, voltage levels at the DC buses, and active power flows at every DC line. In order to compare easily the solution obtained with different degrees of simplification of converter losses modeling, a few indicators that summarize how far the solution obtained with the simplified losses modeling is with respect to the benchmark case are defined. As the objective function depends only on the active power generated by the units, and as active power flows are in general significantly higher than reactive power flows, the comparison will be carried out just in terms of differences of real power.

- **System costs**

Given that the *Complete* modeling provides the benchmark value of the O.F., the deviation of the other three modeling approaches (*Avg*, *Prop* and *Lss*) can be measured in relative terms as follows (4.4):

$$\Delta OF_{\%}^{Avg,Prop,Lss} = \frac{OF^{Avg,Prop,Lss} - OF^{Complete}}{OF^{Complete}} \times 100\% \tag{4.4}$$

- **Active power flow differences**

After solving the OPF, as many power flows as number of branches will be generated. In order to measure how close the solution of the simplified methods are with respect to the *Complete* modeling, the Mean Absolute Error (MAE) is proposed. Notice that positive and negative deviations are not compensated among them. Therefore, a null MAE will be obtained only in case the power flows are exactly the same. MAE is defined as follows:

$$MAE^{Avg,Prop,Lss} = \frac{1}{n}\sum_{l=1}^{n}\left|f_l^{Avg,Prop,Lss} - f_l^{Complete}\right| \tag{4.5}$$

where n is the total number of observations (i.e., number of lines), $f_l^{Avg,Prop,Lss}$ stands for the active power flow at branch l obtained with the approximated method *Avg*,

Prop or *Lss*, and $f_l^{Complete}$ is the actual value obtained with the complete modeling. The MAE of AC and DC power flows will be calculated separately in order to identify whether the impact of converter losses modeling is more relevant in one type of network than in the other. More detailed description can be found in the Section 4.1.3.

Evaluation Method

In order to take into account the dependence of the impact of converter losses on the characteristic of the power system, the the essential steps of the proposed approach can be described as follows:

1. Select a set of possible hybrid AC/DC power systems Ξ
2. For every system $\xi \in \Xi$ build a set of K demand vectors $\boldsymbol{d}^{\xi}$ where each component d_i^{ξ} represents the demand at every node i: $\boldsymbol{d}^{\xi,1}, \ldots, \boldsymbol{d}^{\xi,k}, \ldots, \boldsymbol{d}^{\xi,K}$. Demand vectors $\boldsymbol{d}^{\xi,k}$ can be obtained by multiplying the nominal demand level at every node by a factor that can range from a minimum value to a maximum one with a predetermined step size. In case the demand profiles follow any particular correlation, without loss of generality, these demand scenarios could be generated applying some more sophisticated techniques.
3. For every demand vector k simulate the optimal operation of the power system by running the OPF model presented in Chapter 3 with the complete modeling of converter losses, and with the three simplified approaches (*Avg*, *Prop* and *Lss*)
4. Compute the values of $\Delta OF_{\%}^{Avg,Prop,Lss}$ and $MAE^{Avg,Prop,Lss}$

Notice that this method is completely general and could be used to compare the solution of any OPF model with respect to the accurate solution whenever it is possible to find it.

4.1.3 Case Study

System Description

The case study systems are built based on a Modified IEEE Two Area RTS-96 (MRTS) network (Wong et al., 1999). Fig. 4.1 and Fig. 4.2 provides the single line diagrams of the two hybrid AC/DC power systems (7-Terminal and 9-Terminal that will be referred to as 7T and 9T) that are going to be studied.

Both systems share exactly the same AC network. 7T system consists of two separate MTDC mainly functioning as interconnections between the two areas (Fig. 4.1), while the 9T (Fig. 4.2) system has a more meshed configuration overlaying on the complete AC network. All the lines parameters of AC branches can be found in (Wong et al., 1999).

In the MRTS network, interconnection 107-203 is replaced by a 3-terminal MTDC network with an additional offshore wind farm (buses 301 and 302) in between. Lines 113-215 and 123-217 are replaced by a 4-terminal MTDC network. The reference (slack) buses for AC system are buses 113, 213 and 302 respectively. Two generators, located at bus 107 and 201, are disabled and replaced by the offshore wind farm at bus 302. Different cost coefficients assigned to generators can be found in Table C.3 (Zimmerman et al., 2011). All power injections and voltage levels at VSCs are considered decision variables.

Regarding the input data, 7T system is identical to the one used in (Beerten et al., 2012). To construct 9T system from 7T system, reference buses remain unchanged. $DC4$ and $DC5$ are relocated to AC buses 104 and 118 respectively. In addition, two extra DC buses ($DC8$ and $DC9$) are positioned at AC buses 219 and 206. The two corresponding converters are assigned the same parameters as the ones in $DC6$ and $DC7$ accordingly, while the others keep the same as in the 7T network. All power injections and voltage levels at VSCs are considered decision variables.

The penalty cost for non-served active and reactive power is set to be 1000 \$/MW and 1000 \$/Mvar respectively (Leveque, 2007). The ratios α used in (4.2) are calculated from computing the accurate losses at every converter, and by averaging the ratios obtained for different demand levels of the reference case and for all the converters. For each of the systems, all converters are assigned the same average value. The detailed converter and grid data are available in Appendix C (Beerten and Belmans, 2015; Zhao et al., 2017).

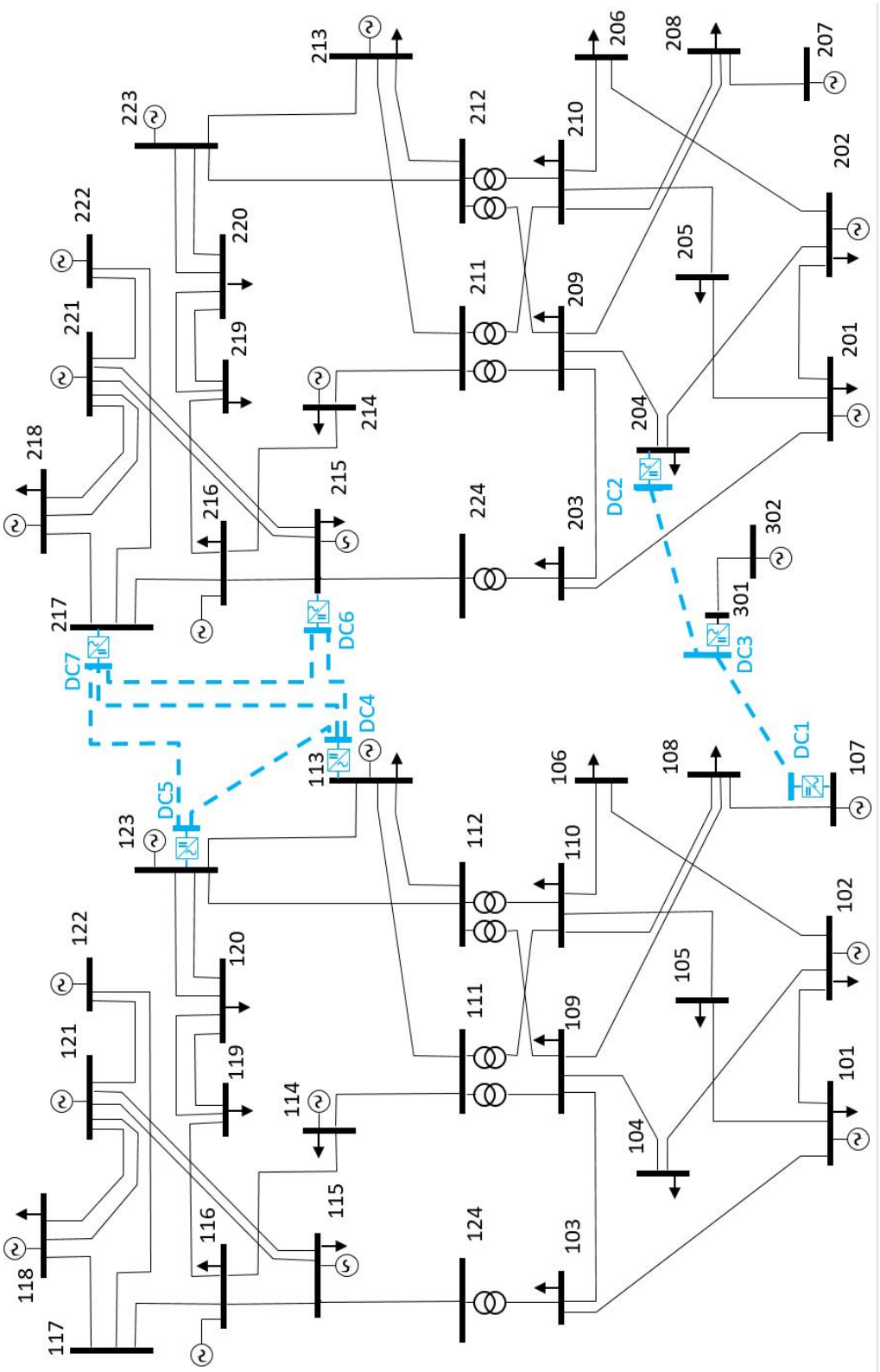

Fig. 4.1 IEEE Two Area RTS-96 with a7-Terminal HVDC networks

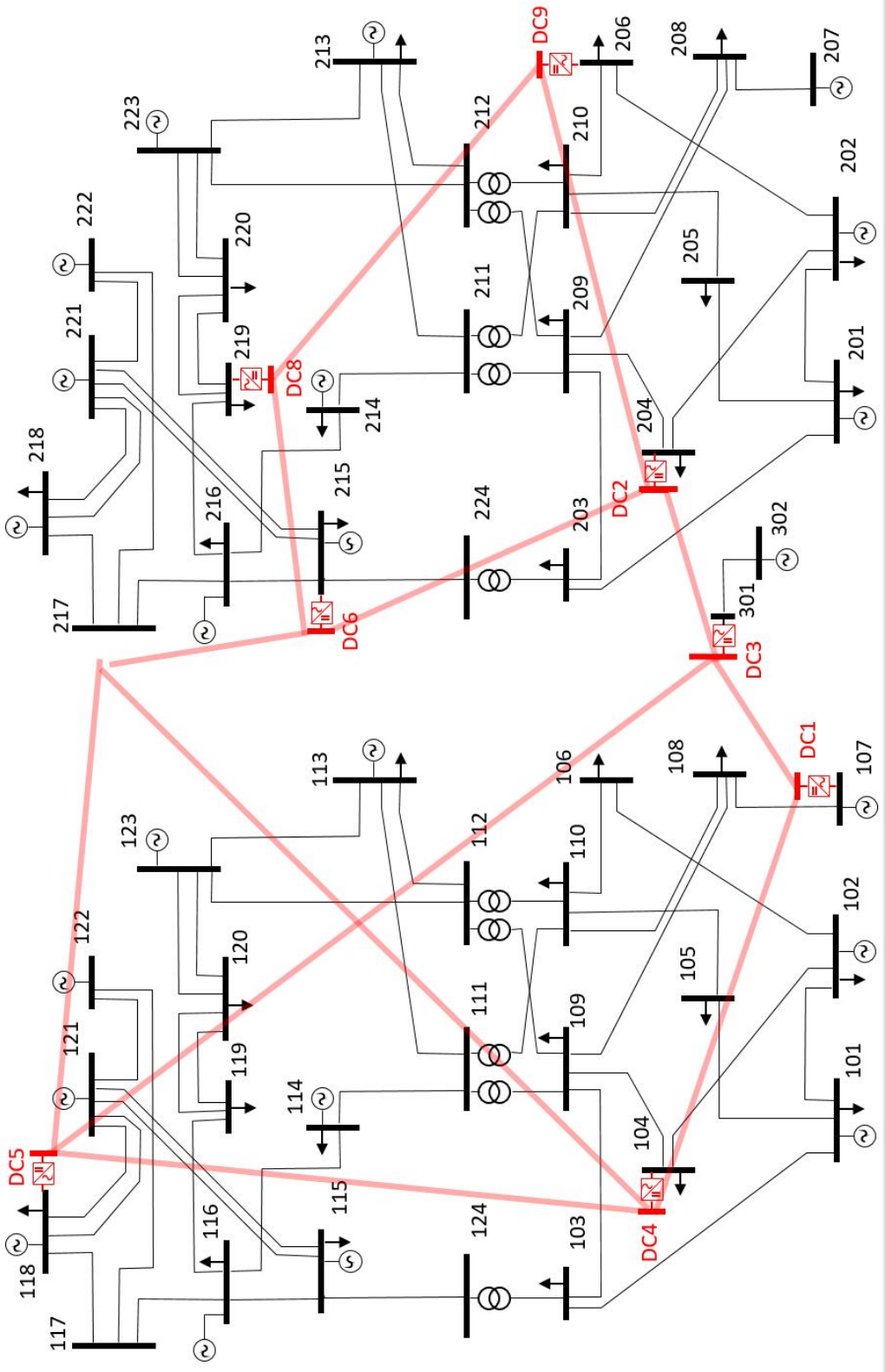

Fig. 4.2 IEEE Two Area RTS-96 with a 9-Terminal HVDC networks

Results

As in previous case studies and (Feng et al., 2014), IPOPT solver (GAMS, 2015) has been chosen given its good performance for solving large-scale nonlinear problems. Following the approach proposed in Section 4.1.2, the demand scenarios have been built by multiplying the nominal demand at every node by a factor ranging from 0.6 to 1.05 with a step size of 0.05 p.u. These limits have been identified as the ones than ensure the feasibility of the optimization problem for the topologies under study, given that unit-commitment decisions are given as input data, and therefore, it is not possible to decrease the output power below certain limits, and neither to exceed a maximum power.

Systems	**7T**			**9T**		
Modeling Methods	*Lss*	*Avg*	*Prop*	*Lss*	*Avg*	*Prop*
0.60	-0.25	0.03	0.86	-0.28	-0.13	0.43
0.65	-0.16	-0.07	-0.09	-0.13	0.05	-0.05
0.70	-0.39	-0.20	0.25	-0.11	0.22	0.13
0.75	-0.28	0.20	-0.01	-0.25	0.24	0.26
0.80	-0.31	-0.07	-0.04	-0.41	0.42	0.04
0.85	-0.23	0.26	0.05	-0.24	0.12	0.23
0.90	-0.22	0.65	0.05	-0.33	0.30	0.14
0.95	-0.26	0.50	0.45	-0.44	-0.14	0.74
1.00	-0.69	-0.04	0.08	-0.75	-0.03	0.21
1.05	-0.53	0.01	0.24	-0.25	0.11	0.61

Table 4.1 O.F. deviation in Percentage [%] (7T and 9T)

The economic impact (in % of variation of the objective function) is shown in Table 4.1 according to the expression presented in (4.4). It can be seen that the impact is close to $|1|$ % in many cases (the highest mismatches have been highlighted for each case). For instance, in the 7T system, the objective functions difference reaches 0.86% with the *Prop-* modeling while for the 9T system, such difference reaches -0.75% with *Lss-* modeling. Extrapolating these percentage to a bigger system where the size of the DC grid is comparable in relative terms as the ones used in the example cases, it could be concluded that the way the converter losses are modeled can have a significant economic implication on the overall operational costs. Notice that the *Lss-* modeling provides lower operating costs for every demand scenario as it ignores the converter losses ($\Delta OF_{\%}^{Lss} \leq 0$). For *Avg-* and *Prop-* modeling methods it cannot be identified

any particular pattern of how the values of $\Delta OF_{\%}^{Avg}$ and $\Delta OF_{\%}^{Prop}$ vary with respect to the demand.

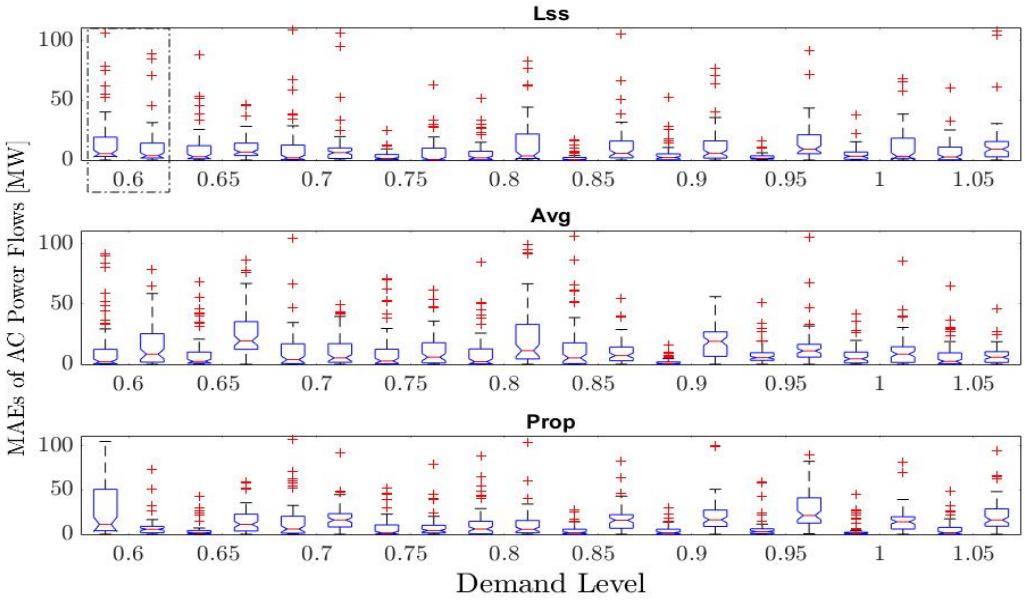

Fig. 4.3 MAE of AC Power Flows [MW] (7T/9T)

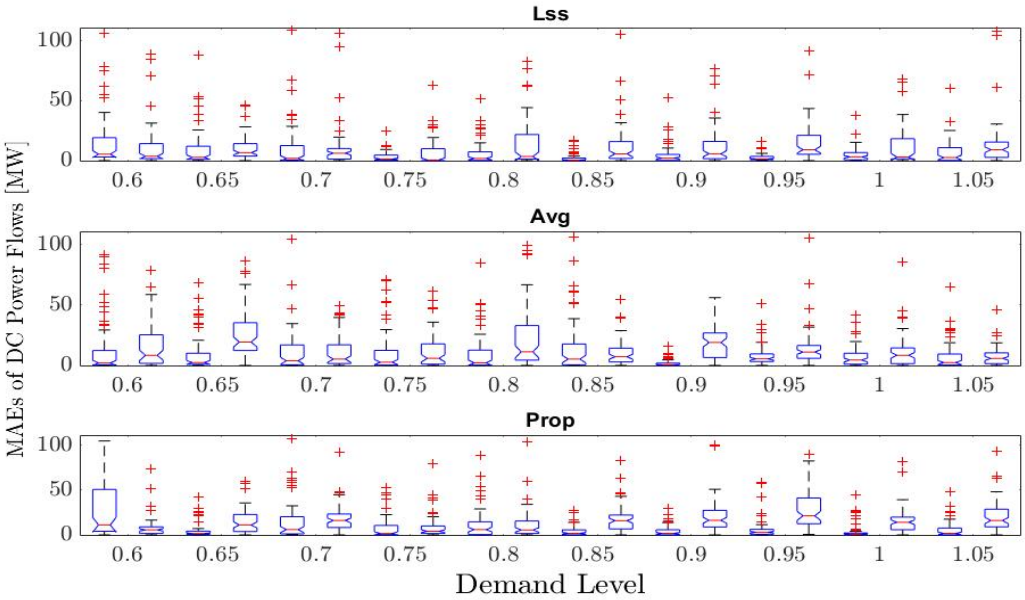

Fig. 4.4 MAE of DC Power Flows [MW] (7T/9T)

Regarding the impact on power flows, AC and DC lines are analyzed separately for each modeling method by comparing their MAE according to (4.5). The results of 7T and 9T systems are plotted together by pairs for each demand factor value. For instance, the dash-dotted rectangular box in Fig. 4.3 shows the boxplots for the 7T (on the left) and 9T (on the right) systems for the demand level of 0.6. Figs. 4.3 and 4.4 present the boxplots of the absolute differences of power flows at every AC and DC line respectively for every demand level. For a given box-plot, the straight horizontal line in red represents the obtained MAE for all lines in that demand level scenario. In this case study, the widely acknowledged definition of boxplot, also known as box-whisker diagram, is adopted (Upton and Cook, 1996; Zwillinger and Kokoska, 1999). The blue box contains 50% of the data set once the outliers (marked as "+" in red) have been discarded (i.e. lower and upper boundaries are 25^{th} and 75^{th} percentiles). Tables 4.2 and 4.3 provide the numerical values.

Systems	**7T**			**9T**		
Modeling Methods	*Lss*	*Avg*	*Prop*	*Lss*	*Avg*	*Prop*
0.60	16.98	13.42	23.94	13.81	16.30	12.70
0.65	10.29	9.33	4.74	10.18	17.07	13.24
0.70	9.96	10.79	17.18	9.83	11.95	14.35
0.75	2.95	11.13	7.42	6.65	12.84	11.54
0.80	6.28	9.32	11.38	12.91	17.96	14.80
0.85	2.08	13.25	3.81	11.70	11.64	14.20
0.90	4.61	1.82	3.98	13.31	16.14	15.51
0.95	2.59	7.79	6.11	15.20	13.36	17.68
1.00	4.74	7.38	3.89	12.98	12.34	13.92
1.05	6.53	7.00	5.81	12.98	9.66	15.37
Mean	**6.70**	**9.10**	**8.82**	**11.96**	**13.93**	**14.33**

Table 4.2 MAE of AC Power Flows [MW]

It is important to highlight that for both 7T and 9T systems, AC branch power flows differences are in general smaller when compared to DC branches. In addition, AC flows MAE are higher 70% of the studied cases in the 9T system. However, for the DC flows the behavior is the opposite one: only 10% of the studied cases the DC flows MAE is higher for the 9T system. Therefore, for these study cases it could be concluded that the more meshed the DC grid is, the higher the impact on AC flows are due to not modeling the converter losses in an accurate manner. However, for the DC flows, the more meshed the DC grid is, the lower the impact on DC flows.

Systems	**7T**			**9T**		
Modeling Methods	*Lss*	*Avg*	*Prop*	*Lss*	*Avg*	*Prop*
0.60	52.42	89.23	65.57	20.67	20.55	17.15
0.65	65.24	58.85	26.69	13.53	21.51	16.35
0.70	57.64	46.73	71.61	18.00	15.81	16.17
0.75	20.98	63.30	49.05	13.32	17.32	12.89
0.80	30.92	46.84	52.20	20.89	23.70	20.25
0.85	12.56	73.98	18.46	18.99	15.48	16.65
0.90	28.23	10.83	19.99	21.05	21.34	19.90
0.95	13.16	33.31	36.70	20.15	17.70	23.73
1.00	17.88	28.78	26.91	20.98	16.93	17.72
1.05	35.14	29.59	25.75	18.16	11.64	18.29
Mean	**33.42**	**48.15**	**39.29**	**18.57**	**18.20**	**17.91**

Table 4.3 MAE of DC Power Flows [MW]

Another interesting finding is that *Lss*- modeling outperforms other two methods for AC branches in both systems (the average MAE values 6.70 and 11.96 are lower than the ones of *Avg*- and *Prop*- approaches). However, for DC branches, *Lss*- modeling only outperforms for the 7T case. For the 9T case the best approach is the proportional method. What is more important is that in all these cases, the power flow differences of DC branches (in MW) are very large considering their maximum capacities. For instance, even for the lowest average mismatch case (the *Prop*- modeling for the 9T system), the value 17.91 MW is very relevant taken into account that the capacity of the lines is 100 MW (see Table C.7).

4.1.4 Conclusion

In this analysis, converter losses have been modeled in the most accurate way according to the state-of-the-art, and three alternative approaches (lossless, proportional and average) have also been implemented. As the impact assessment can depend on the level of deployment of the DC grid, two systems have been studied: one with only interconnecting DC lines (7T system) and another one with a very meshed configuration (9T system).

Obtained results show that the OPF solution is highly dependent on how converter losses are modeled. From the study case, it can be concluded that when the system is not heavily meshed, the lossless approach is the best way if complete modeling of converter losses is not possible. However, for meshed DC grids, none of the considered simplified

approaches outperforms when analyzing the AC and DC power flow mismatches. Therefore, the main conclusion that can be drawn from this study is that not modeling the converter losses in an appropriate manner could lead to very different power flow values compared to the accurate formulation, especially for the DC branches. Apart from the pure operational point of view, this issue should be taken into account when planning the expansion of future MTDC networks.

Chapter 5

Technical-Economic Impact Assessment of a North Sea HVDC grid on the pan-European System

This chapter shows the application of the LP-OPF model presented in Chapter 3 to assess the technical-economic impact of a possible HVDC network deployed at the North Sea on the European electric power system.

5.1 Introduction

As explained in Chapter 1, the concept of the *supergrid* is seen as a promising solution to help to integrate larger amounts of RES generation in the power system, and therefore, to contribute to mitigate global climate change. Whether this *supergrid* will eventually be developed or not is somewhat uncertain. However, what can be assured is that its potential development will be made in a gradual manner over time. Given that there is a great potential for offshore wind energy in the North Sea, it seems logical to think that the future HVDC network will be built through the interconnection of more and more offshore wind farms, both among themselves, and between these farms and the conventional AC systems of different countries. In addition, OPF models are commonly used not only for power system operation, but also for planning purposes. However, as previously discussed in Chapter 2 and 3, conventional OPF models only consider AC systems. Few works have considered HVDC systems under an optimization context (Baradar et al., 2013; Cao et al., 2013; Feng et al., 2014). Among them, (Wang, 2013b)

is the only work that covers both aspects but with a small size system of 32 buses. Consequently, there is a need for new models that fit real-life practice and the LP-OPF model presented in Chapter 3 can contribute to make operation and planning studies of large-scale systems. Furthermore, solving large-scale networks (for example, European network) with TEP models is prohibitively expensive or even impossible if considering inter-temporal links and uncertainties (Fitwi, 2016; Lumbreras Sancho, 2014; Zhang, 2013). The proposed LP-OPF model is able to deal with large-scale hybrid networks by reducing the complexity of the problem and enhancing tractability. Meanwhile, it tackles the problem of underinvestment resulted from neglecting system losses (as shown in (Fitwi, 2016)), by taking into account all the detailed representation of networks and converters losses.

5.1.1 Review of offshore wind development in EU

Meeting the rising energy requirements in a sustainable, secure and competitive manner is one of the main challenges of current power systems. In order to achieve such goal, a larger integration of RES is needed. Offshore Wind Farms (OWFs) are expected to supply a significant portion of future energy needs and, in that sense, the European Wind Energy Association (EWEA) estimated in 2011 that 150 GW of offshore wind capacity would be installed by 2030, producing 562 TWh of electricity annually to cover 14% of the EU's electricity demand (Arapogianni et al., 2011). However, a careful analysis of the trend during the last years regarding the evolution of OWF installed capacity in Europe makes such estimation too optimistic unless potential barriers are overcome. Thus, in the last report Key trends and statistics 2017 published by *WindEurope.org*, the expected offshore wind power cumulative capacity to 2030 is 72.2 GW for the central scenario, 49.5 GW for the low scenario, and 98.93 GW for the high scenario (WindEurope, 2018). Next figure shows the EU cumulative installed capacity of OWF during the time period 1991-2017 (Fig. 5.1).

Despite the obvious increasing trend, the original EWEA estimation would imply to increase the current installed capacity by a factor of 10. Table 5.1, Table 5.2, and Table 5.3 show the capacity installed by each country in each one of the covered years, where only the countries with not-null installed capacity have been included.

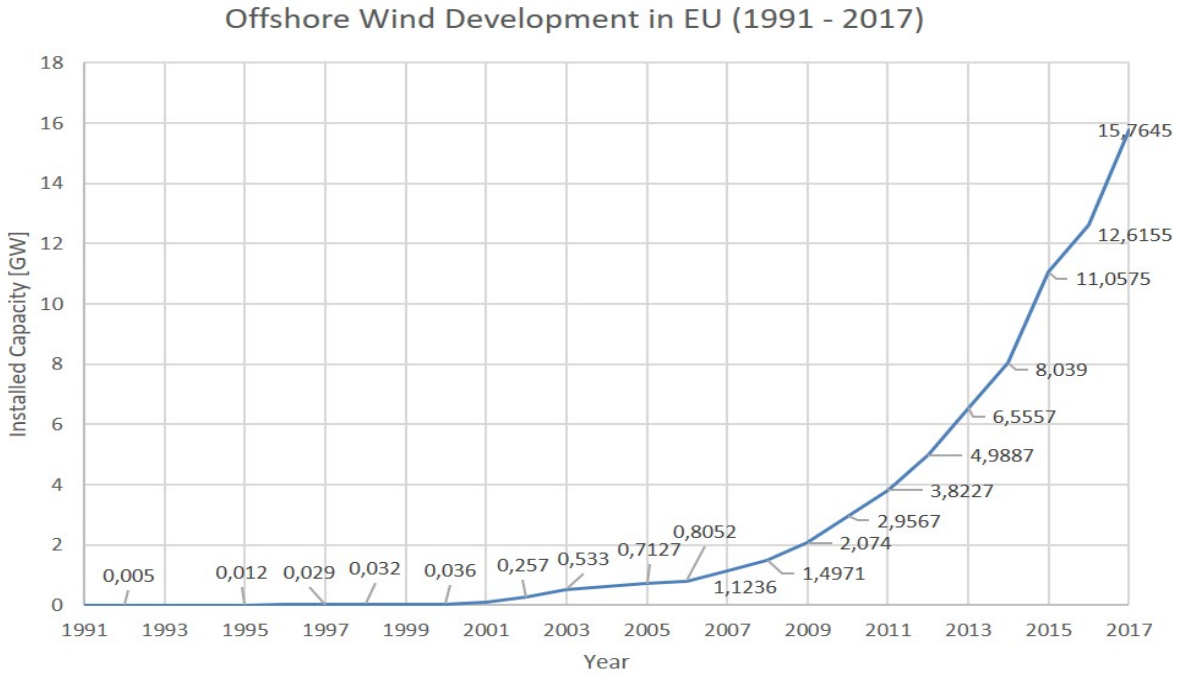

Fig. 5.1 EU Offshore wind development from year 1991 to 2017 (GW of installed capacity)

Country/Year	**1991**	**1992**	**1993**	**1994**	**1995**	**1996**	**1997**	**1998**	**1999**
Accumulated [GW]	0.005	0.005	0.005	0.007	0.012	0.029	0.029	0.032	0.032
Annual Total [MW]	4.95	0	0	2	5	16.8	0	2.8	0
Denmark	4.95				5				
Netherlands				2		16.8			
Sweden									2.8

Table 5.1 Offshore installed capacity per year and country [MW] during 1991-1999

Country/Year	**2000**	**2001**	**2002**	**2003**	**2004**	**2005**	**2006**	**2007**	**2008**	**2009**
Accumulated [GW]	0.036	0.087	0.257	0.536	0.623	0.713	0.805	1.123	1.490	2.074
Annual Total [MW]	3.8	50.5	170	279	89.7	90	92.5	318	366	576.7
Belgium									30	
Finland									24	
Germany					4.5		2.5		5	30
UK	3.8			4	60	90	90	100	187	284.4
Denmark		40	160	233						230
Netherlands				19				108	120	
Sweden		10.5	10	23				110		30
Norway										2.3
Ireland					25.2					

Table 5.2 Offshore installed capacity per year and country [MW] during 2000 - 2009

Country/Year	**2010**	**2011**	**2012**	**2013**	**2014**	**2015**	**2016**	**2017**
Accumulated [GW]	2.957	3.823	4.988	6.557	8.039	11.058	12.616	15.765
Annual Total [MW]	882.73	866.35	1165.6	1568	1483.3	3018.5	1558	3149
Belgium	165		184.5	192	141			165
Finland	2.3							60
France								2
Spain				5				
Germany	50	108.3	80	240	528.9	2282.4	813	1247
UK	458.4	752.45	854.2	733	813.4	566.1	56	1680
Denmark	207.03	3.6	46.8	350				-5
Netherlands						180	691	
Sweden				48		-10		
Portugal		2					-2	

Table 5.3 Offshore installed capacity per year and country [MW] during 2010 - 2017

During the early stages of OWF industry development, the distances between the wind turbines and the shore were small. For instance, the world's first OWF project named Vindeby (Denmark) started in 1991, and consisted of 11 wind turbine generators (WTG) (450 kW each) that were placed 2 km from the coast. In 2012, the average distance to shore of the new installed OWF was 29 km, and in 2017 this value was 41 km[1]. The selection of the most appropriate technology depends basically on the distance from the existing AC network, and for low distances AC transmission systems are preferred. In any case, there is a need to be able to capture offshore wind resources at higher distances, where wind energy resources can be more abundant taking advantage of the last technological advances of WTGs and power electronics. In this framework new OWFs are being built at 1) rising distances to shore, and 2) for higher levels of transmitted power. These two factors limit the feasibility of High Voltage Alternating Current (HVAC) transmission schemes (CIGRE, 2013a). In (Ergun and Hertem, 2016) it is discussed that the breakeven distance of High Voltage Direct Current (HVDC) system interconnected by cables is about 120 km in terms of total costs, although the decision to choose HVDC instead of HVAC depends on the particularities of the project, and such breakeven distance could be smaller.

5.1.2 Storyline

Under the context of the *BestPaths* project as described in Section 1.1.2, in order to assess the impact of *BestPaths* technologies, it is necessary to perform simulations on two scenarios. Both scenarios are forward looking year 2030 with detailed network representations. One considers *BestPaths* technologies while another takes into account the capabilities of *BestPaths* technologies, such as HVDC grids, AC corridors repowering techniques (HTLS conductor, DLR, etc.), together with an expansion on the network. The objective is to study the economic benefit that could be brought by proposed technologies.

The entire expansion can be divided into two parts: 1) North Sea Offshore Grid (NSOG) expansion which mainly utilize HVDC technologies to host more offshore wind resources and 2) continental AC corridors repowering which is meant to increase transmission capacity. Since this thesis focuses on HVDC technologies and offshore wind integration assessment, the chapter will concentrate on the NSOG expansion part.

[1]Source: https://windeurope.org

To carry out the case study, two scenarios are also built, simulated and compared (later referred as *Reference* and *NS HVDC* scenarios respectively). Building of these two networks are described in detail in the following sections. The purpose of the case study is to assess how much techno-economic impact it can bring to the Continental Europe (CE) with additional offshore infrastructure.

5.2 System Description

5.2.1 Reference scenario

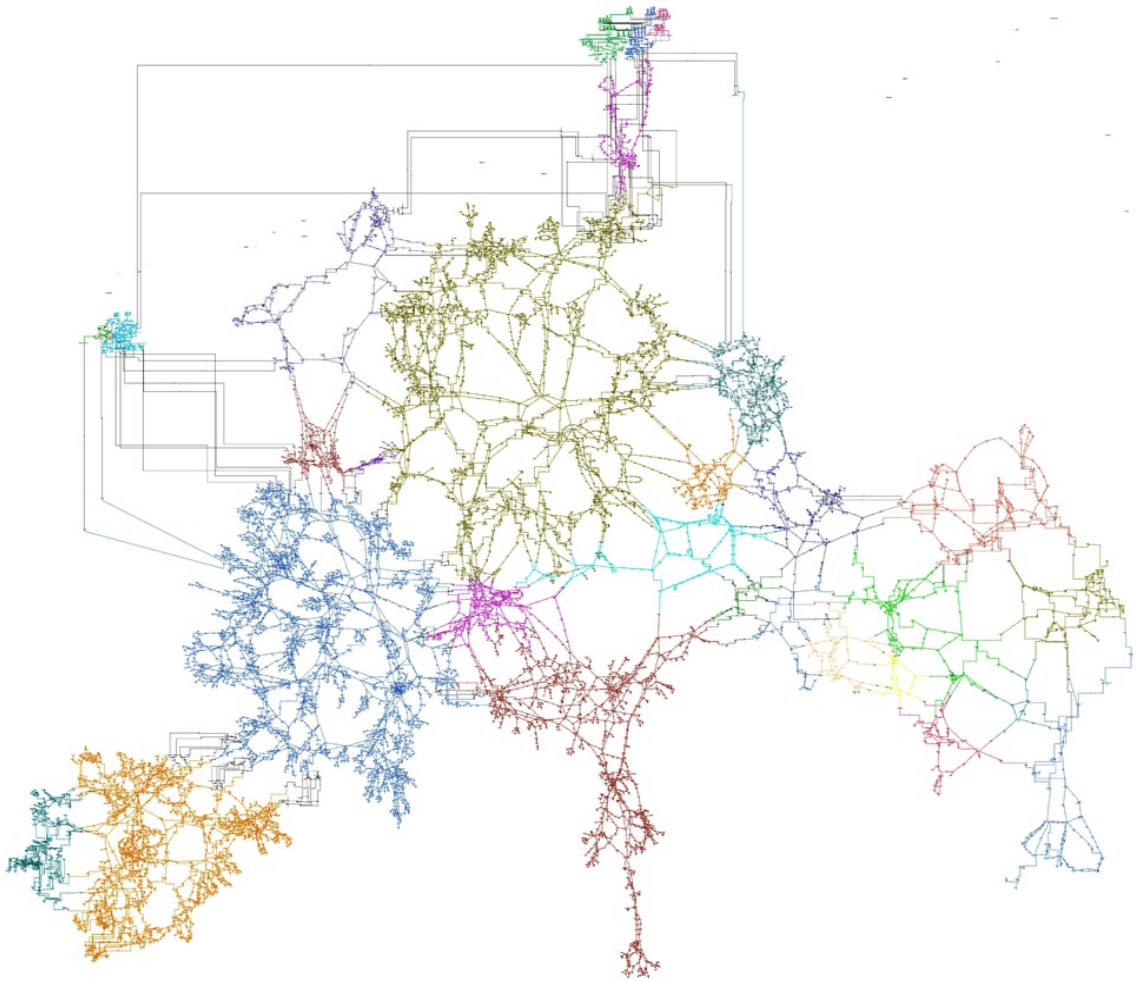

Fig. 5.2 Reference Network

The *Reference* network topology is built based on the reduced network provided as input in the context of *BestPaths* project. The original network has combined different sources of data: ENTSO-e, TYNDP2016 and e-Highway2050 project. After the network reduction, only parts that are at voltage level 220 kV and above remain. For the original combinatorial network, the CE part is provided by ENTSO-e, while UK and Scandinavia region are represented in a highly aggregated way with few nodes per country (which was developed in the e-Highway2050 project). Transmission projects which are ought to be commissioned before 2030 (and included in TYNDP 2016) are also considered in the *Reference* and *NS HVDC* scenarios. Initial load and generation data are based on statistical fact sheet and power statistic data base published by ENTSO-e (ENTSO-e, 2016, 2017), while the projection for 2030 is based on the EUCO30 scenario (IIASA, 2017). Details concerning *Reference* data set are included in the (Zhao et al., 2018). The summary of the *Reference* network characteristics is depicted in Table 5.4 and the schematic illustration is shown in Fig.5.2.

Elements	**Amount**	**Type**	**Amount**
Network Nodes/Buses	7789	AC	7483
		DC	306
Lines	8927	AC	8783
		DC	144
RES Generators	299	Solar PV	42
		Offshore Wind	9
		Onshore Wind	248
Hydroelectric Power Plants	171	Pumped Storage	84
		Other Hydroelectric	87
Loads	3413	-	-
2 Winding Transformers	1148	-	-
Converters	306	-	-
Conventional Generators	765	-	-

Table 5.4 Summary of the *Reference* network characteristics

Regarding the North Sea offshore part, there are in total 9 aggregated offshore nodes with each representing a certain region of the North Sea wind resources. This is aligned with the starting point of the expansion model which are used to build the *NS HVDC* scenario. More details are explained in the next section. A schematic illustration is shown later.

OWFs	Installed Capacity GW
117_ns	6.299
118_ns	3.149
119_ns	0.525
120_ns	0.525
121_ns	2.172
122_ns	2.534
123_ns	7.964
124_ns	1.629
125_ns	0.543
Total	**25.34**

Table 5.5 Summary of North Sea OWFs in *Reference* scenario

5.2.2 Building NS HVDC scenario

Methodology

Building a credible scenario on an HVDC network in the North Sea that takes advantage of the possibility of having multi-terminal systems leads to several difficulties. The first one is that apart from the network developments that are taken into account in the TYNDP 2016, there is no clear consensus on the HVDC Offshore Grid architectures that could be implemented in the coming years. In addition, governance constraints among involved countries can affect notably the final adopted design. Therefore, a state-of-the-art review is firstly performed on several HVDC Offshore Grid architectures and research projects where the study case is the European system, namely: OffshoreGrid (Decker et al., 2011), EWEA (Fichaux et al., 2009) and Friends of the Supergrid (FOSG) (FOSG, 2010). The features of those networks are summarized in Table 5.6.

It can be observed that all the studies are considerably out-of-date, meanwhile the assumptions are rather diverse. It is needed to keep in mind that to find an optimal development for a transmission system is an extremely challenging task. Not only because the size and complexity of the resulting optimization problem is very high, but also because some aspects such environmental, social, and governance issues, are difficult to be modeled in a quantitatively manner. All the previous reviewed research work have considered pure transmission expansion problems. However, it is important to highlight that building *NS HVDC* scenario is a more complex problem than a traditional TEP problem as the development of the offshore grid involves making

Projects	Features
OffshoreGrid	• Proposed in 2011 considering a potential capacity of 126 GW offshore wind, amount to 13.330 TWh in 25 years.
Split Design	• Development is planned in three steps which requires a long time, "*realization within a reasonable time frame raises challenges*". • Step 3 development is rather ambitious which contains a central node connecting 4 nodes, "*a variety of new technologies needed for safe and secure operation, particularly with respect to power flow control mechanisms, security issues, increased capacity and reduction of energy losses*": - The key issue to be tackled is MT operation: DC CB - TSO lacks of experience with MT operation • It builds nodes in areas where the projects are canceled[4].
EWEA	• Proposed in 2009. It considers 150 GW installed capacity producing 563 TWh annually in 2030 which according to the evolution of the development of the off-shore industry in Europe seems too optimistic.
2030 time frame	• The proposal does not cover all North Sea wind potentials. • The designed topology connects DC nodes with 4 other nodes.
FOSG	• Proposed in 2010. It considers 23 GW of offshore wind installed capacity (from the Firth-of-Forth, Dogger-Hornsea, Norfolk Bank, German and Belgian Offshore clusters) which does not capture the current known potential wind resources.
Phase I	• The design is based on the concept of a superNode[5] that does not consider the individual converters representation. • Central node located in the North sea portion belonging to the UK has 5 links. • Extendable to onshore: beneficial from the overall European perspective.

[3] Current state of North Sea OWFs development can be accessed here: http://www.4coffshore.com/offshorewind.

[4] The SuperNode interconnects HVDC links with offshore wind parks via a small islanded AC network (node).

Table 5.6 Summary of features of previously proposed offshore grids

decisions not only regarding the construction of new lines, but also the installation of additional wind farms. Thus, it is a Generation and Transmission Expansion Planning (GTEP) problem.

Therefore, with the aim of avoiding being conditioned by any type of restriction, it has been decided to use an expansion planning model called Offshore Grid Expansion Model (OGEM) (Dedecca, 2017), focused on the specificities of the North Sea that is able to find the optimal integrated HVDC network to host the optimal amount of available wind resource potential keeping a right balance between investment costs and operational saving. The model has used a simplified network representation to enhance the tractability. The overall planning problem consists of determining the optimal transmission capacities that should (or should not) be installed among the nodes of the grid, as well as the generation capacities, i.e., OWFs that should be installed at the pre-selected offshore nodes. More details regarding the description of the model and assumptions can be found in (Dedecca et al., 2018; Zhao et al., 2018).

The initial system is based on the e-Highway 2050 project. It has 103 on shore nodes (to represent the CE, UK and Scandinavia region) and 9 offshore nodes interconnected through HVAC and PTP HVDC lines. The model considers three possible offshore transmission technologies, i.e., HVAC, PTP HVDC and MTDC, which are characterized by their corresponding techno-economic parameters. HVAC are connected directly to AC nodes, while PTP HVDC and MTDC are connected to AC nodes through converters. DC CBs are considered for MTDC network. The model considers 25.34 GW of offshore wind power installed capacity as starting point with additional potential of 25.75GW in 2030 (Table 5.5) (James et al., 2017), and assess the profitability of adding extra capacity to reach a maximum of 115 GW total capacity in 2050. The maximum possible installed capacities aligns with e-Highway2050 project (e-Highway2050, 2015). As a result of applying OGEM, four additional OWFs were built (together with original 25.34 GW resulting in a final installed capacity of 45.52 GW in total which allows to capture 173 TWh/year of energy) and 8 additional lines (3 AC lines and 5 DC lines constituting 2 MTDC grids) at the end of 2030. Thereafter, these investment decisions (both generation and transmission) are plugged back into the *Reference* network to form *NS HVDC* scenario.

Finally, the schematic illustration of NSOG for both *Reference* and *NS HVDC* scenarios are shown in Fig. 5.3. Existing connections are represented by black solid lines. Please note that each node is an aggregated node that represents wind installed capacity within a certain area. In order to differentiate between existing OWFs and

OWFs	Installed Capacity GW
117_ns	6.299
118_ns	3.149
119_ns	0.525
120_ns	0.525
121_ns	2.172
122_ns	2.534
123_ns	7.964
124_ns	1.629
125_ns	0.543
106_ns	3.540
111_ns	4.968
112_ns	11.055
114_ns	0.614
Total	**45.52**

Table 5.7 Summary of North Sea OWFs in *BP HVDC* scenario

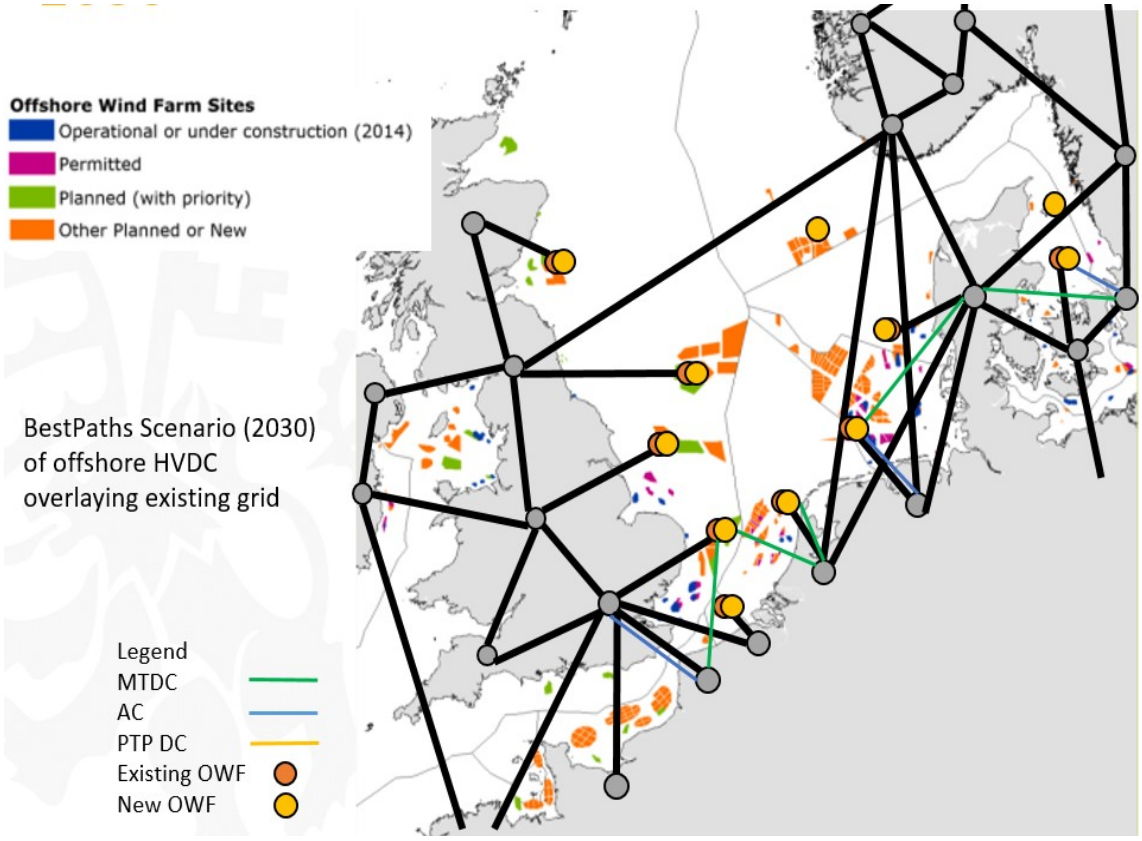

Fig. 5.3 NSOG Expansion Plan for 2030. The legend on the top-left corner and the background map is from ECOFYS (Cole et al., 2014)

candidate offshore wind clusters (that will be decided by the OGEM model), the 9 offshore nodes in the *Reference* scenario are represented by orange circles with black periphery and the new offshore wind clusters or OWFs are depicted in light-orange circles (in total, there are 11 nodes). The model assumes that adding new wind farms in the nodes where there is already existing installed generation will entail the development of new lines. In addition, it considers the possibility to install new wind farms in the candidate nodes characterized by a maximum wind resource that could be captured. For illustrative purpose, the aggregated nodes that represents expansion of existing ones are placed close to the existing ones.

It is important to highlight that the offshore grid involves the participation of several actors that can belong to multiple levels, ranging from the sub-national entities in charge of network planning studies, until the European institutions responsible for defining the energy policy. The fact that the new corridors allow not only to connect wind farms developed by each country with its own AC system, but also serve as additional interconnection ties between different countries, represents a quite difficult challenge from the planning point of view. In this sense, the model OGEM allows to include or not a set of constraints derived from governance issues that may condition the development of the network. In order to achieve the most efficient design, the model has been run removing such set of constraints that have been proven to hinder the deployment of MTDC grid (Dedecca et al., 2018). This approach is aligned with the recommendation provided in (Zhao and García-González, 2018) regarding the need to foster a coordinated planning of both AC and DC future networks.

One thing worth to mention is that OGEM model is not oriented to produce a very detailed network representation of the wind-farm assets and detailed grid modelling. It is rather oriented to provide a regulatory insight to assess the impact of governance constraints for future expansion and therefore it has some limitations. For example, a highly aggregated network is used to reduce the complexity of the optimization problem and to enhance the tractability of the problem. Despite this fact, the model takes into account the impact of the investment cost required to build the new infrastructures according to the total capacity installed and the type of line built (AC, HVDC point-to-point, or HVDC multiterminal). In addition, security constraints are not considered in the model for the same reason. Meanwhile, since UK and Scandinavia region are already represented with DC links (Fig. 5.3), profitability is the only considered factor when building connections between this region with the continental Europe. It can be

observed that between UK and France, the model has decided to build an AC link. This may appear inappropriate and unrealistic.

In all ways, the focus of this case study is to demonstrate the applicability of the model, and at the same time to show an example on how to assess a large-scale system (e.g., pan-European) from a techno-economic perspective. Whether or how to build a practical NSOG is out of the scope here.

Analysis of the NSOG with and without consideration of DC CB cost

As discussed in the barriers identification of demos 1 and 2 of (Zhao and García-González, 2018), DC CB is an indispensable component for MTDC system protection and CB costs can go up to one sixth of the cost of a converter station (CIGRE, 2013a). In Fig. 5.3, OGEM has assumed the commercial availability of DC CBs. However, the related investment costs are very high. In order to assess the impact of DC CBs cost on the entire NSOG topology, the expansion problem was solved again assuming null DC CB cost. It is important to notice that this assessment has been carried out just to assess the impact of this cost parameter which is subject to uncertainty.

As a result, complete network topology is generated. Since this part of the analysis is out of the scope of the thesis, for simplicity, expansion results are not shown here but can be referred to in (Zhao et al., 2018). It is difficult to compare visually the obtained grids with and without DC CB costs, since the total investment level depends on two factors: length of the lines and related capacity. In order to compare the two cases, the total products of lengh (km) and capacity (GW) for each transmission technology are listed respectively (Table 5.8). It is possible to check that the non consideration of DCCB cost increases the installed capacity of MTDC grids.

Type	**MTDC [km.GW]**	**AC [km.GW]**	**PTP DC [km.GW]**
with DC CB cost	9312.87	4855.53	5375.04
without DC CB cost	11815.27	1991.03	4913.79

Table 5.8 Transmission investment level comparison

On one hand, MTDC investment costs (including DC CB cost) could be lower than an equivalent PTP HVDC grid, since each node would only need one converter to absorb and inject power. On the other hand, it is not necessary for the OGEM to favor a MTDC structure since in that case, power flows through lines are constrained by

power flow equations, while for PTP links, the capacity is only limited by the thermal capacities. Therefore, there is a trade off between savings from converter investment for MTDC network and additional power flow constraints.

In this assessment, it is indeed observed that without consideration of DC CB cost, OGEM shifts the investment and intends to invest more in MTDC network rather PTP DC links or AC lines, i.e., from 9312.87 km.GW to 11815.27 km.GW.

5.3 Case Study

In the case study, for the sake of brevity, eight days with extreme conditions are chosen according to the demand and RES conditions. Since some days are overlapped with the others, in total, five days are simulated for demonstration purposes of the assessment (shown in Table 5.9). It shall be noted that if one wants to assess the system in a comprehensive manner, the whole year simulation would be needed. To explain further how the subscript of the notation were formed: the first one or two letters in small case indicates either hourly (with h) or daily (with d) or both (with hd); the consecutive two letters can be seen as a group, of which the first capital letter refers to RES (with R) or Demand (with D), then the situation is peak (with p) or valley (with v).

Selected Days	**Features**	**Notation**
D_{20}	the day when hourly demand peak occurs the day when hourly RES valley occurs	D_{hDpRv}
D_{21}	the day when daily demand peak occurs	D_{dDp}
D_{54}	the day when hourly RES peak occurs the day when daily RES peak occurs	D_{hdRp}
D_{177}	the day when daily RES valley occurs	D_{dRv}
D_{226}	the day when hourly demand valley occurs the day when daily demand valley occurs	D_{hdDv}

Table 5.9 Selected Days for Techno-Economic Impact Assessment

In the case study, the penalty cost for non-served active power is set to be 1000 €/MW (Leveque, 2007). All generators are identified and categorized into five types: combined cycle units, hydro plants, nuclear plants, coal thermal plants and RES. Cost information is assigned accordingly (Zhao et al., 2018). For hydro units, prior to running the LP-OPF model, a high level scheduling model is assumed to provide hydro-thermal coordination. In each hour, a maximum and minimum production

level is given as input in order to constrain the total energy it allows to produce. In addition, coal and combined cycle units are subject to an extra environmental cost. Carbon price is set to 7.6 €/ton (Healy et al., 2016). Emission factors for coal and combined cycle plants are assumed to be 0.9 ton/MWh and 0.4 ton/MWh respectively (Lopez-Pena Fernandez, 2014).

Indicators	**Abbreviation**	**Unit**	**Definition**
Operating Cost	O.C.	M€	generation unit production cost
Energy non-Served	ENS	%	share of energy not supplied
RES Penetration	RES	GWh	total RES generation
RES Curtailment	RES Curt.	%	share of RES not dispatched
CO_2 Emission	Ems.	Mton	emission due to thermal unit productions

Table 5.10 List of Techno-Economic Impact Assessment Indicators

Results shown in this section are generated by using CPLEX solver with a tolerance of 1E-3. In order to demonstrate how an HVDC infrastructure can be assessed from a techno-economic point-of-view, several indicators are proposed and listed in Table 5.10 for comparison.

5.3.1 Results

In Table 5.11, factors contributing to economic impact are presented. In the picked days for both scenarios, the lowest operating cost (O.C.) happens on the demand valley day (first row) and the highest O.C. happens on the hourly demand peak day while hourly RES presence is the lowest (fifth row) in the system. With more RES introduced in the system, the second highest O.C. happens on the demand peak day (second row). The O.C. is continuously lowered on the RES peak day (third row). Finally, on the RES valley day (fourth row), the O.C. is slightly higher than demand valley day. Variations in O.C. consequently have an impact on the environment with more or less carbon emissions which is shown in Table 5.13 and will be discussed further later.

It can be clearly observed that with the support of additional NS HVDC infrastructures, operational cost savings can be obtained in all cases. Even in the demand valley day, the O.C. has decreased 1.6% which amounts to 438 M€ annual savings. Information on Capital Expenditure (CAPEX) is normally unavailable, and in general, it is hard to make sensible estimation. Nevertheless, given the expected operating time

Days	Reference			NS HVDC			Comparison	
	O.C. [M€]	ENS [%]	RES [GWh]	O.C. [M€]	ENS [%]	RES [GWh]	ΔO.C. [%]	ΔRES [%]
D_{hdDv}	79.0	0.0	1285.6	77.8	0.0	1351.7	-1.6	5.1
D_{dDp}	247.4	0.1	1115.2	236.9	0.1	1300.6	-4.2	16.6
D_{hdRp}	145.1	0.0	2169.4	136.9	0.0	2352.2	-5.7	8.4
D_{dRv}	91.1	0.0	956.9	87.7	0.0	1096.2	-3.7	14.6
D_{hDpRv}	257.5	0.1	1037.3	246.9	0.1	1222.5	-4.1	17.9

Table 5.11 Economic Impact of *Reference* and *NS HVDC* Scenarios without consideration of RES in Distribution Level

scope, variations in OPEX could provide a lump sum of how much investment would be allowed in order to be cost-effective for the long term.

In this case study, result on ENS reduction is not obvious since there are not much ENS within the system. However, RES penetration has shown a significant increase, in particular, days that have less RES available. Please note here, since both networks have only taken into account the part that is 220 kV and above, the RES level indicated in the table only refers to high voltage level, i.e., Transmission Level (TL). Together with renewable energy at the Distribution Level (DL), the total RES penetration within the system is shown in Table 5.12.

Days	Reference			NS HVDC			Comparison
	TL [GWh]	DL [GWh]	Total [GWh]	TL [GWh]	DL [GWh]	Total [GWh]	ΔRES [%]
D_{hdDv}	1285.6	2724.4	4010.0	1351.7	2724.4	4076.1	1.65
D_{dDp}	1115.2	2276.0	3391.2	1300.6	2276.0	3576.6	5.47
D_{hdRp}	2169.4	2860.3	5029.6	2352.2	2860.3	5212.4	3.63
D_{dRv}	956.9	2467.3	3424.2	1096.2	2467.3	3563.5	4.07
D_{hDpRv}	1037.3	2322.0	3359.3	1222.5	2322.0	3544.5	5.51

Table 5.12 RES penetration level of *Reference* and *NS HVDC* Scenarios with consideration of RES in Distribution Level

Without consideration of DL (Table 5.11), looking at column ΔRES in % and again, the lowest increment happens in the demand valley day and highest occurs on the hourly demand peak day with hourly lowest RES. It shows the same order when comparing O.C. in M€. On the day where the highest RES is available, the support that brought by the additional NS infrastructure is modest (8.4%). Although one day

(24-hour snapshots) simulation cannot regard as conclusive, this may shed some light on when additional transmission projects start to become less cost-effective, thus less appealing to TSOs.

Table 5.13 shows the environmental impact that NS infrastructure could bring to the system. Although (Jones et al., 2018) demonstrated that daily emission is averaged to 2.79 Mton considering a pan-European perspective, which is relatively higher than the emission presented in the table. It is needed to keep in mind that both *Reference* and *NS HVDC* Scenarios have only considered system at transmission level, which implies that effect of thermal units located at distribution level are not computed as net demand generation values are given for that nodes. For example, in Spain, there are many cogenerations at the distribution level which have similar emission factor as gas units (Lopez-Pena Fernandez, 2014). Those units are not included in the studied scenarios which contribute to the lower values of emission.

The largest emission reduction occurs on the day with peak RES. Essentially, the more RES the system is able to host, the less energy conventional units (coal, combined cycle, etc.) need to produce, the less emission it could have overall within EU. However, when the system does not have much demand or have too much demand, the impact coming from the additional NS infrastructure is not substantial despite the economic savings. For example, on the day demand valley occurs, emission is only dropped by 0.9% and when the hourly and daily demand peak occurs, emission reductions are 1.9% and 2% respectively.

Days	**Reference**		**NS HVDC**			**Comparison**	
	Ems. [Mton]	RES Curt. [%]	Ems. [Mton]	RES Curt. [%]	*RES Curt. [%]	ΔEms. [%]	Δ*RES Curt. [%]
D_{hdDv}	0.541	15.5	0.536	15.4	14.7	-0.9	-5.6
D_{dDp}	2.399	24.5	2.350	28.4	23.1	-2.0	-5.5
D_{hdRp}	1.242	22.8	1.160	26.8	23.5	-6.6	3.3
D_{dRv}	0.616	22.2	0.581	23.0	19.9	-5.7	-10.6
D_{hDpRv}	2.368	29.3	2.324	33.6	26.8	-1.9	-8.6

* denotes normalized RES curtailment

Table 5.13 Environmental Impact of *Reference* and *NS HVDC* Scenarios

For RES curtailment comparison, since the total RES available for both scenarios are different, one additional column is added to normalize by equating the total amount of RES available. In all cases except the day with peak RES, it shows remarkable decrease in RES curtailment. In particular, when RES valley occurs, the RES curtailment reduction reaches maximum, i.e., 10.6%. On the contrary when it is the RES peak day, RES curtailment has increased by 3.3%. This is reasonable considering that in *Reference* scenario, there is already a significant amount of RES available in the system. Therefore, in the future when considering expansion of the network for RES integration, it must be noted that extra infrastructure may not help if the system has already been loaded with massive RES. It is important to know when the marginal benefit contributed by additional lines or generators start to lose.

During the simulation of selected days, in total 7 lines are identified as congested which is shown in Table 5.14. In addition, Table 5.15 presents the cross-comparison among the two scenarios. × marked in the Y/N column indicates that the line is congested and ♯ column shows the times of congestion occurrences. Since *NS HVDC* scenario has incorporated more offshore wind towards the continents, two more lines are congested which are not in *Reference* scenario: line 12 and line 5056. One is an interconnector between Germany and Denmark, another is a transmission line within France. This leads to the conclusion that with future development of transmission lines based on HVDC technology, the reinforcement of the existing AC grid will be necessary to accommodate increased injections of HVDC lines. Thus, a coordinated planning of both AC and DC future network is essential to achieve the full potential of the hybrid network.

Line ♯	**From Country**	**To Country**	**From Bus**	**To Bus**
No.	No.	No.	ID	ID
9	Bosnia and Herzegovina	Hungry	BA910535	HR922472
10	Serbia	Hungry	RS927759	HR922327
11	Bulgaria	Greek	BG911235	GR921301
12	Germany	Denmark	DE915466	DK916219
324	Austria	EU*	AT910383	XRU_MN21_OV
5056	France	France	FR920202	FR918753
7709	France	Luxembourg	FR918753	LU923874

* denotes that the node does not belong to any region or area specifically

Table 5.14 Buses of the congested AC Lines

Line ♯		9		10		11		12		324		5056		7709	
		Y/N	♯	Y/N	♯	Y/N	♯	Y/N	♯	Y/N	♯	Y/N	♯	Y/N	♯
Reference	D_{hdDv}			×	24										
	D_{dDp}	×	15	×	1	×	1			×	1			×	6
	D_{hdRp}	×	3	×	2										
	D_{dRv}	×	2	×	17										
	D_{hDpRv}					×	6			×	3			×	6
NS HVDC	D_{hdDv}			×	24							×	3		
	D_{dDp}	×	14	×	1	×	1			×	2			×	4
	D_{hdRp}	×	18	×	3	×	4	×	1						
	D_{dRv}	×	1	×	1							×	3		
	D_{hDpRv}									×	7			×	4

Table 5.15 Congestion level of *Reference* and *NS HVDC* Scenarios

Days	Reference					NS HVDC				
	AC	**DC**			**Total**	**AC**	**DC**			**Total**
		Line	Converter	**subTotal**			Line	Converter	**subTotal**	
D_{hdDv}	541.9	25.1	70.6	95.7	637.6	541.8	24.4	81.5	105.9	647.6
D_{dDp}	749.5	27.7	71.4	99.0	848.6	777.0	27.7	82.3	110.0	887.0
D_{hdRp}	811.7	28.0	72.4	100.4	912.2	820.1	28.3	82.5	110.8	930.9
D_{dRv}	543.9	24.9	70.5	95.4	639.3	530.4	25.3	81.5	106.8	637.2
D_{hDpRv}	742.4	26.4	71.3	97.7	840.1	775.6	27.3	82.2	109.6	885.2

Table 5.16 System Losses of *Reference* and *NS HVDC* Scenarios [GWh]

Table 5.16 shows the impact that the NSOG have on the CE from the technical perspective in terms of system losses. It can be seen clearly that in both scenarios, DC system losses are not negligible as claimed in (Zhao et al., 2017), in particular the converter losses. In all cases, DC part of the system losses has increased with the additional NSOG. While AC system losses mainly have increased except for the day demand valley occurs: the losses have kept around the same level. It can also be observed that when there are large amount RES available or when there is a heavy demand, more power can be expected to circulate within the system, therefore more system losses are generated: the three days/cases with either RES peak or demand peak, total system losses are around 900 GWh while two other days/cases are around 650 GWh. Moreover, since network development generally decreases losses and energy efficiency can thus be measured through the reductions of system losses (ENTSO-e, 2015b), in this case study, only when daily RES valley happens, the energy efficiency benefit was achieved: 639.3 vs. 637.2 GWh.

Finally, problem size is compared by indicating number of constraints, number of variables and nonzero elements. While CPU time and number of iterations used, which defines the computational burden, are shown subsequently.

Problem Features	**Reference**	**NS HVDC**
Constraints	72610	72821
Variables	135804	136213
Nonzero Elements	385621	386707
CPU Time [*s*]	180.625	262.843
Iterations	75040	91588

Table 5.17 Problem Size and Computational Burden Comparison

Chapter 6

Barriers Towards the European Supergrid

This chapter first reviews the motivations towards an European supergrid in order to meet the energy targets. Then it examines the state-of-the-art and soon-to-be available technologies. Among them, the most promising ones are identified. Finally, it dedicates one section on elaborating the main barriers that prevents the development and deployment of those technological solutions[1].

6.1 Introduction

The 2020 Climate and Energy Package, also known as 20-20-20 targets, was established by the European Commission (EC) through binding legislation in 2009. Several actions have been taken by the European Union (EU) to achieve such goal, such as setting mandatory national targets to meet a 20% renewable energy for the overall share of energy by 2020, a reduction of 20% greenhouse gas (GHG) by 2020 (80-95% by 2050 (EC, 2011)) compared to 1990 levels (EC, 2009). In this spirit, transmission grid plays a key role for decarbonization of the energy system. Despite the increasing need in transmission capacity to meet the energy policy targets, infrastructures are developing slowly due to complex permitting processes, inappropriate regulatory framework and public opposition (Van Nuffel et al., 2017).

[1]This chapter draws on Q. Zhao, J. García-González, R. Gaspari, "Technological solutions and barriers identification for transmission system development to help renewable energy sources integration," submitted for publication to *Renewable & Sustainable Energy Reviews* 2018.

According to the National Renewable Energy Action Plans (NREAP) submitted by each MS, wind energy is the crucial component to achieve this objective: in total 209.6 GW installed capacity can be expected by 2020 in the EU (Gonzalez and Lacal-Arantegui, 2016). Towards this end, the concept *supergrid* has been proposed to interconnect distant areas as many RES are available in remote locations (Gordon, 2006). The *supergrid* is seen as a promising solution to harness geographically dispersed low-carbon energy sources (such as offshore wind and solar). It does not only serve to this single purpose, but also it is impelled by a number of drivers. Due to the intermittent and less predictable nature of RES, fast balancing is essential to assure system reliability. Transnational interconnections not only are instruments for better security of supply, but also facilitate the cross-border trading and the integration of wholesale electricity markets (Van Hertem and Ghandhari, 2010). A future *supergrid* would serve as a backbone based on the existing transmission system. This in parallel requires strong upgrades and expansions of the European grid since present high voltage transmission infrastructures have already been constraining the development of renewables (ECF, 2010; Nature, 2008). The European project e-Highway 2050 finalized in 2015 has shown that transmission network bottlenecks result in severe load sheddings and significant RES curtailments (e-Highway2050, 2015).

Driven by the increasing need for additional transmission capacity, both national and transnational, substantial amount of investments can be expected for strengthening the network. The International Energy Agency (IEA) estimated an investment in transmission infrastructure of OECD Europe at $158 billion for the period of 2014 - 2035, which amounts to 144 000 km , additional lines and 421 000 km refurbishments (IEA, 2014). The Ten-Year Network Development Plan (TYNDP) published in 2014 by ENTSO-e foresees an expenditure of €150 billion on transmission projects until 2030, which represents yet only a subset of the entire needed investments faced by TSOs (Van Nuffel et al., 2017). Although the EC has addressed the importance of energy infrastructure and transmission grid, in particular since 2010 (EU, 2010a,b), the ambitious goals for network expansion stand in stark contrast to the slow progress in reality during the last decade: investment levels indicated in the national development plans are lagging behind (Van Nuffel et al., 2017). Even critical projects can face significant delays: several interconnection projects are still stuck in the planning phase (EC, 2007).

Reasons for insufficient expansion and modernization of the grid are manifold. Besides the technical barriers that hamper the development of transmission network,

the lack of financing, the existence of public opposition to the development of new lines and a complex regulatory framework are also obstacles preventing new projects to be developed.

A variety of technical solutions is nowadays available for connecting RES as well as reinforcing current transmission networks based on two principles: one is the overarching technology that is investigated in this thesis, i.e., HVDC; another is AC transmission. Current planning of European transmission systems consider both HVDC and AC OHLs as potential alternatives. However, the latter one is the most preferred option for many TSOs due to both technical and economic advantages. This fact can be confirmed by calculating the figures given in TYNDPs: The TYNDP 2010-2020 suggests that more than half of the projects (55%) are new AC OHL at 400 kV, around 16% of the projects are refurbishment of existing AC lines, and only 25% of the projects are new DC links (mainly subsea cables) (ENTSO-e, 2010); in the later version TYNDP 2014, 120 projects were proposed for the next decade which amounts to roughly 48 000 km of new or renovated lines. Despite the increasing trend observed in using HVDC technologies, AC is expected to remain the prominent technology, as a total of 25 000 km of AC lines are either planned to be built or upgraded (ENTSO-e, 2014).

The European project *BestPaths* (as seen in Section 1.1.2) gathers experts trying to validate technical feasibility with five large-scale demonstrations and to quantify the impacts and benefits of innovative technologies that would finally lead to larger transmission capacity and system flexibility (BestPaths, 2014 - 2018). Inspired and supported by the European project, the purpose of this chapter is to shed light on the current technology advances for policy makers, providing them with an overview of various options for future transmission infrastructure development. In addition, this chapter also includes a discussion on economic and regulatory barriers based on the feedback received from different stakeholders.

6.2 Technology Development

The overarching challenge faced by the existing European transmission network is the deficient capacity that holds back massive RES integration meeting the EU targets in the long term (ECF, 2010). In order to tackle this issue, this section is dedicated to address two questions below first by reviewing state-of-the-art technological solutions (for either repowering or expanding transmission capacity) and identifying the most promising ones:

1. Which are the current and future available technologies that should be considered when repowering and expanding the network?

2. Given the above spectrum of technologies, how could these solutions contribute to the network upgrade and expansion?

6.2.1 Status Quo

To answer *Question 1)*, it is necessary to provide an overview on current and forward-looking technological advances beyond the state-of-the-art. Different technologies that are considered investment options are briefly mentioned in TYNDP 2010-2020 (ENTSO-e, 2010). The Friend of the Supergrid (FOSG) has further reviewed in (FOSG, 2014), both from AC and DC perspective, the technologies that are able to interconnect RES and expand the existing grid. However, both references are out-of-date, leaving concepts such as insulated cross-arms, Dynamic Line Rating (DLR) systems and DC superconducting links out of the discussion.

Nevertheless, the *BestPaths* project aims to validate the capabilities of several novel network technologies that are considered promising and bring affordable solutions before 2020. In next section, analyzed and proposed technology developments that will be discussed individually are shown.

6.2.2 Technologies for Supergrid

To answer how the spectrum of technologies could contribute to the network upgrade and expansion (*Question 2*), it would be very valuable to collect information from concerned parties. The high representativeness of different types of agents in the *BestPaths* project consortium (TSO's, RES companies, manufactures and research centers) offers a great advantage. Participated partners include but not limited to:

- TSOs: REE, RTE, Elia, Statnett, etc.
- RES companies: Iberdrola, etc.
- Manufactures: ABB, Siemens, GE, etc.
- Research Institutes: Sintef, CIRCE, etc.

Consequently, in addition to external research, a replicability[2] survey has been designed and conducted in several stages. The first part of the survey consisted of particular questions addressing each demo participant. The second part of the survey was further divided into three aspects, i.e., technical, economic and regulatory. Lists of questions/barriers were given to all the demo partners to either rank the importance or express their opinions. Finally, workshops and interviews/bilateral meetings were held for further clarification and information exchange.

Section 6.2.3 and 6.2.4 are devoted to give a general description of the key technologies/concepts that are listed in Table 6.1. It includes the two basic transmission principles, i.e., AC and DC, both for repowering and expanding purposes for the existing network. Interoperability associated with converters is further discussed in Section 6.2.5. Apart from a qualitative description, the main advantages and disadvantages of each options will also be highlighted. More technical details can be found through project deliverables (BestPaths, 2014 - 2018).

AC Transmission	**DC Transmission**
High Temperature Low Sag conductor	Converter Technology
Insulated cross-arm	Underground and submarine cable
Innovative OHL concepts: • Robotic mounting of air warning marker • Composite foundation • Composite tower	Insulator for HVDC OHL
Innovative repowering process: • Live-line working • Conductor car • Insulator changing technology	High Temperature Low Sag conductor
Dynamic Line Rating system	Superconducting link

Table 6.1 Main Technology Developments

6.2.3 AC Transmission

High Temperature Low Sag (HTLS) conductors

The traditional AC OHL is a mature solution when considering network reinforcement. OHL technology is very well established and has been used for decades. However, due

[2]Replicability refers to duplication of a system component at another location or time with different boundary conditions (Sigrist et al., 2016).

to high visual impact, electromagnetic field (EMF), significant right-of-way, etc., which consequently result in long consultation and permitting process, new developments are urged. As projected in (Buijs et al., 2011), new materials are used for conductors allowing high temperature and low sag. This allows to increase transmission capacity. HTLS conductors with composite materials for cores are believed to have the highest potential. The studies were firstly initiated in 2004. (Reddy and Chatterjee, 2016) reveals the technology development over the past years. Nowadays, several HTLS types are available on the market. However, long time reliability is not yet proven since it requires service experience exceeding 40 years. Up to now, there is no HTLS technology that has been operated more than that. Future investigations need to be carried out focusing on long-term behavior and aging process.

Insulated cross-arms

Conventionally, there are only two options when considering updating of transmission capacity of an existing line: either by adding additional circuits or by increasing the voltage. Neither of these solutions can be easily put into practice. However, by replacing normal cross-arms with insulated ones, voltage level can be raised. Consequently, transmission capacity can be increased up to ten times of the original values. The inquiry of insulated cross-arms in light of new tower designs was firstly launched by Elia[3] in 2008 (Goffinet et al., 2017). This technology is mature today and has been implemented in a number of countries already as pilot projects Europe-widely, e.g., Belgium, Spain and Italy.

Innovative OHL concepts

Innovation is believed to be the key driver to achieve a sustainable and modernized power system. Consequently, three technologies have been developed for OHLs, namely robotic mounting of Air Warning Marker (AWM), composite foundation and composite pylons. Robotic mounting helps save manpower that need to be devoted when placing AWMs. Conventional foundation and tower are made of concrete. When transportation of concrete is difficult and power lines are planned to be built far away from roads or built-up areas, e.g., mountains, composite foundations is valuable in rocky terrain. Similarly, composite towers can be very useful due to their low weight. In *BestPaths*

[3]Elia is Belgium's HV TSO (30 kV to 380 kV).

project, all current solutions are designed according to Statnett[4] specifications and currently still under development stage.

Innovative repowering process

Live-line working has a long tradition. The earliest history of such concept dates back in 1913 in the USA and 1933 in Europe (Lovrencic et al., 2017). The tools and methods are constantly evolving to meet the challenges in day to day operation (RTE, 2013). To explore the concept, a new type of conductor car has been developed using new generation of materials (Gocsei et al., 2017). In addition, insulator changing technologies (including associated protective equipment) have been recently explored (BestPaths, 2014 - 2018). All technologies are currently in progress of on-site testing. This allow maintenance work on existing OHLs without the need to switch off the lines.

Dynamic line rating (DLR) technology

The idea of DLR system is not new. It aims to monitor lines and handle sag effectively so that normal conductor can be operated the same way as high temperature conductors. Consequently, a higher capacity can be achieved. A thorough review is provided in (Michiorri et al., 2015) from both historical and practical perspectives. However, new solutions are being developed nowadays: renovative DLR systems based on low-cost sensors and other novel solutions such as new modeling techniques and algorithms for the system to calculate and predict line ratings. At present, developed sensors are close to a commercial stage. These solutions are able to measure parameters related to conductors. However, there is a lack of experience among TSOs and utilities to calculate weather conditions with data provided, especially wind. From software perspective, i.e., algorithms to forecast ampacity, there is lack of consensus on the most appropriate models.

6.2.4 DC Transmission

Converter technology

Converter stations are crucial components to develop a future supergrid which allows massive integration of RES, in particular offshore wind (Van Hertem and Ghandhari, 2010). As presented in Chapter 2, currently there are two main types used in HVDC

[4]Statnett is a Norwegian state-owned enterprise responsible for owning, operating and constructing the stem power grid in Norway.

transmission systems: conventional line-commutated CSCs, and self-commutated VSCs. The research carried out in this thesis has proven that converter losses are not negligible and have a significant impact on the optimal system operation (Zhao et al., 2017). Driven by the need to reduce operational losses, MMC (a type of VSCs) was firstly developed by Siemens and then gradually become the trend and adopted by the three major European HVDC manufacturers, i.e., Siemens, ABB, GE (previously Alstom) (FOSG, 2014). Currently, HB MMC is the state-of-the-art technology for large offshore wind farms. However, FB MMC is seen as a more promising solution due to its fault blocking capability.

In addition to the HB and FB MMC solutions, a new converter technology (buffer-reactor free HB VSC with a special converter transformer) has been recently proposed by Toshiba due to numbers of advantages. This converter offers small footprint and leakage flux, and it provides high reliability using Injection-Enhanced Gate Transistors (IEGTs) which were firstly invented by Toshiba in 1993 (Kitagawa et al., 1993). At present, the innovative design of the converter transformer is in a preliminary stage, under development for HV and full-scale.

Underground and submarine cables

Cables are another important component to be considered for power transmission and interconnecting systems in addition to converter stations. Typical HVDC cables consist of six parts, namely, conductor core, semiconductor screen, main insulation, sheath, armoring, and associated accessories. Depending on the different characteristics of dielectric materials, different electrical, mechanical and thermal performances can be resulted for cables (Chen et al., 2015). The two main types of cables (depending on the insulation systems) are extruded and paper-lapped (or oil-impregnated). Thereinto, paper-lapped cables can be further categorized into OF and MI ones. MI and OF cables have been the mainstream of DC cable systems since 1954 until the first application of extruded cables in Gotland Island (80kV) in 1999 (Ghorbani et al., 2014; Murata et al., 2013). Extruded HVDC cable systems show a great potential due to a number of advantages, such as higher operational temperature, no fear of oil leakage, lower weight, simpler and faster installation process. In addition, ongoing test carried out in the cable industry are positive about allowing polarity reversal for HVDC extruded cables. In any case, these extruded cables are the preferred option for VSC technology. Compared to the highest operating voltage level (600 kV) that paper-lapped cables have achieved, the rated voltage of commercially available extruded cables are still

at 320 kV (Chen et al., 2015). In August of 2014, ABB has successfully tested and qualified an extruded HVDC system at 525 kV level (including joints and terminations) up to 2600 MW for both land and subsea purposes (Gustafsson et al., 2014). After the launch by ABB, recently in 2017, NKT[5] announced their latest R&D result, a new 640 kV extruded HVDC cable system that is able to transmit power up to at least 3 GW, for underground application (Bergelin et al., 2017).

Insulation for HVDC OHLs

Insulators tested in *BestPaths* follow a modular design to deal with both current and voltage requirements. One of the critical procedures for designing an HVDC OHL is to decide on the size of external insulation. Specific dielectric materials are required for this purpose. In the early years, ceramics were adopted and there is a standard published under reference IEC 61325 (George and Lodi, 2009). Later, composite materials were more used since 1980s (Engelbrecht et al., 2012). There are two key aspects that need to be analyzed when sizing it, i.e., environmental stress and dielectric strength. Therefore, to assist on future development, it is important to provide more accurate characterization of the components and improved definition of sizing criteria based on the severity of the environmental conditions, with a focus on the insulators that are already commercial solutions. In particular, the use of special composite insulators and adoption of Room Temperature Vulcanizing (RTV) silicon coating.

HTLS conductors

Replacing conventional OHLs with HTLS conductors and converting AC lines into HVDC are usually seen as the two alternatives to overcome the transmission capacity limits (Balser et al., 2012). (Nogales et al., 2009) has provided a comparison between the two technologies. In (Douglass et al., 2016) it is suggested that HTLS conductor is unlikely to be used for lines that have constant high power transfer in day to day operation like HVDC. However, the idea to apply HTLS technology on HVDC lines has been proposed and implemented in the High Voltage Test Laboratory at Ricerca sul Sistema Energetico (RSE[6]) (BestPaths, 2014 - 2018). Therefore, issues related to optimal choice and size of conductors for HVDC OHLs are investigated. It

[5]NKT A/S (formerly NKT Holding A/S) is an industrial holding company with interests in power cables and wires as well as optical components, lasers and crystal fibres.

[6]RSE is a publicly owned company with the Italian energy service manager (GSE S.p.A) as its sole shareholder. It carries out research into the field of electrical energy with special focus on national strategic projects funded through the Fund for Research into Electrical Systems.

mainly depends on two aspects: 1) maximization of flexibility in transmission capacity and 2) minimization of corona and electromagnetic effects. Use of innovative HTLS conductors for HVDC purpose, adopting new HTLS core materials, manage to increase the transmission capacity compared to traditional conductors. It allows an increase in the conductive area, meanwhile a reduction of ohmic losses.

Superconducting links

Superconducting materials have a huge current rating which are at least 150 times greater than copper, since they are almost perfect conductors with no electrical resistance. Therefore, superconducting cables provide a new way to enhance transmission capacity by increasing the current instead of voltage.

The idea to deploy superconducting material for transmitting GW of power has been around for decades (Garwin and Matisoo, 1967). Nowadays, several demonstrative projects have been commissioned and operated worldwide (Thomas et al., 2016). However, new materials and designs are evolving constantly.

MgB_2 was discovered in early 1950s, but not applied as a superconductor until 2001 (Buzea and Yamashita, 2001). Compared to other superconductors such as Nb_3Sn, it has a relatively high critical temperature of 39 K and low cost due to abundance of raw material Mg and B. Soon after the discovery of MgB_2 superconducting use, a new company that manufactures industrial MgB_2 wires was established in 2003 (Ballarino and Flukiger, 2017).

It is critical to validate the cutting-edge MgB_2 technology. Novel MgB_2 superconducting cable prototypes made of MgB_2 round wires for high-power electricity transfer were realized by CERN[7] and investigated in depth. In one of the demonstrations of BestPaths, the objective is to develop a full-scale 3.2 GW HVDC superconducting cable system operating at 320 kV and 10 kA in He gas, with hybrid current leads and HV cable insulation in liquid N_2 (BestPaths, 2014 - 2018).

Finally, in order to maintain the MgB_2 cable operation temperature, a dedicated cooling plant including fluid circulation system is needed. More technical details that are project specific can be found in (Ballarino et al., 2016).

[7]The European Organization for Nuclear Research.

6.2.5 Interoperability

VSC makes meshed MTDC systems technically feasible, overcoming the technical barriers of CSCs (CIGRE, 2013a). Although, the need of standardization and interoperability among different vendors has been pointed out previously in (Cole et al., 2011; Van Hertem and Ghandhari, 2010), there is no real experience in testing the compatibility of different equipment for large systems. In order to develop a HVDC grid, all equipments from different manufacturers would need to be compatible. Different technologies and control algorithms are allowed for VSCs, however, they shall not interfere with each other. A high level of harmonization need to be achieved among vendors to ensure reliable system operation while not compromising the competition among manufactures. At present, neither VSCs nor MTDC systems have any kinds of standardization requirements. Consequently, multivendor interoperability (IOP) is an important issue that could lead to potentially several problems such as induced oscillations on the DC buses. To overcome these problems, it is essential to provide recommendations for specification and hardware control implementation which would ensure maximum IOP for multivendor solutions. At the moment of writing this thesis, only one standard has been found that is under drafting by the International Electrotechnical Commission (IEC), technical committee 115, titled as "Road Map on Standardization of HVDC Technology" (IEC, 2017).

6.3 Barrier Identification

In this section, all the identified barriers (economic, technical and regulatory) that harness the deployment of the technical solutions shown in previously are carefully addressed.

Since financial or economic instruments are implied under the regulatory framework, section 6.3.1 provides an overall brief discussion. Then for each technology development listed in Table 6.1, barriers from technical and regulatory perspective are analyzed more in depth in Section 6.3.2 (AC transmission) and 6.3.3 (DC transmission) respectively.

6.3.1 Economic Barriers

Advantages of using innovative technologies to repower and expand EU transmission grid are potentially large. However, the uncertainties associated with the balance between costs and benefits are tremendous. Therefore, economic viability needs to be carefully

examined before any huge investment in transmission network reinforcement take place. This can be perceived as the biggest barrier for any type of novel solution. Moreover, to allocate costs appropriately among involved parties is not a trivial task. The most recommended methodology is the "beneficiary pays" principle which distributes costs accordingly to the benefits acquired by each beneficiary. The difficulties not only lie on finding a common CBA that all parties agree upon, but on the fact that the quantification of the expected benefits can be very challenging (lack of data, size of the problem, tailor-made modeling to capture the features of the technological solutions, computational burden, etc.). In general, this kind of CBA must follow the steps below:

- To define scenarios representing both business as usual and plausible scenarios considering future transmission investments where the assessed technologies are replicated in promising locations.
- To collect data from the pan-European perspective (including continental Europe, UK and Nordic countries) and build a coherent and comprehensive network data set.
- To apply simulation/optimization models as the one proposed in this thesis to perform impact assessment reflecting transmission projects' added value.
- The techno-economic viability can be measured through a number of indicators, e.g., RES curtailments, CO_2 emissions, Operational Expenditure (OPEX) variations, energy non-served, etc. The indicators can be calculated through network studies by running models with predefined scenarios (network, generation, demand, etc.).

The procedure to carry out such a study is neither obvious nor straightforward. The first difficulty is to obtain the needed data to build the scenarios due to confidentiality reasons and the lack of public sources containing detailed information. Secondly, the impact assessment is a mid to long term study which requires to simulate hourly system operations for a period of time, e.g., one year, taking into account uncertainties of future system development (conventional generations, demands, planned transmission assets, renewable generation profiles). To prepare a consistent data set that represents adequately future power system is challenging, especially when they are provided by different entities. Moreover, it is essential to strike a balance between the complexity of the network representation and computational effort. Meanwhile, the model developed

should be complex enough to capture relevant features but simple enough to allow affordable computation for large-scale systems.

In case the savings in the operational costs are higher than the required investment costs, the economic barriers could be overcome.

6.3.2 AC Transmission

Use of HTLS conductors and insulated cross-arms

HTLS conductors with composite matrices and insulated cross-arms together form a compact design in order to raise transmission capacity. Despite being mature technologies that have been implemented in real projects, proper functioning of the solutions can be influenced by the particularities of the developing site.

For HTLS conductors, loading cases (ice and wind) could excess the limit of existing towers which were designed for different nominal conditions. There are also certain HTLS conductor technologies which are better suited for specific loading conditions. For insulated cross-arms that entail the replacement of old OHLs, the required investments might represent a serious obstacle. In addition, TSOs need to be aware that new methodologies or tools need to be developed and reach a mature stage for carrying out the maintenance of these kind of towers.

The current and also the first ever insulated cross-arm was designed assuming a middle-European environment by Belgium's TSO, Elia, i.e., certain environmental parameters (e.g., low level of pollution, lighting and ice load, etc.) were utilized. Therefore, the solution specification complies with Elia's standards. However, each country has different loading cases which could excess the mechanical capabilities of the insulated cross-arm. High declivity could also affect the stability of the pivoting vees. In one words, mechanical stability of the system could be endangered in the case of deployment in an improper environment. So far, several pilot projects were implemented in Europe. If other countries would like to implement this technology with different environmental conditions and subject to special national standards, the solution would need particular adaptations.

According to the feedback gathered from the carried-out survey, from the regulation side, long term reliability of HTLS conductors and insulated cross-arms have not been proved yet, and aging mechanisms remain uncovered at present for both technologies. TSOs are usually conservative and require high standards of reliability and maturity for system components. Therefore, they could be reluctant on this regard to accept

the solutions and consider neither HTLS conductors nor insulated cross-arms as primary candidates for uprating transmission capacity. National or local regulation could also impede potential deployment due to domestic constraints derived from national standards: (CTC, 2011) indicates that in US different states have their own requirements (diameter, weight, core strength, maximum resistance, etc.) on conductor sizes, so are the MSs in Europe. In the case of HTLS conductors, there is lack of standardizations (testing, qualifying, fitting, etc.). This results in complications when it is needed to implement in another location. For example, during the tender process (to introduce HTLS to the Irish transmission network), a list of detailed specifications was drawn considering a number of standards to ensure that the selected conductors comply with the requirements (design, supply, test and installation) of all aspects (Geary et al., 2012).

Some IEC open standards are currently in development, e.g., IEC 62818 (titled "Fiber Reinforced Composite Core used as Supporting member material") for composite core and IEC 63089 (titled "Overhead Electrical Stranded Conductors Composite Core Reinforced") for HTLS conductors with composite core. From a long-term perspective, more standards need to be developed.

The main barriers for HTLS conductors and insulated cross-arms can be summarized as follows:

- HTLS conductors
    1. Extra effort is required to adapt to a different environment.
    2. Long term reliability is not proven yet, while TSOs are conservative.
    3. There is a lack of standardization.
    4. Cost-effectiveness is not evident at this stage.
- Insulated cross-arms
    1. Current solution is designed based on Elia's specification, assuming middle-Europe environment conditions (rain, temperature, etc). In case other countries would like to replicate such technology, under different environmental conditions and subject to special national standards, the solution needs to be adapted accordingly.
    2. Insulated cross-arms is part of the compact design which entails replacement of old OHLs. It can be difficult for TSOs and public to accept it.

3. There is no standard configuration and requires special design to adapt to particularities of the developing site.

Innovative OHL concepts and repowering process

Innovative OHL concept along with repowering process mean to optimize the repowering process complementarily. For robotic mounting, markers have to be tailor made in correct size and with an interface so that the robot is capable of handling the marker and place them properly. Composite foundation requires specific location where it has solid rock/bedrock. On one hand, this could restrict the deployment of the technology geographically; on the other hand, manpower to remove solid rock/bedrock for conventional transmission line construction can be replaced by implementing such technology given natural resources (TOBIN, 2013). In addition, unlike conventional foundation, composite foundation may not be able to withstand forest/bush fire. Regarding live-line working, despite the solution complies with some mandatory standards, to name a few: EN 50374, EN 50110-1, IEC 60895, etc., it does not allow adaptations to a different working conditions without further adjustments. The main difficulties are due to different possible combinations among tower, insulator and conductors at HV which lead to difference in available clearances.

From the regulation side, risk-aversion might be the biggest barrier for the deployment of all these technologies. TSOs and entrepreneurs have strong tradition adopting old-fashioned manual mounting of AWM and concrete/steel foundations. In addition, live-line activities need to be very carefully examined due to strict personal safety criteria and this could slow down the replication process.

Furthermore, discrepancies among national regulations could discourage the deployment of these technologies. All current solutions are designed according to Statnett[8] specifications. Existing regulatory frameworks are not directly applicable for novel concepts of OHLs. In some cases, there are regions where live-line working is not supported (e.g., Austria, Netherland (CIGRE, 2013b)). In other cases, this issue has not been paid enough attention to (e.g., Slovenia (Lovrencic et al., 2017)). Thus, it is necessary to establish standards/rules, including required clearances, exposure limits of electric and magnetic files, geographies and environmental circumstances, etc.. In case where regulations exist, modifications and/or extensions of current standards are entailed in order to introduce new equipment and technologies to the system.

[8]Statnett is a Norwegian state-owned enterprise responsible for owning, operating and constructing the stem power grid in Norway.

For example, recently in the HV Laboratory of Budapest University of Technology and Economic, a conductor car using new materials (composite) and adhesives is being developed (Gocsei et al., 2017). Current standards consider conductor car as a conductive, metal structure. Due to novel material selection and design principle, adjustments are needed. Consequently, CENELEC[9] CLC/TC78[10] has accepted the request of modification for existing IEC 50374 standard.

The main barrier for innovative OHL concepts (robotic AWM, composite foundation and tower) and repowering process can be summarized as follows:

- OHL concept (robotic AWM, composite foundation and tower)
    1. Composite foundation requires specific location where it has solid rock/bedrock.
    2. Current solution is designed according to Statnett's specifications which could result in future barriers as regulations and standards differ in regions.
    3. Risk-aversion of TSOs who might prefer traditional manual mounting of AWMs, and use of concrete/steel foundations
- Innovative repowering process
    1. Although the solution complies with mandatory standards (e.g. EN 50374, EN 50110-1, IEC 60895, etc.), it needs to adapt to different working conditions.
    2. Due to novel material selection and new design principle, modification and/or extension of current standards are required.

Dynamic line rating technology

DLR system is capable of increasing the transmission capacity through more efficient use of existing assets. It provides more flexibility for operating the lines without complex permitting and installation processes.

There have been lots of attempts by TSOs to develop DLR systems, yet no definite conclusion is achieved on which combination of measurements and algorithms represents the optimal solution (ENTSO-e, 2015a). The algorithms used in practical

[9]CENELEC is the European Committee for Electrotechnical Standardization and is responsible for standardization in the electrotechnical engineering field.

[10]CLC/TC78 is the technical body to prepare CENELEC standards for work equipment, devices and tools, including personal protective equipment used for work on or near live electrical systems or installations.

implementations of DLR have to be fine-tuned according to the particularities of each location. Although low-cost sensors are successfully developed recently along with new modeling techniques, methodologies to measure weather conditions as well as algorithms to forecast ampacity are not proven to be robust yet (BestPaths, 2014 - 2018): how environment conditions could affect the operations, as well as how temperature and strain would evolve during operation remain obscure. Experiments in real facilities are needed in order to reach a more mature state. This entails that current solution cannot be easily replicated in a different location without carrying out fine adjustments. As a result, the extra costs for the re-design and required tests might represent a significant barrier.

From the regulatory perspective, despite the benefits that it could offer, TSOs in EU can be reluctant to invest in such technology due to the current remuneration schemes adopted. Most of the TSOs' revenue are based on Regulatory Asset Base (RAB) and they are not acknowledged by efficient grid management and operation. Therefore, there is a lack of incentives to invest in technologies like DLR system as these type of expenses are counted towards operational expenses.

Moreover, more intense coordination among TSOs is needed for such application on infrastructures at a transnational level. Lack of standardization and harmonization among national network codes create operational difficulties. The fact that beneficiaries and associated benefits remain vague would further block the investments in these solutions.

The main barriers for DLR can be summarized as follows:

1. Lack of experience among TSOs and utilities to forecast required weather conditions for this application.

2. Given the limited experience, all models used to forecast ampacity have to be fine-tuned according to the particularities of each location. Lack of consensus on the best models to be used in each case.

3. TSOs are not properly incentivized to invest in DLR systems. TSOs' revenue in EU are based on a Regulatory Asset Base and they are not acknowledged by efficient grid management and operation, i.e., they are not remunerated for operating the grid efficiently.

6.3.3 HVDC Transmission

An HVDC system consists of mainly two components: converter stations and DC conductors/cables. In this section, barriers concerning both HVDC components are thoroughly discussed.

Converter technology

Converter stations are key components of HVDC systems. There is a variety of possible configurations and manufactures available and need to be carefully examined. Although VSCs enable the possibility of HVDC systems with MTDC configurations, many technical challenges remain:

- DC breaker: When fault occurs, DC breakers are critical elements to isolate the faulted lines instead of shutting down the entire MT system which is not acceptable for the future supergrid scenario. Several solutions are already available (Barnes and Beddard, 2012), however, none of them have been implemented and used in real projects.

- Hybrid system operation, protection and control: In the future, both offshore and onshore networks will have to be operated together with AC grids. Once a supergrid is established, an unprecedented coordination among TSOs and the DC grid needs to be achieved. Given more degrees of freedom of operation for such a power system, it is more complicated to maintain stability and reliability to ensure security of supply. Furthermore, suitable protection strategies are needed on top of DC breakers to guarantee the reliability of the DC grid (Cole et al., 2011). The developed control strategies must be able to detect, identify and isolate the faults, to open the faulted lined within milliseconds, while ensure that the AC system is not affected (Van Hertem and Ghandhari, 2010).

- Standards and IOP issues: At present, no standardization of MTDC exists despite its expected importance. Since the supergrid has to incorporate a wide range of products from different vendors, the IOP is very important as different technologies from different manufactures must be compatible in order to function properly together. Until now, the reasons that can compromise the IOP of HVDC grids is still an open question. The only attempt to investigate IOP has assumed a centralized coordination of converters via a Master Control (MC) (BestPaths, 2014 - 2018). Yet, whether this scheme is acceptable or not remains controversial.

Besides, strong coordination is also needed between MC and the underlying AC network(s). This potentially raises a series of regulatory complications which will be discussed further in Section [sub:Regulatory]. Finally, a multinational DC grid code must be available for the future development of MTDC grids (Pierri et al., 2017).

Underground and submarine cables

For both underground and submarine cables (including accessories: joints and terminations), adaptations are needed for different working conditions, since different interactions can be expected. According to the feedback received from technical experts belonging to Nexans[11] when developing this thesis, cable size is large when high operation voltage is targeted. Consequently, transportation and handling of such cables can be very challenging. In particular, for underground land cables, large bending radius may limit the installation and civil works could be a problem in a population-densed area.

HTLS conductors

Currently, the solution is not commercially available. Several prototypes have been developed for the SACOI[12] link ("SACOI3") according to the specificity of this site.

The main barrier from the technical perspective is due to the use of composite material in the core. Their performance is limited by the temperature. Although these materials have been studied in other application (at moderate temperature) and no specific problems are shown, it requires a study more in depth about the behavior at a continuous regime of high temperature. In case of poor performance, new matrix solutions need to be studied and developed. Tests and field experience will tell more about possible challenges to face.

Insulator for HVDC OHLs

Environmental conditions play a key role when designing the external insulation. Depending on the weather severity, reevaluation is certainly needed for current commer-

[11]Nexans S.A. is a French company which manufactures copper and optical fiber cable products for the infrastructure, industrial and construction markets.

[12]The HVDC Italy–Corsica–Sardinia (also called SACOI; Sardinia–Corsica–Italy) is an HVDC interconnection used for the exchange of electric energy between the Italian mainland, Corsica and Sardinia.

cially available solutions to be applied in different locations. For example, the pollution performance of insulation which is affected by both pollution and wetting conditions can vary significantly. Consequently, the final selection of the OHL insulation type and insulation level could be different (Vladimirskii, 2015). This entails an extra amount of costs before deployment. Nevertheless, both design criteria and experience can be used for future reference and it is not very difficult to make adjustment in order to adapt to another set of standards.

Superconducting links

Currently, MgB_2 superconducting links are still on an experimental R&D phase and therefore it cannot be considered as a mature technology. The superconductor used in *BestPaths* project was designed to transmit 10 kA. It could be easily increased by adding superconducting wires. However, this creates a technological lock concerning current rating of converter stations since the conducted survey indicates that presently available HV converter do not deliver rating over 2 kA. Therefore, converter current rating can present as a technical constraint for future replication of such superconductor link at this moment. Nevertheless, discussions have been conducted with the converter manufacturers suggesting that 5-6kA is plausible, and with converters operating in parallel, 10kA could be achieved in theory.

Furthermore, the system has adopted double fluid circulation, i.e., helium (He) for the low temperature conductor, nitrogen (N) for the dielectric medium. It entails that a pumping and cooling station is needed ideally fitting with power substations (in average every 50 km) along the cable route which can be prohibitive for system operators. Besides, the crossing of areas with a topography of steep inclines will lead to high pressures and a special design is needed for the cooling system in this case. For N which is denser than He, the duplication of cryogenic stations would assume the acquisition of specific land for new builds and installations. This can be problematic for industrial deployment. One way to unleash this issue would be the use of liquid hydrogen (H) due to several advantages such as low boiling point (20.3 K), large latent heat, low viscosity coefficient, etc. [39], to replace N for long links.

Moreover, although a conduit with diameter of $25mm$ represents only $2m^3$ per kilometer of cable, using of nature resources like helium gas as a cooling medium can be an issue. Using liquid H could also alleviate on this regard. However, one needs to bear in mind that experience with liquid H at a large-scale is insufficient so far and needs more investigation.

Finally, it must be highlighted that superconducting links cannot be considered as classic branches embedded in the network for operation mainly due to its significant transmission capacity. Management of an outage is more complex than a HVAC branch in a meshed grid. Moreover, good harmonization shall be reached with the converters' control and protection. In case of a cable breakdown, the power must be shared by the other lines within the meshed grid. The discussion in e-Highway 2050 shows that the maximum transit that can be managed by TSOs is between 3 GW and 10 GW. The demonstration targets a value of 3.2 GW which can be considered under the feasible margin. In principle, it can be properly managed without excessive difficulty. Nevertheless, the actual limit can vary notable from case to case depending on the specific location where the solution has to be commissioned.

The main barriers for DC superconducting links can be summarized as follows:

1. Although current solution still is not mature for large-scale deployment, outcomes obtained in the demo are rather promising. Additional policies are needed to incentivize innovation at the TSO level, and in particular to deploy this innovative idea in order to gain experience.

2. The conductor was designed to transmit 10 kA. Presently available HV converters do not deliver current rating over 2 kA. However, either by increasing the maximum current of HV converters, or by operating them in parallel, this barrier could be overcome.

3. Pumping and cooling station is needed ideally fitting with power substations (in average every 50km) along the cable route which can represent a serious barrier for system operators. However, for shorter links less than 50 km this would not be a barrier.

4. Crossing areas with steep inclines can lead to high pressure and a special design is needed for the cooling system in this case. This could limit the applicability of this technology in certain places.

5. Currently there is no standard (except regulations concerning safety) for MgB_2 wires as the concept is very innovative.

6. From regulatory perspective, there is a lack of support to test so innovative technologies. Strong collaboration is expected in case of interconnectors using superconducting link among TSOs. As it is capital intensive, measures to facilitate access to co-financing (including European funds) could help the deployment.

Regulatory barriers associated with HVDC technology

As a result of energy infrastructure development, environmental concerns such as EMF, footprint, visual impact, etc. raise public opposition. Thus, the lack of sufficient public acceptance is one of the major barriers for investments in transmission assets (Battaglini et al., 2012). Apart from this common barrier, HVDC projects (both onshore and offshore projects) have to deal with the following considerations:

- National, transnational policies

National support schemes play a key role in promoting investments in promising technologies and they have major influence over technology choice. Inappropriate or insufficient support can lead to discouragement of technology development. From the conducted survey, serious doubts are raised concerning that current policy framework does not guarantee to move forward the build-up of HVDC grids.

Under the scope of entire pan-European, national targets and standards vary from country to country which makes cross-border grid investment more difficult. In this sense, a stable legal and regulatory framework must be ensured in order to attract the required investments. For instance, UK has established so called the Cap & Floor regime (C&F) for the purpose of encouraging investment in electricity interconnectors. The cap sets the maximum amount of revenue to ensure that it is not excessive, while ensuring that adequate returns can be received by equity investors. The floor sets the minimum amount of revenue that an interconnector is able to collect to cover its costs. In this way, risk is appropriately mitigated for project developers (OFGEM, 2016).

Moreover, permitting or licensing process for energy infrastructures (for both onshore and offshore) is rather complex and time-consuming which results in long delays and large administrative costs. Comparatively speaking, the onshore part is the most critical for planning and permitting of submarine interconnectors (van den Berg et al., 2013). For interconnections involving multiple countries, regulation is even more complicated. The cable route needs to obtain approval from all involved countries. To reach an agreement on cost allocation based on common criteria, like benefits, is very challenging. Thus, standardized processes that rationalize the work developed by involved TSOs are crucial to ease the permitting procedure.

- Financial instrument

Currently, HVDC projects are capital intensive with high upfront investment costs demanding long-term funding and they are taken care by TSOs. Substantial investments

can be expected on energy infrastructure in the coming future. However, investment levels indicated in the national development plans do not keep up the pace with increasing need in transmission capacity. Measures to facilitate access to co-financing (including European funds) and other institutional investors are needed (Van Nuffel et al., 2017).

In addition, investments in HVDC technologies can be perceived as high risk compared to conventional ones due to uncertainties resulted from future cost and revenue levels. However, this risk could be mitigated through a regulation framework that fosters long term contracts.

Finally, the remaining effect of the financial crisis that swept the international economy one decade ago is still limiting the national budgets to support for both domestic and transnational deployment of HVDC infrastructures (Pierri et al., 2017).

- Operation of HVDC supergrid

The existence of a HVDC supergrid overlaying the AC grid of several countries calls for a joint coordination of such infrastructure. Despite some researchers have studied the best strategies for carrying out a decentralized OPF in the presence of HVDC grids, it is necessary to study which is the best framework for operating the supergrid given that the set point of the converters affects the DC flow of the HVDC grid, and consequently impacts on the AC flows within each country (Iggland et al., 2014).

- Standardization

Only HVDC cables (both land and submarine) have standards that are fully accepted internationally. At present, standards do not exist for VSC design and control strategy which results in IOP issues for multivendor solutions. Similarly, insulation for OHLs and HTLS conductors do not have standards neither. This causes problems for both TSOs and manufactures. On one hand, operational difficulties and reliability issues must be faced by TSOs. On the other hand, manufacturers must be ready to modify the technologies and the relevant test procedures accordingly to each MSs' specific requirements.

- Legal and intellectual property (IP)

This barrier is referring to converter technology specifically. Potentially, inequity can be resulted among MSs due to grid operator(s)' intentions so that converters may

be assigned different roles. Therefore, to resolve problems with ownership, governance and coordination of a MTDC network is neither trivial nor straightforward.

In addition, in attempts to resolve IOP issues that are resulted from multivendor solution, some specified functions cannot be implemented due to legal and IP protections. This further create a barrier for implementing a MTDC network.

6.4 Conclusion

In times of massive deployment of RES, current transmission grid expansion progresses rather slowly and remains challenging. Development of renewables and modernization of the infrastructure need to be synchronized to meet the 2020 targets. Although the growing need for more investments and the potential benefit of having a interconnected pan-European grid are well perceived by MSs, there are obstacles covering a wide range of problems.

In this chapter, the latest and most promising technologies for uprating and expanding network are reviewed thanks to the support of EC on the *BestPaths* project. The merits of each technology are discussed individually. Barriers hampering transmission investments are carefully addressed from economic, technical and regulatory perspectives. The analysis suggested the following conclusions.

First and foremost, the primary barriers that impedes grid expansion are not technical or financial, but from regulatory perspective such as lack of appropriate regulatory frameworks, standardizations and public acceptance.

Secondly, in order to build and properly operate a future transnational HVDC grid it is paramount to define a regulatory framework to coordinate the actions of involved TSOs and to provide clear schemes regarding the ownership and governance of the grid assets. In the same vein, the development of technical standards is essential to ensure the interoperability among different vendors and the adoption by the TSOs of the new technologies developed in *BestPaths* project. The new transmission lines based on HVDC technology will be indispensable in the future European transmission network, and the reinforcements of the existing AC grid will be necessary to accommodate increased injections of HVDC lines. Thus, a coordinated planning of both AC and DC future networks is essential to achieve the full potential of both technologies.

Regarding the innovation, it is necessary the development of new policies to incentivize TSOs' investment in some of *BestPaths* technologies taking into account their specificities. Fostering DLR technologies would imply a change in the retribution

schemes for TSOs that should include the acknowledgement and remuneration for efficient grid management and operation. On the other hand, some of the developed technologies are rather capital intensive, as the case of superconducting links, and therefore measures to ease the access to co-financing (including European funds) could help its deployment.

Finally, there is the lack of a complete data set that could be used for network analysis (planning and operation) under a pan-European perspective. In this sense, the European Commission should develop and maintain an open common reference framework of European network scenarios and models for the pan-European Transmission System. The model should include electrical data and geographical layout of the transmission grid; information about generators, including capacity, type and location in the transmission grid; and distribution of power demand; updated grid scenarios along with expected grid scenarios for different time horizons considering the recommendations coming from TYNDP 2018, Projects of Common Interest and some relevant European projects such as e-Highways2050. This set of baseline scenarios would be a strong asset for future EU-funded research projects as it would avoid overlap and effort in this recurring task. In addition, an open set of scenarios would allow their unrestricted use (apart from due credit) for different research initiatives.

Chapter 7

Summary, Conclusion and Future Work

7.1 Summary

Providing low-carbon power across Europe relies on a strongly integrated and liquid energy market, supported by upgraded and new trans-national transmission networks. This calls attention to VSC HVDC systems in the vision of developing a future *supergrid*, as well as research effort in order to fully understand all aspects related to the hybrid AC/DC grids.

Towards this end, this thesis has been developed addressing different perspectives of hybrid AC/DC systems.

To study the steady-state behavior of a hybrid network, OPF models for AC grids needed to be expanded to incorporate MTDC networks. They are essential not only for operation, but also for planning purposes. Therefore, two OPF models have been developed including considerations of VSC MTDC systems with all the system losses taken into account. One is a detailed nonlinear formulation which is computationally expensive and that has been used mainly as a benchmark model. Special attention has been paid to converter loss modeling differentiating when the converter acts as a rectifier or as an inverter. Results have shown that the OPF solution is highly dependent on how converter losses are modeled. Not modeling the converter losses in an appropriate manner could lead to very different power flow values compared to the accurate formulation, especially for the DC branches. Apart from the pure operational point of view, this issue should be taken into account when planning the expansion of future MTDC networks. The other OPF model is a linearized version of

the OPF formulation which means to analyze potential benefits provided by embedded VSC-MTDC systems at the steady-state operation of the transmission grid. Analysis has been carried out on two systems (14-bus and 50-bus) to assess the goodness of the linearized model benchmarking with the nonlinear one. To demonstrate the applicability of the model, this linearized model has been used on a system at the pan-European level, and following the CBA guide established by ENTSO-e to assess the benefit, an example case has been presented. This has required to build a potential 2030 HVDC infrastructure in the North Sea which has been obtained by using a state-of-the-art expansion model for offshore wind networks. Results show that MTDC grid in the North Sea helps to integrate more RES to continental Europe implying lower operating costs and less carbon emissions, while potentially it could lead to more congestion in the continental AC network.

Finally, this thesis has also analyzed and identified several the most promising transmission technologies (including both AC and DC) among the the state-of-the-art and soon-to-be available ones. Barriers that could impede the future development of the *supergrid* are also identified and carefully examined.

7.2 Conclusion

Starting from PTP or B2B HVDC connections between isolated or asynchronous grids, eventually evolving into multivendor systems and finally meshed DC networks, VSC MTDC is considered one of the most attractive options towards the *supergrid* as discussed in the thesis. However, there are many challenges that remain unsolved.

The thesis has focused on the steady-state analysis of hybrid networks from a medium-term scope under different perspectives. It endeavors to address the main research question emanating from modeling and analytical perspectives of the MTDC system. To answer the overall research question "What are the main techno-economic impacts of VSC-MTDC systems, under the scope of the pan-European transmission network, considering large integration of offshore wind generation?" posed in Chapter 1, two objectives were presented.

Regarding objective 1, the main contribution and conclusion can be summarized as follows:

- Two mathematical models are proposed to cope with VSC MTDC from both operation and planning perspective. Both models have taken into account detailed modeling of the converters with a special attention paid to modeling their losses.

- Technical impact of introducing of HVDC networks is not negligible, especially the modeling of system losses. In case of a large deployment of HVDC networks, the impact of their converter stations on the control, operation and planning of the whole power system needs to be carefully examined.

- Not modeling the converter losses in an appropriate manner could lead to very different power flow values compared to the accurate formulation, especially for the DC branches. Apart from the pure operational point of view, this issue should be taken into account when planning the expansion of future MTDC networks.

Regarding objective 2, the main contribution and conclusion can be summarized as follows:

- A system dataset at pan-European level was gathered by combining ENTSO-e, TYNDP2016 and e-Highway2050 project, including load and generation data. The reduced grid takes into account all the nodes with voltage level of 220 kV and above and has been provided as input data in the context of *BestPaths* project. The reduction of the grid process has not been carried out in the thesis.

- The grid was reduced from a total of 17138 nodes 16551 lines and to a total of 7754 nodes and 8923 lines.

- To demonstrate the applicability of the LP-OPF model, it has been used to assess the technical-economic impact of a possible HVDC network deployed at the North Sea on the European electric power system.

- Results show that additional HVDC infrastructures can effectively save operating costs and increase RES integration. However, in various days with different RES and demand scenarios, the cost savings and RES penetration could vary a lot. For example, compared to a demand off-peak day , operational costs could be saved more on a demand peak day.

- With more RES integrated in the system, more congestions can be expected within the original system.

- Moreover, emission can also be reduced as a result of additional HVDC infrastructure. Nevertheless, depending on the scenario, more emission reduction does not always imply less RES curtailment. In some extreme day with excessive RES, there could be even more RES curtailment while remarkable reduced emission.

- Having said all of the above, whether VSC MTDC projects are overall economically beneficial or not depends on many factors and they are case-dependent. Cost and benefit of such HVDC application need to be carefully justified before implementation in real life. The model developed in this thesis can serve for that purpose.

- A future *supergrid* would serve as a backbone based on the existing transmission system. Nevertheless, reasons for insufficient expansion and modernization of the grid are manifold. Among all the barriers identified, the main ones can be concluded as follows:

    1. The primary barriers that hold back grid expansion are not technical or financial, but from regulatory perspective such as lack of appropriate regulatory frameworks, standardizations and public acceptance.
    2. In order to build and properly operate a future transnational HVDC grid, it is paramount to define a regulatory framework to coordinate the actions of involved TSOs and to provide clear schemes regarding the ownership and governance of the grid assets.
    3. A coordinated planning of both AC and DC future networks is essential to achieve the full potential of both technologies.
    4. It is necessary the development of new policies to incentivize TSOs' investment in some of technologies taking into account their specificities, such as DLR.
    5. There is a lack of a complete data set that could be used for network analysis (planning and operation) under a pan-European perspective.

7.3 Future Work

The thesis focused on the techno-economic impact assessment of embedded VSC-MTDC systems on the AC networks from a centralized point-of-view in the steady-state. Although the research carried out tried to cover different aspects regarding HVDC systems, it only represents a tip of the iceberg. Some interesting research questions, which have not been elaborated in this work, are formulated here as inspiration for future research.

From the modeling perspective:

- In the proposed OPF models, security constraints, i.e., $N-1$ criterion are not considered. They could have an impact when planning future HVDC grids.
- Nonlinear optimization techniques could be investigated to calculate the solutions for NLP-OPF and to try to ensure a global optimum this has been a trend in the last decade for AC system where DC-OPF has been questioned, and including embedded HVDC systems add another level of complexity that deserves more research.
- The thesis has considered a centralized point-of-view by minimizing total costs. To study the hybrid network under a market scenario, i.e., an equilibrium problem while different areas that try to maximize their own benefit, could represent a very interesting research line.

From the analysis perspective:

- This thesis has focused on the steady-state analysis of hybrid networks. Dynamic interaction between AC and VSC-MTDC systems could be investigated in order to understand the benefits from using VSC-MTDC systems in the improvement of the system stability and reliability.
- Preferred topology of an MTDC could be studied by extending the models proposed in this thesis.
- Algorithms could be investigated for the purpose of finding the optimal location to place the VSCs in a AC grid.

References

Roadmap 2050: a practical guide to a prosperous, low-carbon Europe. Technical report, European Climate Foundation (ECF), The Hague, 2010.

Engineering Transmission Lines with High Capacity Low Sag - ACCC Conductors. Technical report, CTC Global Corporation, 2011. ISBN: 978-0-615-57959-7.

Live Working - A Cutting-Edge Technique. Technical report, Reseau de transport d'electricite, 2013.

World Energy Investment Outlook - Special Report. Technical report, International Energy Agency, 2014.

Road Map on Standardization of HVDC Technology. Technical report, IEC TC 115, 2017.

Elisabeth N. Abildgaard and Marta Molinas. Modelling and Control of the Modular Multilevel Converter (MMC). *Energy Procedia*, 20:227–236, January 2012. ISSN 1876-6102. doi: 10.1016/j.egypro.2012.03.023.

R. Adapa. High-Wire Act: HVdc Technology: The State of the Art. *IEEE Power and Energy Magazine*, 10(6):18–29, November 2012. ISSN 1540-7977. doi: 10.1109/MPE.2012.2213011.

N. Alguacil, A.L. Motto, and A.J. Conejo. Transmission expansion planning: a mixed-integer LP approach. *IEEE Transactions on Power Systems*, 18(3):1070–1077, August 2003. ISSN 0885-8950. doi: 10.1109/TPWRS.2003.814891.

B. R. Andersen. HVDC transmission-opportunities and challenges. In *The 8th IEE International Conference on AC and DC Power Transmission*, pages 24–29, March 2006. doi: 10.1049/cp:20060006.

Athanasia Arapogianni, Jacopo Moccia, David Williams, and Joseph Phillips. Wind in our Sails - The coming of Europe's offshore wind energy industry. Technical report, The European Wind Energy Association, November 2011.

Jos Arrillaga, Y. H. Liu, and Neville R. Watson. *Flexible Power Transmission: The HVDC Options*. Wiley, Chichester, England ; Hoboken, NJ, 1 edition edition, October 2007. ISBN 978-0-470-05688-2.

Urban Axelsson, Anders Holm, Christer Liljegren, Kjell Eriksson, and Lars Weimers. Gotland HVDC Light Transmission - World's First Commercial Small Scale DC Transmission. In *15TH International Conference and Exhibition on Electricity Distribution*, Nice, France, 1999.

M. P. Bahrman and Brian K. Johnson. The ABC of HVDC Transmission Technologies. *IEEE power & energy magazine*, pages 1–7, 2007. ISSN 1540-7977.

A. Ballarino and R. Flukiger. Status of MgB2 wire and cable applications in Europe. *Journal of Physics: Conference Series*, 871, July 2017. ISSN 1742-6588, 1742-6596. doi: 10.1088/1742-6596/871/1/012098.

A. Ballarino, C. E. Bruzek, N. Dittmar, S. Giannelli, W. Goldacker, G. Grasso, F. Grilli, C. Haberstroh, S. Hole, F. Lesur, A. Marian, J. M. Martinez-Val, L. Martini, C. Rubbia, D. Salmieri, F. Schmidt, and M. Tropeano. The BEST PATHS Project on MgB2 Superconducting Cables for Very High Power Transmission. *IEEE Transactions on Applied Superconductivity*, 26(3):1–6, April 2016. ISSN 1051-8223. doi: 10.1109/TASC.2016.2545116.

S. Balser, S. Sankar, R. Miller, A. Rawlins, M. Israel, T. Curry, and T. Mason. Effective Grid Utilization: A Technical Assessment and Application Guide. Technical report, National Renewable Energy Laboratory (NREL), USA, 2012.

M. Baradar and M. Ghandhari. A Multi-Option Unified Power Flow Approach for Hybrid AC/DC Grids Incorporating Multi-Terminal VSC-HVDC. *IEEE Transactions on Power Systems*, 28(3):2376–2383, August 2013. ISSN 0885-8950. doi: 10.1109/TPWRS.2012.2236366.

M. Baradar, M.R. Hesamzadeh, and M. Ghandhari. Second-order cone programming for optimal power flow in vsc-type ac-dc grids. *IEEE Transactions on Power Systems*, 28(4):4282–4291, Nov. 2013. ISSN 0885-8950. doi: 10.1109/TPWRS.2013.2271871.

Mike Barnes and Antony Beddard. Voltage Source Converter HVDC Links - The State of the Art and Issues Going Forward. *Energy Procedia*, 24(Supplement C):108–122, January 2012. ISSN 1876-6102. doi: 10.1016/j.egypro.2012.06.092.

Antonella Battaglini, Nadejda Komendantova, Patricia Brtnik, and Anthony Patt. Perception of barriers for expansion of electricity grids in the European Union. *Energy Policy*, 47(Supplement C):254–259, August 2012. ISSN 0301-4215. doi: 10.1016/j.enpol.2012.04.065.

J. Beerten and R. Belmans. Development of an open source power flow software for high voltage direct current grids and hybrid AC/DC systems: MATACDC. *Transmission Distribution IET Generation*, 9(10):966–974, 2015. ISSN 1751-8687. doi: 10.1049/iet-gtd.2014.0545.

J. Beerten, S. Cole, and R. Belmans. A sequential ac/dc power flow algorithm for networks containing multi-terminal vsc hvdc systems. In *Power and Energy Society General Meeting, 2010 IEEE*, pages 1–7, Jul. 2010. doi: 10.1109/PES.2010.5589968.

J. Beerten, S. Cole, and R. Belmans. Generalized steady-state vsc mtdc model for sequential ac/dc power flow algorithms. *IEEE Transactions on Power Systems*, 27 (2):821–829, May 2012. ISSN 0885-8950. doi: 10.1109/TPWRS.2011.2177867.

Jef Beerten. *Modeling and Control of DC Grids*. Ph.D. Thesis, Katholieke University Leuven, Belgium, 2013.

Pehr Bergelin, Marc Jeroense, Tobias Quist, and Hans Rapp. 640 kV extruded HVDC cable system. Technical report, NKT Group GmbH, 2017.

BestPaths. Best Paths Project, 2014 - 2018. URL http://www.bestpaths-project.eu/.

A. Brooke, D. Kendrick, and A. Meeraus. *GAMS: A User's Guide*. The Scientific Press, Redwood City, California, 1992.

Patrik Buijs, David Bekaert, Stijn Cole, Dirk Van Hertem, and Ronnie Belmans. Transmission investment problems in Europe: Going beyond standard solutions. *Energy Policy*, 39(3):1794–1801, March 2011. ISSN 0301-4215. doi: 10.1016/j.enpol.2011.01.012.

Cristina Buzea and Tsutomu Yamashita. Review of superconducting properties of MgB2. *Superconductors, Science & Technology*, November 2001. doi: https://doi.org/10.1088/0953-2048/14/11/201. arXiv: cond-mat/0108265.

C. Cagigas and M. Madrigal. Centralized vs. competitive transmission expansion planning: the need for new tools. In *2003 IEEE Power Engineering Society General Meeting (IEEE Cat. No.03CH37491)*, volume 2, page 1017 Vol. 2, July 2003. doi: 10.1109/PES.2003.1270450.

Jun Cao, Wenjuan Du, Haifeng Wang, and S.Q. Bu. Minimization of Transmission Loss in Meshed AC/DC Grids With VSC-MTDC Networks. *IEEE Transactions on Power Systems*, 28(3):3047–3055, August 2013. ISSN 0885-8950. doi: 10.1109/TPWRS.2013.2241086.

Nilanjan Chaudhuri, Balarko Chaudhuri, Rajat Majumder, and Amirnaser Yazdani. *Multi-terminal Direct-Current Grids: Modeling, Analysis, and Control*. John Wiley & Sons, September 2014. ISBN 978-1-118-96053-0. Google-Books-ID: sGiCBAAAQBAJ.

G. Chen, M. Hao, Z. Xu, A. Vaughan, J. Cao, and H. Wang. Review of high voltage direct current cables. *CSEE Journal of Power and Energy Systems*, 1(2):9–21, June 2015. doi: 10.17775/CSEEJPES.2015.00015.

R. D. Christie. Power Systems Test Case Archive - UWEE, 1993. URL https://www2.ee.washington.edu/research/pstca/.

CIGRE. VSC TRANSMISSION. Technical Report Ref.269, CIGRE Working Group B4.37, Apr. 2005.

CIGRE. HVDC Grid Feasibility Study. Technical report, CIGRE Working Group B4.52, April 2013a.

CIGRE. Live Work – A Management Perspective. Technical Report 561, Cigre Joint Working Group B2/B3.27, December 2013b. ISBN: 978-85873-256-2.

CIGRE. Guide for the Development of Models for HVDC Converters in a HVDC Grid. Technical report, CIGRE Working Group B4.57, Dec. 2014.

CIGRE. TB 675 General guidelines for HVDC electrode design. Technical report, CIGRE Working Group B4.61, 2017. URL https://e-cigre.org/publication/675-general-guidelines-for-hvdc-electrode-design.

Stijn Cole. *Steady-state and dynamic modelling of VSC HVDC systems for power system Simulation*. PhD thesis, PhD dissertation, Katholieke University Leuven, Belgium, 2010.

Stijn Cole, K. Karoui, T. K. Vrana, O. Fosso, J. Curis, A. Denis, and C. C. Liu. A European supergrid: present state and future challenges. In *17th Power Systems Computation Conference, Stockholm*, 2011.

Stijn Cole, Pierre Martinot, Stephane Rapoport, Georgios Papaefthymiou, and Valerio Gori. Study of the Benefits of a meshed offshore grid in Northern Seas Region. Technical report, European Commission, July 2014.

B. Cui and X. A. Sun. A New Voltage Stability-Constrained Optimal Power-Flow Model: Sufficient Condition, SOCP Representation, and Relaxation. *IEEE Transactions on Power Systems*, 33(5):5092–5102, September 2018. ISSN 0885-8950. doi: 10.1109/TPWRS.2018.2801286.

R. de Dios, F. Soto, and A.J. Conejo. Planning to expand? *IEEE Power and Energy Magazine*, 5(5):64–70, September 2007. ISSN 1540-7977. doi: 10.1109/MPE.2007.904764.

S. de la Torre, A.J. Conejo, and J. Contreras. Transmission Expansion Planning in Electricity Markets. *IEEE Transactions on Power Systems*, 23(1):238–248, February 2008. ISSN 0885-8950. doi: 10.1109/TPWRS.2007.913717.

Jan De Decker, Paul Kreutzkamp, Pieter Joseph, Achim Woyte, Simon Cowdroy, Peter McGarley, Leif Warland, Harald Svendsen, Jakob Völker, Carolin Funk, Hannes Peinl, Jens Tambke, Lüder von Bremen, Katarzyna Michalowska, and George Caralis. Offshore Electricity Grid Infrastructure in Europe. Technical report, October 2011. URL http://www.offshoregrid.eu/images/FinalReport/offshoregrid_fullfinalreport.pdf.

Joao G. Dedecca. OGEM: The Offshore Grid Exploratory Model. Technical report, October 2017. URL https://zenodo.org/record/1006739#.W0yWDUh1yUk.

João G. Dedecca, Sara Lumbreras, Andrés Ramos, Rudi A. Hakvoort, and Paulien M. Herder. Expansion planning of the North Sea offshore grid: Simulation of integrated governance constraints. *Energy Economics*, April 2018. ISSN 0140-9883. doi: 10.1016/j.eneco.2018.04.037. URL http://www.sciencedirect.com/science/article/pii/S0140988318301622.

A. H. Dominguez, A. H. E. Zuluaga, L. H. Macedo, and R. Romero. Transmission network expansion planning considering HVAC/HVDC lines and technical losses. In *2016 IEEE PES Transmission Distribution Conference and Exposition-Latin America (PES T D-LA)*, pages 1–6, September 2016. doi: 10.1109/TDC-LA.2016.7805606.

Richard C. Dorf, editor. *The Electrical Engineering Handbook*. CRC Press, Boca Raton, 1 edition edition, 2000. ISBN 978-0-8493-2177-1.

D.A. Douglass, R.G. Stephen, and G.C. Sibilant. Use of HTLS in New Line Designs. In *2016 CIGRE-IEC Colloquium*, Montreal, QC, Canada, 2016.

e-Highway2050. Europe's future secure and sustainable electricity infrastructure - e-Highway2050 project results. Technical report, e-Highway2050 Project, November 2015.

EC. Inquiry pursuant to Article 17 of Regulation (EC) No 1/2003 into the European gas and electricity sectors (Final Report). Technical report, European Commission, 2007.

EC. Directive 2009/28/EC of the European Parliament and of the Council of 23 April 2009 on the promotion of the use of energy from renewable sources and amending and subsequently repealing Directives 2001/77/EC and 2003/30/EC, 2009.

EC. Communication from the Commission to the European Parliament, the Council, the European Economic and Social Committee and the Committee of the Regions: Energy Roadmap 2050, 2011.

EdisonTechCenter. The History of Alternating Current: AC Power History, 2014a. URL http://www.edisontechcenter.org/AC-PowerHistory.html.

EdisonTechCenter. The History of Alternating Current: History of Electrification, 2014b. URL http://www.edisontechcenter.org/HistElectPowTrans.html.

EdisonTechCenter. Oskar von Miller - Electrical Pioneer and Business Leader, 2015. URL http://www.edisontechcenter.org/OskarVonMiller.html.

Electrosuisse. Technology is our business - René Thury, 2011. URL https://www.electrosuisse.ch/fileadmin/user_upload_electrosuisse/Verband/Verlag/Pioniere/Pioniere_S_bis_Z/ThuryR.pdf.

C.S. Engelbrecht, J.P. Reynders, I. Gutman, K. Kondo, C. Lumb, A. Pigini, V. Sklenicka, and D. Wu. Outdoor insulation in polluted conditions: guidelines for selection and dimensioning Part 2: The DC Case. Technical Report TB518, CIGRE WG C4.303, Paris, December 2012.

Engineering and Technology History. Thomas Edison's 1882 Pearl Street Generating Station, 2010. URL http://ethw.org/w/images/a/ae/Edison_and_Pearl_Street%2C_Text%2C_031410.pdf.

ENTSO-e. Ten Year Network Development Plan 2010 - 2020. Technical report, ENTSO-e, Brussels, Belgium, 2010.

ENTSO-e. Ten Year Network Development Plan 2014. Technical report, ENTSO-E, Brussels, Belgium, 2014.

ENTSO-e. Dynamic line rating - CE TSOs current practice. Technical report, ENTSO-e RGCE SPD WG, March 2015a.

ENTSO-e. ENTSO-E Guideline for Cost Benefit Analysis of Grid Development Projects. Technical report, ENTSO-e, February 2015b.

ENTSO-e. ENTSO-e Power Statistics - Monthly Domestic Values. Technical report, ENTSO-E, 2016. URL https://www.entsoe.eu/data/power-stats/monthly-domestic/.

ENTSO-e. Statistical Fact Sheet 2016. Technical report, ENTSO-E, 2017. URL https://docstore.entsoe.eu/Documents/Publications/Statistics/Factsheet/entsoe_sfs_2016_web.pdf.

Hakan Ergun and Dirk Van Hertem. Comparison of HVAC and HVDC technologies. In *HVDC Grids: For Offshore and Supergrid of the Future*, pages 79–96. Wiley-Blackwell, 2016. ISBN 978-1-119-11524-3. doi: 10.1002/9781119115243.ch4. URL https://onlinelibrary.wiley.com/doi/abs/10.1002/9781119115243.ch4.

V. L. M. Escobar, L. R. A. Romero, Z. A. H. Escobar, and R. R. A. Gallego. Long term transmission expansion planning considering generation-demand scenarios and HVDC lines. In *2016 IEEE PES Transmission Distribution Conference and Exposition-Latin America (PES T D-LA)*, pages 1–6, September 2016. doi: 10.1109/TDC-LA.2016.7805617.

EU. Energy 2020 - A strategy for competitive, sustainable and secure energy. Technical report, European Union, Belgium, November 2010a.

EU. Energy infrastructure priorities for 2020 and beyond - A Blueprint for an integrated European energy network. Technical report, European Union, 2010b.

Wang Feng, Anh Le Tuan, L.B. Tjernberg, A. Mannikoff, and A. Bergman. A new approach for benefit evaluation of multiterminal vsc-hvdc using a proposed mixed ac/dc optimal power flow. *IEEE Transactions on Power Delivery*, 29(1):432–443, Feb. 2014. ISSN 0885-8977. doi: 10.1109/TPWRD.2013.2267056.

Nicolas Fichaux, Justin Wilkes, Frans Van Hulle, and Aidan Cronin. Oceans of Opportunity. Technical report, European Wind Energy Association, September 2009.

Desta Zahlay Fitiwi, Luis Olmo, Michel Rivier, Fernando de Cuadra, and José Ignacio Perez-Arriaga. Finding a representative network losses model for large-scale transmission expansion planning with renewable energy sources. *Energy*, December 2015.

Desta Zahlay Fitwi. *Strategies, Methods and Tools for Solving Long-term Transmission Expansion Planning in Large-scale Power Systems.* PhD thesis, Comillas Pontifical University,KTH Royal Institute of Technology, Delft University of Technology, 2016. URL http://repository.tudelft.nl/assets/uuid:e0f7045a-8cbf-42fb-8ba2-4fb15514f197/Elta_Koliou_binnenwerk.pdf.

N. Flourentzou, V.G. Agelidis, and G.D. Demetriades. Vsc-based hvdc power transmission systems: An overview. *Power Electronics, IEEE Transactions on*, 24(3): 592–602, March 2009. ISSN 0885-8993. doi: 10.1109/TPEL.2008.2008441.

FOSG. Position Paper on the EC Communication for a European Infrastructure Package. Technical report, FOSG, Brussels, December 2010. URL http://www.smartgrids-cre.fr/media/documents/dossiers/supergrids/Position_paper_EC_Communication_European_Infrastructure.pdf.

FOSG. Roadmap to the supergrid technologies. update report. Technical report, Friends of the Supergrid (FOSG), Mar. 2014.

Stephen Frank, Ingrida Steponavice, and Steffen Rebennack. Optimal power flow: a bibliographic survey I. *Energy Systems*, 3(3):221–258, April 2012a. ISSN 1868-3967, 1868-3975. doi: 10.1007/s12667-012-0056-y.

Stephen Frank, Ingrida Steponavice, and Steffen Rebennack. Optimal power flow: a bibliographic survey II. *Energy Systems*, 3(3):259–289, April 2012b. ISSN 1868-3967, 1868-3975. doi: 10.1007/s12667-012-0057-x. URL http://link.springer.com/article/10.1007/s12667-012-0057-x.

Jiao Fu, Zhichang Yuan, Yizhen Wang, Shukai Xu, Wei Wei, and Yu Luo. Control strategy of system coordination in Nanao multi-terminal VSC-HVDC project for wind integration. In *2014 IEEE PES General Meeting | Conference Exposition*, pages 1–5, July 2014. doi: 10.1109/PESGM.2014.6938929.

GAMS. GAMS — The Solver Manuals, October 2015. URL http://www.gams.com/help/topic/gams.doc/solvers/allsolvers.pdf.

R. L. Garwin and J. Matisoo. Superconducting lines for the transmission of large amounts of electrical power over great distances. *Proceedings of the IEEE*, 55(4): 538–548, April 1967. ISSN 0018-9219. doi: 10.1109/PROC.1967.5575.

A. Gavrilovic. AC/DC system strength as indicated by short circuit ratios. In *International Conference on AC and DC Power Transmission*, pages 27–32, September 1991.

R. Geary, T. Condon, T. Kavanagh, O. Armstrong, and J. Doyle. Introduction of high temperature low sag conductors to the Irish transmission grid. In *CIGER Session*, Paris, 2012.

J. M. George and Z. Lodi. Design and selection criteria for HVDC overhead transmission lines insulators. In *Conference on Power Systems CIGRE Canada, Toronto*, 2009.

H. Ghorbani, M. Jeroense, C. O. Olsson, and M. Saltzer. HVDC Cable Systems - Highlighting Extruded Technology. *IEEE Transactions on Power Delivery*, 29(1): 414–421, February 2014. ISSN 0885-8977. doi: 10.1109/TPWRD.2013.2278717.

H. Ghorbani, A. Gustafsson, M. Saltzer, and S. Alapati. Extra high voltage DC extruded cable system qualification. In *2015 International Conference on Condition Assessment Techniques in Electrical Systems (CATCON)*, pages 236–241, December 2015. doi: 10.1109/CATCON.2015.7449542.

P. Girdinio, P. Molfino, M. Nervi, M. Rossi, A. Bertani, and S. Malgarotti. Technical and compatibility issues in the design of HVDC sea electrodes. In *International Symposium on Electromagnetic Compatibility - EMC EUROPE*, pages 1–5, September 2012. doi: 10.1109/EMCEurope.2012.6396841.

Udana N. Gnanarathna, Aniruddha M. Gole, Athula D. Rajapakse, and Sanjay K. Chaudhary. Loss Estimation of Modular Multi-Level Converters using Electro-Magnetic Transients Simulation. In *Proc. Int. Conf. Power Syst. Transient (IPST)*, 2011.

G. Gocsei, B. Nemeth, B. G. Halasz, J. Meixner, and B. Magyar. Development of a new type of conductor car from design to assembly. In *2017 12th International Conference on Live Maintenance (ICOLIM)*, pages 1–5, April 2017. doi: 10.1109/ICOLIM.2017.7964106.

J. F. Goffinet, I. Gutman, and P. Sidenvall. Innovative insulated cross-arm: Requirements, testing and construction. In *2017 12th International Conference on Live Maintenance (ICOLIM)*, pages 1–7, April 2017. doi: 10.1109/ICOLIM.2017.7964158.

Antonio Gomez-Exposito, Antonio J. Conejo, and Claudio Canizares. *Electric Energy Systems: Analysis and Operation*. CRC Press, Boca Raton, 1 edition edition, July 2008. ISBN 978-0-8493-7365-7.

Javier Serrano Gonzalez and Roberto Lacal-Arantegui. A review of regulatory framework for wind energy in European Union countries: Current state and expected developments. *Renewable and Sustainable Energy Reviews*, 56:588–602, 2016. ISSN 13640321. doi: 10.1016/j.rser.2015.11.091.

F. Gonzalez-Longatt, J. Roldan, and C. A. Charalambous. Power flow solution on multi-terminal HVDC systems: supergrid case. In *International Conference on Renewable Energies and Power Quality (ICREPQ'12), Santiago de Compostela, Spain*, 2012.

S. Gordon. Supergrid to the rescue. *Power Engineer*, 20(5):30–33, October 2006. ISSN 1479-8344.

Anders Gustafsson, Markus Saltzer, Andreas Farkas, Hossein Ghorbani, Tobias Quist, and Marc Jeroense. The new 525 kV extruded HVDC cable system. Technical report, ABB, August 2014.

Temesgen Mulugeta Haileselassie. *Control, Dynamics and Operation of Multi-terminal VSC-HVDC Transmission Systems*. Ph.D. Thesis, Norwegian University of Science and Technology, 2012. URL http://www.diva-portal.org/smash/record.jsf?pid=diva2:589072.

H Hamzehbahmani, H Griffiths, A Haddad, and D Guo. Earthing requirements for HVDC systems. In *2015 50th International Universities Power Engineering Conference (UPEC)*, pages 1–7. IEEE, September 2015. ISBN 978-1-4673-9682-0. doi: 10.1109/UPEC.2015.7339768. URL http://ieeexplore.ieee.org/document/7339768/.

Sean Healy, Verena Graichen, and Sabine Gores. Trends and projections in the EU ETS in 2016. Technical Report 24, European Environment Agency, Denmark, 2016. ISBN 978-92-9213-817-2 ISSN 1977-8449 doi:10.2800/71685.

Reza Hemmati, Rahmat-Allah Hooshmand, and Amin Khodabakhshian. State-of-the-art of transmission expansion planning: Comprehensive review. *Renewable and Sustainable Energy Reviews*, 23:312–319, July 2013. ISSN 1364-0321. doi: 10.1016/j.rser.2013.03.015.

M. R. Hesamzadeh, N. Hosseinzadeh, and P. J. Wolfs. Economic assessment of transmission expansion projects in competitive electricity markets - an analytical review. In *2008 43rd International Universities Power Engineering Conference*, pages 1–10, September 2008. doi: 10.1109/UPEC.2008.4651531.

M. Huneault and F. D. Galiana. A survey of the optimal power flow literature. *IEEE Transactions on Power Systems*, 6(2):762–770, May 1991. ISSN 0885-8950. doi: 10.1109/59.76723.

E. Iggland, R. Wiget, S. Chatzivasileiadis, and G. Anderson. Multi-Area DC-OPF for HVAC and HVDC Grids. *IEEE Transactions on Power Systems*, PP(99):1–10, 2014. ISSN 0885-8950. doi: 10.1109/TPWRS.2014.2365724.

E3MLab & IIASA. Technical report on Member State results of the EUCO policy scenarios. Technical report, E3MLab & IIASA, January 2017. URL https://ec.europa.eu/energy/sites/ener/files/documents/20170125_-_technical_report_on_euco_scenarios_primes_corrected.pdf.

Rhodri James, Guy Henley, Stefanie Hintze, Andrew Conway, and Jérôme Guillet. Comparative Analysis of International Offshore Wind Energy Development. Technical report, IEA RETD TCP, 2017.

Dave Jones, Alice Sakhel, Matthias Buck, and Patrick Graichen. The European Power Sector in 2017. State of Affairs and Review of Current Developments. Technical report, Agora Energiewende and Sandbag, January 2018.

Dragan Jovcic and Khaled Ahmed. *High Voltage Direct Current Transmission: Converters, Systems and DC Grids*. John Wiley & Sons, September 2015. ISBN 978-1-118-84666-7. Google-Books-ID: xjmCCgAAQBAJ.

Gilbert King. Edison vs. Westinghouse: A Shocking Rivalry, 2011. URL https://www.smithsonianmag.com/history/edison-vs-westinghouse-a-shocking-rivalry-102146036/.

M. Kitagawa, I. Omura, S. Hasegawa, T. Inoue, and A. Nakagawa. A 4500 V injection enhanced insulated gate bipolar transistor (IEGT) operating in a mode similar to a thyristor. In *Proceedings of IEEE International Electron Devices Meeting*, pages 679–682, December 1993. doi: 10.1109/IEDM.1993.347221.

Xiangyu Kong and Hongjie Jia. Techno-Economic Analysis of SVC-HVDC Transmission System for Offshore Wind. In *Power and Energy Engineering Conference (APPEEC), 2011 Asia-Pacific*, pages 1–5, March 2011. doi: 10.1109/APPEEC.2011.5748839.

M. Korytowski. Uno Lamm: The Father of HVdc Transmission [History]. *IEEE Power and Energy Magazine*, 15(5):92–102, September 2017. ISSN 1540-7977. doi: 10.1109/MPE.2017.2711759.

Prabha Kundur. *Power System Stability and Control*. McGraw-Hill Education, January 1994. ISBN 978-0-07-035958-1. Google-Books-ID: 2cbvyf8Ly4AC.

Elias Kyriakides, Siddharth Suryanarayanan, and Vijay Vittal. *Electric Power Engineering Research and Education*. Power Electronics and Power Systems. Springer International Publishing, New York, NY, 2015. ISBN 978-3-319-17189-0. URL //www.springer.com/gp/book/9783319171890.

la Ville de Genève. Notice d'autorité - Thury, René, December 2006.

A. L'Abbate, G. Migliavacca, G. Fulli, C. Vergine, and A. Sallati. The European research project REALISEGRID: Transmission planning issues and methodological approach towards the optimal development of the pan-European system. In *2012 IEEE Power and Energy Society General Meeting*, pages 1–8, July 2012. doi: 10.1109/PESGM.2012.6344720.

A. U. Lamm. The peculiarities of high-voltage dc power transmission. *IEEE Spectrum*, 3(8):76–84, August 1966. ISSN 0018-9235. doi: 10.1109/MSPEC.1966.5217652.

Allison Lantero. The War of the Currents: AC vs. DC Power, 2014. URL https://energy.gov/articles/war-currents-ac-vs-dc-power.

G. Latorre, R. D. Cruz, J. M. Areiza, and A. Villegas. Classification of publications and models on transmission expansion planning. *IEEE Transactions on Power Systems*, 18(2):938–946, May 2003. ISSN 0885-8950. doi: 10.1109/TPWRS.2003.811168.

X. Lei, B. Buchholz, and D. Povh. Analysing subsynchronous resonance phenomena in the time- and frequency domain. *European Transactions on Electrical Power*, 10(4): 203–211, July 2000. ISSN 1546-3109. doi: 10.1002/etep.4450100402.

V. F. Lescale. Modern HVDC: state of the art and development trends. In *1998 International Conference on Power System Technology, 1998. Proceedings. POWERCON '98*, volume 1, pages 446–450, August 1998. doi: 10.1109/ICPST.1998.729003.

Francois Leveque, editor. *Competitive Electricity Markets And Sustainability*. Edward Elgar Pub, Feb. 2007. ISBN 978-1-84542-921-8.

X. Li, Z. Yuan, J. Fu, Y. Wang, T. Liu, and Z. Zhu. Nanao multi-terminal VSC-HVDC project for integrating large-scale wind generation. In *2014 IEEE PES General Meeting | Conference Exposition*, pages 1–5, July 2014. doi: 10.1109/PESGM.2014.6939123.

Zehong Liu, Liying Gao, Zuli Wang, Jun Yu, Jin Zhang, and Licheng Lu. R&D progress of +/- 1100kv UHVDC technology. *B4-201-2012, CIGRE Session*, 2012.

Alvaro Lopez-Pena Fernandez. *Evaluation and Design of Sustainable Energy Policies: An Application to the Case of Spain*. Ph.D. Thesis, Comillas Pontifical University, Madrid, Spain, 2014.

Viktor Lovrencic, Alenka Brezavscek, Milos Pantos, and Bostjan Gomiscek. Contribution of live working to the quality, safety, effectiveness and efficiency of the maintenance processes. *Tehnicki vjesnik - Technical Gazette*, 24(5), 2017. ISSN 13303651, 18486339. doi: 10.17559/TV-20160113105637.

Sara Lumbreras Sancho. *Decision Support Methods for Large-Scale Flexible Transmission Expanssion Planning*. Ph.D. Thesis, Pontifical Comillas University, Madrid, 2014.

K. Meah and S. Ula. Comparative Evaluation of HVDC and HVAC Transmission Systems. In *IEEE Power Engineering Society General Meeting, 2007*, pages 1–5, June 2007. doi: 10.1109/PES.2007.385993.

Andrea Michiorri, Huu-Minh Nguyen, Stefano Alessandrini, John Bjørnar Bremnes, Silke Dierer, Enrico Ferrero, Bjørn-Egil Nygaard, Pierre Pinson, Nikolaos Thomaidis, and Sanna Uski. Forecasting for dynamic line rating. *Renewable and Sustainable Energy Reviews*, 52(Supplement C):1713–1730, December 2015. ISSN 1364-0321. doi: 10.1016/j.rser.2015.07.134.

G. Migliavacca, A. L'Abbate, I. Losa, E. M. Carlini, A. Sallati, and C. Vergine. The REALISEGRID cost-benefit methodology to rank pan-European infrastructure investments. pages 1–7. IEEE, June 2011. ISBN 978-1-4244-8418-8 978-1-4244-8419-5 978-1-4244-8417-1. doi: 10.1109/PTC.2011.6019150.

ModernPowerSystems. 100 years of high voltage DC links, 2007. URL http://www.modernpowersystems.com/features/feature100-years-of-high-voltage-dc-links/.

Yoshinao Murata, Masatoshi Sakamaki, Kazutoshi Abe, Yoshiyuki Inoue, Shoji Mashio, Seiji Kashiyama, Osamu Matsunaga, Tsuyoshi Igi, Masaru Watanabe, and Shinya Asai. Development of high voltage DC-XLPE cable system. *SEI technical review*, 76:55–62, 2013.

Nature. The greener grid. *Nature*, 454:551–552, July 2008. ISSN 0028-0836. URL http://dx.doi.org/10.1038/454551b.

Santiago Cascante Nogales, Jose Antonio Lama Minana, Adrian Alonso, M. Paz Comech, Miguel Garcia-Gracia, and Eduardo Martin. HTLS and HVDC solutions for overhead lines uprating. In *Proc. of the 11th Spanish Portuguese Conference on Electrical Engineering*, pages 1–5, 2009.

C. Oates and C. Davidson. A comparison of two methods of estimating losses in the Modular Multi-Level Converter. In *Proceedings of the 2011-14th European Conference on Power Electronics and Applications (EPE 2011)*, pages 1–10, August 2011.

OFGEM. Cap and floor regime: unlocking investment in electricity interconnectors. Technical report, ofgem, 2016.

M.H. Okba, M.H. Saied, M.Z. Mostafa, and T.M. Abdel-Moneim. High voltage direct current transmission - A review, part I. In *2012 IEEE Energytech*, pages 1–7, May 2012. doi: 10.1109/EnergyTech.2012.6304650.

O. E. Oni, I. E. Davidson, and K. N. I. Mbangula. A review of LCC-HVDC and VSC-HVDC technologies and applications. In *2016 IEEE 16th International Conference on Environment and Electrical Engineering (EEEIC)*, pages 1–7, June 2016. doi: 10.1109/EEEIC.2016.7555677.

Erika Pierri, Ole Binder, Nasser G. A. Hemdan, and Michael Kurrat. Challenges and opportunities for a European HVDC grid. *Renewable and Sustainable Energy Reviews*, 70(Supplement C):427–456, April 2017. ISSN 1364-0321. doi: 10.1016/j.rser.2016.11.233.

Andrés Ramos and Pedro Sanchez-Martin. Modeling Transmission Ohmic Losses in a Stochastic Bulk Production Cost Model. *Institute for Research in Technology, Madrid*, 1997. URL http://www.iit.upcomillas.es/~aramos/papers/losses.pdf.

Hong Rao. Architecture of Nan'ao multi-terminal VSC-HVDC system and its multi-functional control. *Power and Energy Systems, CSEE Journal of*, 1(1):9–18, 2015. URL http://ieeexplore.ieee.org/xpls/abs_all.jsp?arnumber=7086151.

B. Subba Reddy and Diptendu Chatterjee. Analysis of High Temperature Low Sag Conductors Used for High Voltage Transmission. *Energy Procedia*, 90(Supplement C):179–184, December 2016. ISSN 1876-6102. doi: 10.1016/j.egypro.2016.11.183.

Johan Rimez. *Optimal operation of hybrid AC/DC meshed grids*. Ph.D. Thesis, TU Eindhoven, The Netherlands, 2014.

S. Rohner, S. Bernet, M. Hiller, and R. Sommer. Modulation, Losses, and Semiconductor Requirements of Modular Multilevel Converters. *IEEE Transactions on Industrial Electronics*, 57(8):2633–2642, August 2010. ISSN 0278-0046. doi: 10.1109/TIE.2009.2031187.

C. S. Schifreen and W. C. Marble. Charging Current Limitations in Operation or High-Voltage Cable Lines [includes discussion]. *Transactions of the American Institute of Electrical Engineers. Part III: Power Apparatus and Systems*, 75(3), January 1956. ISSN 0097-2460. doi: 10.1109/AIEEPAS.1956.4499370.

SiemensAG. Power Engineering Guide Edition 7.1. Technical report, Siemens Aktiengesellschaft, 2014. URL https://www.energy.siemens.com/hq/en/power-transmission/transformers/assets/pdf/siemens-transformers-power-engineering-guide-7-1.pdf.

Lukas Sigrist, Kristof May, Andrei Morch, Peter Verboven, Pieter Vingerhoets, and Luis Rouco. On Scalability and Replicability of Smart Grid Projects - A Case Study. *Energies*, 9(3):195, March 2016. ISSN 1996-1073. doi: 10.3390/en9030195.

Vijay K. Sood. *HVDC and FACTS controllers : applications of static converters in power systems*. Boston : Kluwer Academic Publishers, 2004. URL http://archive.org/details/springer_10.1007-b117759.

T. Sousa, M. L. dos Santos, J. A. Jardini, R. P. Casolari, and G. L. C. Nicola. An evaluation of the HVDC and HVAC transmission economic. In *Transmission and Distribution: Latin America Conference and Exposition (T D-LA), 2012 Sixth IEEE/PES*, pages 1–6, September 2012. doi: 10.1109/TDC-LA.2012.6401828.

Alfred Still. *Overhead electric power transmission: principles and calculations*. McGraw-Hill, New York, 1913.

B. Stott, J. Jardim, and O. Alsac. DC Power Flow Revisited. *IEEE Transactions on Power Systems*, 24(3):1290–1300, August 2009. ISSN 0885-8950. doi: 10.1109/TPWRS.2009.2021235.

Heiko Thomas, Adela Marian, Alexander Chervyakov, Stefan Stückrad, Delia Salmieri, and Carlo Rubbia. Superconducting transmission lines – Sustainable electric energy transfer with higher public acceptance? *Renewable and Sustainable Energy Reviews*, 55(Supplement C):59–72, March 2016. ISSN 1364-0321. doi: 10.1016/j.rser.2015.10.041. URL http://www.sciencedirect.com/science/article/pii/S136403211501120X.

D. Tiku. dc Power Transmission: Mercury-Arc to Thyristor HVdc Valves [History]. *IEEE Power and Energy Magazine*, 12(2):76–96, March 2014. ISSN 1540-7977. doi: 10.1109/MPE.2013.2293398.

TOBIN. The Grid West Project - Technical Foundation Report. Technical Report Volume 3 Appendix 3.2 of Stage 1 Report, TOBIN Consulting Engineers, Dublin, Ireland, December 2013.

Andrzej M. Trzynadlowski. *Introduction to Modern Power Electronics*. John Wiley & Sons, October 2015. ISBN 978-1-119-00323-6. Google-Books-ID: zRfICgAAQBAJ.

Graham Upton and Ian Cook. *Understanding Statistics*. Oxford University Press, 1996. ISBN 978-0-19-914391-7.

Jan van den Berg, Marieke Maas, Jos Spits, Wouter Meijerman, Pernille Holm Skyt, Betina Haugaard Heron, Søren Klinge, Niels Henrik Hansen, Hans Huibers, Knut Eggenberger, Philipp Strack, Norbert Graefe, Alex Alefragkis, Camiel Masselink, Frank Nobel, Axel Grüneberg, Christoffer Rasch, Jens Pedersen, and Gerjan Emsbroek. D17.2 Reframing planning and permitting for offshore interconnectors. Technical report, the TWENTIES EU Project, 2013.

Dirk Van Hertem and Mehrdad Ghandhari. Multi-terminal vsc hvdc for the european supergrid: Obstacles. *Renewable and Sustainable Energy Reviews*, 14(9):3156–3163, Dec. 2010. ISSN 1364-0321. doi: 10.1016/j.rser.2010.07.068.

Luc Van Nuffel, Koen Rademaekers, Jessica Yearwood, Verena Graichen, María Jose Lopez, Alicia Gonzalez, Juan Luis Martin, Sylvie Ludig, and Foivos Marias. European Energy Industry Investments. Technical report, European Parliament's Committee on Industry, Research and Energy (ITRE), 2017.

L. L. Vladimirskii. Selection and dimensioning of DC overhead line insulation. In *Cigré IEC International Symposium*, 2015.

J. Vobecky, K. Stiegler, M. Bellini, and U. Meier. New Generation Large Area Thyristor for UHVDC Transmission. In *PCIM Europe 2017; International Exhibition and Conference for Power Electronics, Intelligent Motion, Renewable Energy and Energy Management*, pages 1–4, May 2017.

Pal Kristian Myhrer Vormedal. *Voltage Source Converter Technology for Offshore Grids: Interconnection of Offshore Installations in a Multiterminal HVDC Grid using VSC*. M. Sc. Thesis, 2010.

Feng Wang. *On Techno-economic Assessment of a Multi-terminal VSC-HVDC in AC Transmission Systems*. Ph.D. Thesis, Chalmers University of Technology, Sweden, 2013a.

Feng Wang. *On Techno-economic Assessment of a Multi-terminal VSC-HVDC in AC Transmission Systems*. Ph.D. Thesis, Chalmers University of Technology, Sweden, 2013b.

Hualei Wang and M. A. Redfern. The advantages and disadvantages of using HVDC to interconnect AC networks. In *Universities Power Engineering Conference (UPEC), 2010 45th International*, pages 1–5, August 2010.

Shu Wang, Jinxiang Zhu, Lan Trinh, and Jiuping Pan. Economic assessment of HVDC project in deregulated energy markets. In *Electric Utility Deregulation and Restructuring and Power Technologies, 2008. DRPT 2008. Third International Conference on*, pages 18–23. IEEE, 2008.

R. Wiget and G. Andersson. Dc optimal power flow including hvdc grids. In *Electrical Power Energy Conference (EPEC), 2013 IEEE*, pages 1–6, Aug 2013. doi: 10.1109/EPEC.2013.6802915.

Roger Wiget. *Combined AC and Multi-Terminal HVDC Grids–Optimal Power Flow Formulations and Dynamic Control*. Ph.D. Thesis, ETH Zurich, 2015. URL http://www.eeh.ee.ethz.ch/uploads/tx_ethpublications/Dissertation_RogerWiget_final_online.pdf.

WindEurope. Offshore Wind in Europe - Key trends and statistics 2017. Technical report, WindEurope, 2018. URL https://windeurope.org/wp-content/uploads/files/about-wind/statistics/WindEurope-Annual-Offshore-Statistics-2017.pdf.

P. Wong, P. Albrecht, R. Allan, R. Billinton, Q. Chen, C. Fong, S. Haddad, W. Li, R. Mukerji, D. Patton, A. Schneider, M. Shahidehpour, and C. Singh. The IEEE reliability test system-1996. a report prepared by the reliability test system task force of the application of probability methods subcommittee. *IEEE Transactions on Power Systems*, 14(3):1010–1020, Aug. 1999. ISSN 0885-8950. doi: 10.1109/59.780914.

Allen J. Wood and Bruce F. Wollenberg. *Power Generation, Operation, and Control*. John Wiley & Sons, 2nd edition, November 2012. ISBN 978-1-118-58595-5.

Kunpeng Zha, Junzheng Cao, Wenmin Ouyang, Baokui Sun, Chong Gao, and Hongzhou Luan. Design of 6250 A/+- 800 kV UHVDC converter valve. In *13th IET International Conference on AC and DC Power Transmission (ACDC 2017)*, pages 1–6, February 2017. doi: 10.1049/cp.2017.0048.

Hui Zhang. *Transmission Expansion Planning for Large Power Systems*. PhD thesis, Arizona State University, 2013.

Lidong Zhang. *Modeling and Control of VSC-HVDC Links Connected to Weak AC Systems*. Ph.D. Thesis, KTH Electrical Engineering, Royal University of Technology, Stockholm, 2010.

Z. Zhang, Z. Xu, and Y. Xue. Valve losses evaluation based on piecewise analytical method for MMC-HVDC links. *IEEE Transactions on Power Delivery*, 29(3): 1354–1362, June 2014. ISSN 0885-8977. doi: 10.1109/TPWRD.2014.2304724.

Q. Zhao and J. García-González. Deliverable D13.3 Identified Barriers for Replicability. Technical report, the BestPaths EU Project, 2018.

Q. Zhao, J. Garcia-Gonzalez, O. Gomis-Bellmunt, E. Prieto-Araujo, and F. M. Echavarren. Impact of converter losses on the optimal power flow solution of hybrid networks based on VSC-MTDC. *Electric Power Systems Research*, 151:395–403, October 2017. ISSN 0378-7796. doi: 10.1016/j.epsr.2017.06.004.

Q. Zhao, J. García-González, D. Rivas, and N. Galan Hernandez. Deliverable D13.2 Definition and Building of Best Paths Scenario. Technical report, the BestPaths EU Project, 2018.

Jizhong Zhu. *Optimization of power system operation*. Wiley-IEEE ; John Wiley [distributor], Piscataway, N.J.; Chichester, 2nd edition, 2015. ISBN 978-0-470-46697-1 0-470-46697-9 978-0-470-46696-4 0-470-46696-0 978-0-470-29888-6 0-470-29888-X.

R.D. Zimmerman, C.E. Murillo-Sanchez, and R.J. Thomas. MATPOWER: Steady-State Operations, Planning, and Analysis Tools for Power Systems Research and Education. *IEEE Transactions on Power Systems*, 26(1):12–19, February 2011. ISSN 0885-8950. doi: 10.1109/TPWRS.2010.2051168.

Daniel Zwillinger and Stephen Kokoska. *CRC Standard Probability and Statistics Tables and Formulae*. CRC Press, December 1999. ISBN 978-1-58488-059-2 978-1-4200-5026-4. doi: 10.1201/9781420050264.

U. Åström, V. F. Lescale, D. Menzies, Ma Weimin, and Liu Zehong. The Xiangjiaba-Shanghai 800 kV UHVDC project, status and special aspects. In *2010 International Conference on Power System Technology*, pages 1–6, October 2010. doi: 10.1109/POWERCON.2010.5666671.

Appendix A

Leuven 5-bus System with 3-Terminal HVDC Grid Data

This section provides the system data for the Leuven 5-bus system combined with a three bus MTDC overlay grid.

♯	**From**	**To**	r [p.u.]	x [p.u.]	b [p.u.]	p_{max} [MW]
1	1	2	0.0200	0.0600	0.0600	100
2	1	3	0.0800	0.2400	0.0500	100
3	2	3	0.0600	0.1800	0.0400	100
4	2	4	0.0600	0.1800	0.0400	100
5	2	5	0.0400	0.1200	0.0300	100
6	3	4	0.0100	0.0300	0.0200	100
7	4	5	0.0800	0.2400	0.0500	100

Table A.1 AC line data for Leuven 5-bus test case

♯	p_{load} [MW]	q_{load} [MVA]	V_{base} [p.u.]	v_{max} [p.u.]	v_{min}
1	0.0	0.00	345	1.10	0.90
2	20.0	10.0	345	1.10	0.90
3	45.0	15.0	345	1.10	0.90
4	40.0	5.0	345	1.10	0.90
5	60.0	10.0	345	1.10	0.90

Table A.2 AC bus data for Leuven 5-bus test case

♯	p_{max} [MW]	p_{min} [MVA]	q_{max} [MW]	q_{min} [MVA]	A_g [€/MWh]	B_g [€/MW/MWh]	C_g [€/h]
1	250.0	10.0	500.0	-500.0	20.0	0.03	800.0
2	300.0	10.0	300.0	-300.0	20.0	0.03	800.0

Table A.3 Generator data for Leuven 5-bus test case

♯	**From**	**To**	r [p.u.]	p_{max} [MW]
1	3	2	0.0520	100
2	3	5	0.0520	100
3	2	5	0.0730	100

Table A.4 DC line data for Leuven 5-bus test case

♯	**AC Bus**	V_{base} [kV]	v_{max} [p.u.]	v_{min} [p.u.]
1	2	345	1.10	0.90
2	3	345	1.10	0.90
3	5	345	1.10	0.90

Table A.5 DC bus data for Leuven 5-bus test case

Converter	Parameters	Rating & Converter Loss Data $No.$	$1, 2, 3$
$X_{tr}[p.u.]$	0.1121	$P_{dc}[MW]$	100
$R_{tr}[p.u.]$	0.0015	$\pm V_{dc}[kV]$	345
$B_f[p.u.]$	0.0887	$A_v[MW]$	1.1030
$X_c[p.u.]$	0.16428	$B_v[kV]$	0.8870
$R_c[p.u.]$	0.0001	$C_v^{rec}[\Omega]$	2.8850
		$C_v^{inv}[\Omega]$	4.3710

Table A.6 Converter data for Leuven 5-bus test case

Appendix B

IEEE 14-bus System with 5-Terminal HVDC Grid Data

This section provides the system data for the IEEE 14-bus system combined with a five bus MTDC overlay grid.

♯	**From**	**To**	r [p.u.]	x [p.u.]	b [p.u.]	p_{max} [MW]
1	1	2	0.0194	0.0592	0.0528	100
2	1	5	0.0540	0.2230	0.0492	100
3	2	3	0.0470	0.1980	0.0438	100
4	2	4	0.0581	0.1763	0.0340	100
5	2	5	0.0570	0.1739	0.0346	100
6	3	4	0.0670	0.1710	0.0128	100
7	4	5	0.0134	0.0421	0.0	50
8	4	7	0.0	0.2091	0.0	50
9	4	9	0.0	0.5562	0.0	50
10	5	6	0.0	0.2520	0.0	50
11	6	11	0.0950	0.1989	0.0	50
12	6	12	0.1229	0.2558	0.0	50
13	6	13	0.0662	0.1303	0.0	50
14	7	8	0.0	0.1762	0.0	50
15	7	9	0.0	0.1100	0.0	50
16	9	10	0.0318	0.0845	0.0	50

Continued on next page

♯	**From**	**To**	r [p.u.]	x [p.u.]	b [p.u.]	p_{max} [MW]
17	9	14	0.1271	0.2703	0.0	50
18	10	11	0.0821	0.1921	0.0	50
19	12	13	0.2209	0.1999	0.0	50
20	13	14	0.1709	0.3480	0.0	50

Table B.1 AC line data for IEEE14 test case

♯	p_{load} [MW]	q_{load} [MVA]	V_{base} [p.u.]	v_{max} [p.u.]	v_{min}
1	0.0	0.0	138	1.05	0.95
2	21.7	12.7	138	1.05	0.95
3	94.2	19	138	1.05	0.95
4	47.8	-3.9	138	1.05	0.95
5	7.6	1.6	138	1.05	0.95
6	11.2	7.5	138	1.05	0.95
7	0.0	0.0	138	1.05	0.95
8	0.0	0.0	138	1.05	0.95
9	29.5	16.6	138	1.05	0.95
10	9.0	5.8	138	1.05	0.95
11	3.5	1.8	138	1.05	0.95
12	6.1	1.6	138	1.05	0.95
13	13.5	5.8	138	1.05	0.95
14	14.9	5.0	138	1.05	0.95
15	0.0	0.0	138	1.05	0.95

Table B.2 AC bus data for IEEE14 test case

♯	**AC Bus**	p_{max} [MW]	p_{min} [MVA]	q_{max} [MW]	q_{min} [MVA]	A_g [€/MWh]	B_g [€/MW/MWh]	C_g [€/h]
1	1	332.4	0	10	0	20	0.043	0
2	2	140	0	50	-40	20	0.250	0
3	3	100	0	40	0	40	0.010	0
4	6	100	0	24	-6	40	0.010	0
5	8	100	0	24	-6	40	0.010	0
6	15	100	0	0	0	10	0.010	0

Table B.3 Generator data for IEEE14 test case

♯	**From**	**To**	r [p.u.]	p_{max} [MW]
1	1	4	0.0038	50
2	1	5	0.0025	50
3	2	5	0.0038	50
4	2	3	0.0032	50
5	3	4	0.0051	50
6	3	5	0.0051	50
7	4	5	0.0051	50

Table B.4 DC line data for IEEE14 test case

♯	**AC Bus**	V_{base} [kV]	v_{max} [p.u.]	v_{min} [p.u.]
1	1	150	1.1	0.9
2	3	150	1.1	0.9
3	9	150	1.1	0.9
4	13	150	1.1	0.9
5	15	150	1.1	0.9

Table B.5 DC bus data for IEEE14 test case

Converter	Parameters	Rating & Converter Loss Data	
		$No.$	$1-5$
$X_{tr}[p.u.]$	0.10	$P_{dc}[MW]$	100
$R_{tr}[p.u.]$	0.001	$\pm V_{dc}[kV]$	150
$B_f[p.u.]$	0.09	$A_v[MW]$	1.1030
$X_c[p.u.]$	0.16	$B_v[kV]$	0.8870
$R_c[p.u.]$	0.0001	$C_v^{rec}[\Omega]$	2.8850
		$C_v^{inv}[\Omega]$	4.3710

Table B.6 Converter data for IEEE14 test case

Appendix C

MRTS System with 7-Terminal and 9-Terminal HVDC Grid Data

This section provides the system data for the MRTS system combined with a seven bus and nine bus MTDC overlay grid.

C.1 AC Grid Data

♯	p_{load} [MW]	q_{load} [MVA]	V_{base} [p.u.]	v_{max} [p.u.]	v_{min}
101	108	22	138	1.05	0.95
102	97	20	138	1.05	0.95
103	180	37	138	1.05	0.95
104	74	15	138	1.05	0.95
105	71	14	138	1.05	0.95
106	136	28	138	1.05	0.95
107	125	25	138	1.05	0.95
108	171	35	138	1.05	0.95
109	195	40	138	1.05	0.95
110	195	40	138	1.05	0.95
111	0	0	230	1.05	0.95
112	0	0	230	1.05	0.95
113	265	54	230	1.05	0.95

Continued on next page

♯	p_{load} [MW]	q_{load} [MVA]	V_{base} [p.u.]	v_{max} [p.u.]	v_{min}
114	194	39	230	1.05	0.95
115	317	64	230	1.05	0.95
116	100	20	230	1.05	0.95
117	0	0	230	1.05	0.95
118	333	68	230	1.05	0.95
119	181	37	230	1.05	0.95
120	128	26	230	1.05	0.95
121	0	0	230	1.05	0.95
122	0	0	230	1.05	0.95
123	0	0	230	1.05	0.95
124	0	0	230	1.05	0.95
201	108	22	138	1.05	0.95
202	97	20	138	1.05	0.95
203	180	37	138	1.05	0.95
204	74	15	138	1.05	0.95
205	71	14	138	1.05	0.95
206	136	28	138	1.05	0.95
207	125	25	138	1.05	0.95
208	171	35	138	1.05	0.95
209	195	40	138	1.05	0.95
210	195	40	138	1.05	0.95
211	0	0	230	1.05	0.95
212	0	0	230	1.05	0.95
213	265	54	230	1.05	0.95
214	194	39	230	1.05	0.95
215	317	64	230	1.05	0.95
216	100	20	230	1.05	0.95
217	0	0	230	1.05	0.95
218	333	68	230	1.05	0.95
219	181	37	230	1.05	0.95
220	128	26	230	1.05	0.95
221	0	0	230	1.05	0.95

Continued on next page

♯	p_{load} [MW]	q_{load} [MVA]	V_{base} [p.u.]	v_{max} [p.u.]	v_{min}
222	0	0	230	1.05	0.95
223	0	0	230	1.05	0.95
224	0	0	230	1.05	0.95
301	0	0	230	1.05	0.95
302	0	0	230	1.05	0.95

Table C.1 AC bus data for MRTS system test case

♯	**From**	**To**	r [p.u.]	x [p.u.]	b [p.u.]	p^A_{max} [MW]	p^B_{max} [MW]	p^C_{max} [MW]
1	101	102	0.003	0.014	0.461	175	250	200
2	101	103	0.055	0.211	0.057	175	208	220
3	101	105	0.022	0.085	0.023	175	208	220
4	102	104	0.033	0.127	0.034	175	208	220
5	102	106	0.050	0.192	0.052	175	208	220
6	103	109	0.031	0.119	0.032	175	208	220
7	103	124	0.002	0.084	0.000	400	510	600
8	104	109	0.027	0.104	0.028	175	208	220
9	105	110	0.022	0.088	0.024	175	208	220
10	106	110	0.014	0.061	2.459	175	193	200
11	107	108	0.016	0.061	0.017	175	208	220
12	108	109	0.043	0.165	0.045	175	208	220
13	108	110	0.043	0.165	0.045	175	208	220
14	109	111	0.002	0.084	0.000	400	510	600
15	109	112	0.002	0.084	0.000	400	510	600
16	110	111	0.002	0.084	0.000	400	510	600
17	110	112	0.002	0.084	0.000	400	510	600
18	111	113	0.006	0.048	0.100	500	600	625
19	111	114	0.005	0.042	0.088	500	625	625
20	112	123	0.012	0.097	0.203	500	625	625
21	112	123	0.012	0.097	0.203	500	625	625

Continued on next page

♯	**From**	**To**	r [p.u.]	x [p.u.]	b [p.u.]	p^A_{max} [MW]	p^B_{max} [MW]	p^C_{max} [MW]
22	113	123	0.011	0.087	0.182	500	625	625
23	114	116	0.005	0.059	0.082	500	625	625
24	115	116	0.002	0.017	0.036	500	600	625
25	115	121	0.006	0.049	0.103	500	600	625
26	115	121	0.006	0.049	0.103	500	600	625
27	115	124	0.007	0.052	0.109	500	600	625
28	116	117	0.003	0.026	0.055	500	600	625
29	116	119	0.003	0.023	0.049	500	600	625
30	117	118	0.002	0.014	0.030	500	600	625
31	117	122	0.014	0.105	0.221	500	600	625
32	118	121	0.003	0.026	0.055	500	600	625
33	118	121	0.003	0.026	0.055	500	600	625
34	119	120	0.005	0.040	0.083	500	600	625
35	119	120	0.005	0.040	0.083	500	600	625
36	120	123	0.003	0.022	0.046	500	600	625
37	120	123	0.003	0.022	0.046	500	600	625
38	121	122	0.009	0.068	0.142	500	600	625
39	201	202	0.003	0.014	0.461	175	250	200
40	201	203	0.055	0.211	0.057	175	208	220
41	201	205	0.022	0.085	0.023	175	208	220
42	202	204	0.033	0.127	0.034	175	208	220
43	202	206	0.050	0.192	0.052	175	208	220
44	203	209	0.031	0.119	0.032	175	208	220
45	203	224	0.002	0.084	0.000	400	510	600
46	204	209	0.027	0.104	0.028	175	208	220
47	205	210	0.022	0.088	0.024	175	208	220
48	206	210	0.014	0.061	2.459	175	193	200
49	207	208	0.016	0.061	0.017	175	208	220
50	208	209	0.043	0.165	0.045	175	208	220
51	208	210	0.043	0.165	0.045	175	208	220
52	209	211	0.002	0.084	0.000	400	510	600
53	209	212	0.002	0.084	0.000	400	510	600

Continued on next page

♯	**From**	**To**	r [p.u.]	x [p.u.]	b [p.u.]	p^A_{max} [MW]	p^B_{max} [MW]	p^C_{max} [MW]
54	210	211	0.002	0.084	0.000	400	510	600
55	210	212	0.002	0.084	0.000	400	510	600
56	211	213	0.006	0.048	0.100	500	600	625
57	211	214	0.005	0.042	0.088	500	625	625
58	212	223	0.012	0.097	0.203	500	625	625
59	212	223	0.012	0.097	0.203	500	625	625
60	213	223	0.011	0.087	0.182	500	625	625
61	214	216	0.005	0.059	0.082	500	625	625
62	215	216	0.002	0.017	0.036	500	600	625
63	215	221	0.006	0.049	0.103	500	600	625
64	215	221	0.006	0.049	0.103	500	600	625
65	215	224	0.007	0.052	0.109	500	600	625
66	216	217	0.003	0.026	0.055	500	600	625
67	216	219	0.003	0.023	0.049	500	600	625
68	217	218	0.002	0.014	0.030	500	600	625
69	217	222	0.014	0.105	0.221	500	600	625
70	218	221	0.003	0.026	0.055	500	600	625
71	218	221	0.003	0.026	0.055	500	600	625
72	219	220	0.005	0.040	0.083	500	600	625
73	219	220	0.005	0.040	0.083	500	600	625
74	220	223	0.003	0.022	0.046	500	600	625
75	220	223	0.003	0.022	0.046	500	600	625
76	221	222	0.009	0.068	0.142	500	600	625
77	301	302	0.000	0.001	0.000	500	600	625

Table C.2 AC line data for MRTS system test case

♯	**AC Bus**	p_{max} [MW]	p_{min} [MVA]	q_{max} [MW]	q_{min} [MVA]	A_g [€/MWh]	B_g [€/MW/MWh]	C_g [€/h]
1	101	20	16	10	0	130.0000	0.0000	400.6849
2	101	20	16	10	0	130.0000	0.0000	400.6849

Continued on next page

♯	**AC Bus**	p_{max} [MW]	p_{min} [MVA]	q_{max} [MW]	q_{min} [MVA]	A_g [€/MWh]	B_g [€/MW/MWh]	C_g [€/h]
3	101	76	15.2	30	-25	16.0811	0.0141	212.3076
4	101	76	15.2	30	-25	16.0811	0.0141	212.3076
5	102	20	16	10	0	130.0000	0.0000	400.6849
6	102	20	16	10	0	130.0000	0.0000	400.6849
7	102	76	15.2	30	-25	16.0811	0.0141	212.3076
8	102	76	15.2	30	-25	16.0811	0.0141	212.3076
9	107	100	25	60	0	43.6615	0.0527	781.5210
10	107	100	25	60	0	43.6615	0.0527	781.5210
11	113	197	69	80	0	48.5804	0.0072	832.7575
12	113	197	69	80	0	48.5804	0.0072	832.7575
13	113	197	69	80	0	48.5804	0.0072	832.7575
14	114	0	0	200	-50	0	0	0
15	115	12	2.4	6	0	56.5640	0.3284	86.3852
16	115	12	2.4	6	0	56.5640	0.3284	86.3852
17	115	12	2.4	6	0	56.5640	0.3284	86.3852
18	115	12	2.4	6	0	56.5640	0.3284	86.3852
19	115	12	2.4	6	0	56.5640	0.3284	86.3852
20	115	155	54.3	80	-50	12.3883	0.0083	382.2391
21	116	155	54.3	80	-50	12.3883	0.0083	382.2391
22	118	400	100	200	-50	4.4231	0.0002	395.3749
23	121	400	100	200	-50	4.4231	0.0002	395.3749
24	122	50	10	16	-10	0.0010	0	0.0010
25	122	50	10	16	-10	0.0010	0	0.0010
26	122	50	10	16	-10	0.0010	0	0.0010
27	122	50	10	16	-10	0.0010	0	0.0010
28	122	50	10	16	-10	0.0010	0	0.0010
29	122	50	10	16	-10	0.0010	0	0.0010
30	123	155	54.3	80	-50	12.3883	0.0083	382.2391
31	123	155	54.3	80	-50	12.3883	0.0083	382.2391
32	123	350	140	150	-25	11.8495	0.0049	665.1094
33	201	20	16	10	0	130.0000	0.0000	400.6849
34	201	20	16	10	0	130.0000	0.0000	400.6849

Continued on next page

♯	**AC Bus**	p_{max} [MW]	p_{min} [MVA]	q_{max} [MW]	q_{min} [MVA]	A_g [€/MWh]	B_g [€/MW/MWh]	C_g [€/h]
35	201	76	15.2	30	-25	16.0811	0.0141	212.3076
36	202	20	16	10	0	130.0000	0.0000	400.6849
37	202	20	16	10	0	130.0000	0.0000	400.6849
38	202	76	15.2	30	-25	16.0811	0.0141	212.3076
39	202	76	15.2	30	-25	16.0811	0.0141	212.3076
40	207	100	25	60	0	43.6615	0.0527	781.5210
41	207	100	25	60	0	43.6615	0.0527	781.5210
42	207	100	25	60	0	43.6615	0.0527	781.5210
43	213	197	69	80	0	48.5804	0.0072	832.7575
44	213	197	69	80	0	48.5804	0.0072	832.7575
45	213	197	69	80	0	48.5804	0.0072	832.7575
46	214	0	0	200	-50	0	0	0
47	215	12	2.4	6	0	56.5640	0.3284	86.3852
48	215	12	2.4	6	0	56.5640	0.3284	86.3852
49	215	12	2.4	6	0	56.5640	0.3284	86.3852
50	215	12	2.4	6	0	56.5640	0.3284	86.3852
51	215	12	2.4	6	0	56.5640	0.3284	86.3852
52	215	155	54.3	80	-50	12.3883	0.0083	382.2391
53	216	155	54.3	80	-50	12.3883	0.0083	382.2391
54	218	400	100	200	-50	4.4231	0.0002	395.3749
55	221	400	100	200	-50	4.4231	0.0002	395.3749
56	222	50	10	16	-10	0.0010	0	0.0010
57	222	50	10	16	-10	0.0010	0	0.0010
58	222	50	10	16	-10	0.0010	0	0.0010
59	222	50	10	16	-10	0.0010	0	0.0010
60	222	50	10	16	-10	0.0010	0	0.0010
61	222	50	10	16	-10	0.0010	0	0.0010
62	223	155	54.3	80	-50	12.3883	0.0083	382.2391
63	223	155	54.3	80	-50	12.3883	0.0083	382.2391
64	302	350	140	150	-25	11.8495	0.0049	665.1094
65	302	350	140	150	-25	11.8495	0.0049	665.1094

Continued on next page

♯	AC Bus	p_{max} [MW]	p_{min} [MVA]	q_{max} [MW]	q_{min} [MVA]	A_g [€/MWh]	B_g [€/MW/MWh]	C_g [€/h]

Table C.3 Generator data for MRTS system test case

C.2 7-Terminal MTDC Grid Data

♯	From	To	r [p.u.]	p_{max} [MW]
1	1	3	0.0352	100
2	2	3	0.0352	100
3	4	5	0.0828	100
4	4	7	0.0704	100
5	4	6	0.0718	100
6	5	7	0.076	100
7	6	7	0.0248	100

Table C.4 DC line data (7-Terminal) for MRTS system test case

♯	AC Bus	V_{base} [kV]	v_{max} [p.u.]	v_{min} [p.u.]
1	107	150	1.1	0.9
2	204	150	1.1	0.9
3	301	150	1.1	0.9
4	113	300	1.1	0.9
5	123	300	1.1	0.9
6	215	300	1.1	0.9
7	217	300	1.1	0.9

Table C.5 DC bus data (7-Terminal) for MRTS system test case

♯	R_{tr} [p.u.]	X_{tr} [p.u.]	R_c [p.u.]	X_c [p.u.]	B_f [p.u.]	P_{dc} [MW]	$\pm V_{dc}$ [kV]	A_v [MW]	B_v [kV]	C_v^{rec} [Ω]	C_v^{inv} [Ω]
1	0.0010	0.10	0.0001	0.16	0.090	100	150	1.103	0.887	2.885	4.371
2	0.0010	0.10	0.0001	0.16	0.090	100	150	1.103	0.887	2.885	4.371
3	0.0010	0.05	0.0001	0.08	0.045	200	150	2.206	0.887	1.442	2.185
4	0.0005	0.05	0.0001	0.08	0.0	200	300	1.103	1.8	5.94	9.0
5	0.0010	0.10	0.0001	0.16	0.0	100	300	2.206	1.8	11.88	18.0
6	0.0005	0.05	0.0001	0.08	0.0	200	300	1.103	1.8	5.94	9.0
7	0.0010	0.10	0.0001	0.16	0.0	100	300	2.206	1.8	11.88	18.0

Table C.6 Converter data (7-Terminal) for MRTS system test case

C.3 9-Terminal MTDC Grid Data

♯	**From**	**To**	r [p.u.]	p_{max} [MW]
1	1	3	0.0352	100
2	1	4	0.0828	100
3	2	3	0.0352	100
4	2	6	0.0828	100
5	2	9	0.0828	100
6	3	5	0.1656	100
7	4	5	0.1242	100
8	4	7	0.1242	100
9	5	7	0.1242	100
10	6	7	0.0248	100
11	6	8	0.0828	100
12	8	9	0.0828	100

Table C.7 DC line data (9-Terminal) for MRTS system test case

♯	**AC Bus**	V_{base} [kV]	v_{max} [p.u.]	v_{min} [p.u.]
1	107	300	1.1	0.9
2	204	300	1.1	0.9
3	301	300	1.1	0.9
4	104	300	1.1	0.9
5	118	300	1.1	0.9
6	215	300	1.1	0.9
7	217	300	1.1	0.9
8	219	300	1.1	0.9
9	206	300	1.1	0.9

Table C.8 DC bus data (9-Terminal) for MRTS system test case

♯	R_{tr} [p.u.]	X_{tr} [p.u.]	R_c [p.u.]	X_c [p.u.]	B_f [p.u.]	P_{dc} [MW]	$\pm V_{dc}$ [kV]	A_v [MW]	B_v [kV]	C_v^{rec} [Ω]	C_v^{inv} [Ω]
1	0.0010	0.10	0.0001	0.16	0.090	100	300	1.103	0.887	2.885	4.371
2	0.0010	0.10	0.0001	0.16	0.090	100	300	1.103	0.887	2.885	4.371
3	0.0010	0.05	0.0001	0.08	0.045	200	300	2.206	0.887	1.442	2.185
4	0.0005	0.05	0.0001	0.08	0.0	200	300	1.103	1.8	5.94	9.0
5	0.0010	0.10	0.0001	0.16	0.0	100	300	2.206	1.8	11.88	18.0
6	0.0005	0.05	0.0001	0.08	0.0	200	300	1.103	1.8	5.94	9.0
7	0.0010	0.10	0.0001	0.16	0.0	100	300	2.206	1.8	11.88	18.0
8	0.0005	0.05	0.0001	0.08	0.0	200	300	1.103	1.8	5.94	9.0
9	0.0010	0.10	0.0001	0.16	0.0	100	300	2.206	1.8	11.88	18.0

Table C.9 Converter data (9-Terminal) for MRTS system test case

Appendix D

Per Unit Calculations for the Hybrid OPF

In a electrical power system study, it is common to use per unit (p.u.) system to simplify calculations. This is well known in AC systems where the p.u. modeling allows to deal easily with the magnitudes that take very different values depending on the voltage level of each grid zone due to the existence of transformers. As the DC modeling of a hybrid AC/DC grid requires to deal simultaneously with p.u. magnitudes of both the AC and DC sides, in this section a very brief review is provided. In a p.u. system, the physical quantity is expressed as a fraction of a defined base unit quantity which can be defined as follows:

$$per\ unit\ value = \frac{actual\ value}{base\ value} \tag{D.1}$$

There are four basic electrical elements: voltage, power, impedance and current. In per unit notation, some basic relations needs to be kept as shown in Table D.1. Thus only two of the base quantities can be arbitrarily chosen while the other two must follow the relations.

For example, let's consider a three-phase power transmission system that has a rating power of 100 MVA and uses a nominal voltage of 138 kV for transmission. One could arbitrarily select $S_b = 100$ MVA, and keep the nominal voltage 138 kV as the V_b. Then base current and impedance would have: $I_b = S_b/(\sqrt{3} * V_b) = 0.42$ kA, $Z_b = V_b^2/S_b = 190.44\ \Omega$.

Base quantity	**Three Phase AC System**
Power	$S_b = \sqrt{3} * V_b * I_b$
Voltage	$V_b = S_b/(\sqrt{3} * I_b)$
Current	$I_b = S_b/(\sqrt{3} * V_b)$
Impedance	$Z_b = V_b/(\sqrt{3} * I_b) = V_b^2/S_b$
*subscript b indicates the per unit base values	

Table D.1 Per Unit Base Values Calculation of AC systems

In the case of transformers assuming n_L and n_H be the number of turns in primary and secondary winding, one could choose either the low voltage (later referred as V_L) as the base voltage (later referred as V_{bL}) or the high voltage (later referred as V_H) as base voltage (later referred as V_{bH}). Then base currents (I_{bL}, I_{bH}) and base impedances (Z_{bL}, Z_{bH}) for both conventions can be calculated respectively as shown below (Table D.2).

Base quantity	$V_b = V_L$	$V_b = V_H$
Power	S_b	S_b
Voltage	$V_{bL} = V_L = \frac{n_L}{n_H} * V_H$	$V_{bH} = V_H = \frac{n_H}{n_L} * V_L$
Current	$I_{bL} = S_b/V_{bL} = S_b/V_L = \frac{n_H}{n_L} * I_{bH}$	$I_{bH} = S_b/V_{bH} = S_b/V_H = \frac{n_L}{n_H} * I_{bL}$
Impedance	$Z_{bL} = V_{bL}/I_{bL} = V_{bL}^2/S_b = (\frac{n_L}{n_H})^2 * Z_{bH}$	$Z_{bH} = V_{bH}/I_{bH} = V_{bH}^2/S_b = (\frac{n_H}{n_L})^2 * Z_{bL}$

Table D.2 Per Unit Base Values Calculation of Transformers

When performing system studies for a hybrid network, similarly as for AC systems, it is important to define per unit conventions for the DC network as well. The per unit system defined in Table D.3 is used throughout the manuscript. It is important to highlight that p.u. values depends on the number of poles, p, of HVDC configurations.

Base quantity	**DC system**
Power	$P_b = p * V_b * I_b$
Voltage	$V_b = P_b/(I_b * p)$
Current	$I_b = P_b/(V_b * p)$
Impedance	$Z_b = V_b/I_b = p * V_b^2/P_b$
*p indicates the the number of poles	

Table D.3 Per Unit Base Values Calculation of DC systems

To illustrate better, considering a DC system with bipolar scheme (± 138 kV) that has a rating power of 100 MW. It entails that the number of poles, $p = 2$. In the case of asymmetric monopole, $p = 1$. One could again arbitrarily select the $P_b = 100$ MW, and use the pole-to-ground voltage 100 kV as the V_b. Then base current and impedance would have: $I_b = P_b/(V_b * 2) = 0.36$ kA, $Z_b = 2 * V_b^2/P_b = 380.88\ \Omega$.

It is important to notice that the base power value should be kept the same for the entire power system of concern (AC and DC).